7 Jura Mountains

7.1 Interpretation of seismic lines across the rhomb shaped Val de Ruz basin (internal Folded Jura)

A. Sommaruga & M. Burkhard

Contents

7.1.1 Introduction

In 1988, British Petroleum conducted a seismic survey in the canton Neuchâtel where a total of about 300 km of vibro-seismic (and dynamite in rugged topography) profiles were acquired (compare approximate seismic plan published by Swisspetrol 1992). In an agreement between BP, the canton Neuchâtel and the Swiss National Science Foundation, part of this seismic survey from the Val de Ruz area has been obtained for research. These lines permit to extend our knowledge of the local stratigraphy, particularly for thicknesses of layers older than Dogger. Furthermore, for the first time in the central Jura, seismic data permit to constrain the geometry of this fold and thrust belt at depth.

The Val de Ruz is located within the internal part of the central Jura fold and thrust belt (Figure 7.1-1). Among the various cross sections studied by the NRP 20 project, these sections represent the most external parts of the Alpine thrust system. In this context it has to be mentioned that the overall tectonic picture of a cross section through the Alps in Western Switzerland is quite different from Eastern Switzerland, where the "alpine deformation front" is located within the internal part of the Molasse Basin, crossed by an industry section obtained in exchange with the NRP 20 program (Stäuble & Pfiffner 1991). In comparison with this eastern transsect, the "alpine deformation front" in central and western Switzerland is located in a much more external position, beyond the folded and thrust Jura chains (Laubscher 1972; Burkhard 1990). The transition from "undeformed foreland" to shortened cover is located mostly in France and has not been crossed by any of the NRP 20 lines. The French ECORS line from the southwestern termination of the Jura (Damotte et al. 1990; Guellec et al. 1990) is one of the few published seismic sections across the entire Jura. Other seismic profiles from the Jura have become available through NAGRA studies (Laubscher 1985; Noack 1989; Naef & Diebold 1990; Diebold et al. 1991) and small sections published by Bitterli (1972), Suter (1978) and Jordi (1990).
The study area (see Figure 7.1-1) is bordered to the south by lake Neuchâtel, representing the transition between the rather strongly folded Jura chain to the NNW and the very weakly folded/ faulted Molasse Basin to the SSE. Surface geology is quite well known from a series of published 1:25'000 maps of the Geological Atlas of Switzerland and innumerable original 1:5'000 map sheets deposited at the Institut de Géologie at Neuchâtel. Outcropping Mesozoic strata range from uppermost Liassic (strongly tectonized in the Vue des Alpes strike slip zone) to middle Cretaceous. The Mesozoic series are dominated by interlayered marls and limestones. The structural backbone of the characteristic Jura folds is formed by up to 400 m pure gray Malm limestones. This is the major competent formation within the Mesozoic se-

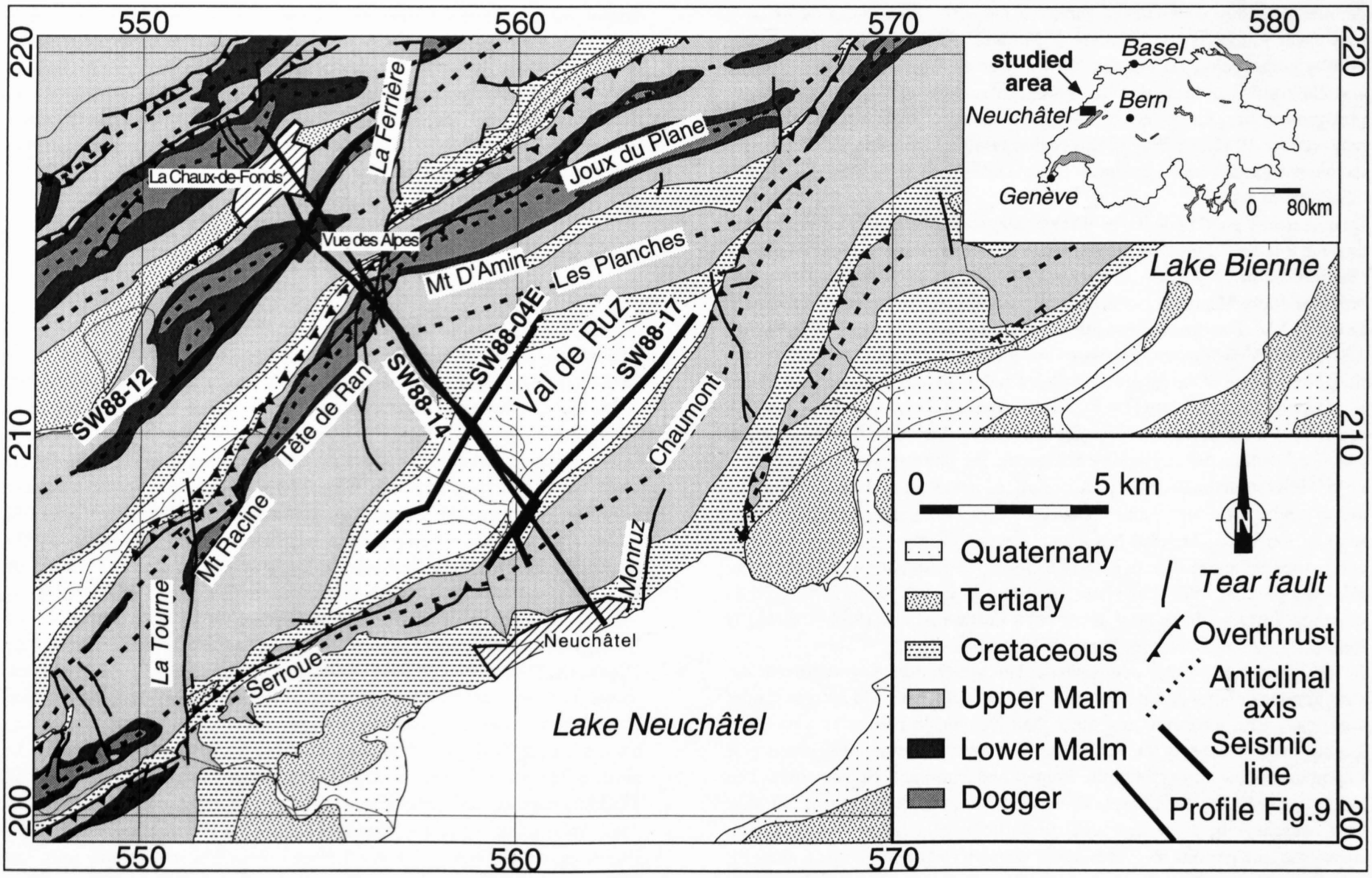

Figure 7.1-1
Structural map of the Val de Ruz area, according to geologic maps 1:25'000 Val de Ruz (Bourquin et al. 1968), Neuchâtel (Frei et al. 1974) and Bienne (Schär et al. 1971). Thick lines represent the approximate position of seismic lines. Major structural elements are labeled. Coordinates are according to the Swiss reference grid.

crease in the percentage of marly interlayers. The Dogger is formed by at least 250 m of a well layered series of coarse grained limestones containing various formations: Dalle nacrée, Calcaire roux sableux, Grande Oolithe (Oberer Hauptrogenstein), Oolithe subcompacte (Unterer Hauptrogenstein) and Calcaire à entroques. The "Aalenian" black shales (ca. 100 m?) corresponding to the Opalinus Ton of the Eastern Jura, contrast strongly with the overlying Dogger limestones. The "Aalenian" itself, some slivers of Liassic and uppermost Triassic (Rhaetian) limestones have been encountered in a recent geotechnical drilling campaign near La Vue des Alpes (Meia pers. comm. 1992). All these layers, including the Aalenian are strongly tectonized and the data do not permit the establishment of stratigraphic thicknesses.

Comparisons of the seismic stratigraphy as encountered in longitudinal lines of the Val de Ruz, have therefore to be made with more distant wells particularly for formations below the Dogger. Figure 7.1-2 shows a compilation of the lithostratigraphy of the Val de Ruz area in comparison with drill hole data from Courtion (Fischer & Luterbacher 1963) in the Molasse Basin south-east of Neuchâtel, Buez (Bitterli 1972) in the French Jura north-west of Neuchâtel and Essertines (Bitterli 1972) in the Molasse Basin south-west of Neuchâtel. The lithostratigraphy of the Val de Ruz is very similar to that of the Courtion drill hole. For all formations above Liassic, Persoz (1982) has shown a good correlation of whole rock and clay mineralogy as well as lithofacies between the Courtion drill hole and the Val de Ruz area. The lithostratigraphy of the Courtion drill hole is also quite similar to that from Buez: the thickness of the "Aalenian"-Liassic and Keuper formations are virtually identical. We therefore suppose that the Val de Ruz area, located in between these two drill holes, could have a comparable stratigraphy at depth (i. e. Liassic and Triassic). In the Essertines drill hole, on the other hand, the stratigraphy is quite different. In particular, the total thickness of Malm is increased by about 50% and shows a considerably more internal, deeper water facies with numerous marl interlayers. The informations on lower Liassic and older formations are unreliable for thickness and stratigraphy because this section was drilled through an anticline close to "the Essertines wrench fault zone" (Jordi 1993), where repetitions in the evaporitic sequence are possible. As an alternative interpretation to the stratigraphic log presented by Bitterli (1972), we suggest that the Keuper thickness in Essetinres is only 200 m and the underlying evaporites correspond to the Muschelkalk formation.

By comparison with Buez, Courtion and Essertines the Keuper formation thickness below the Val de Ruz is expected to be about 200 m of anhydrite and shales, underlain by some 60 m of upper Muschelkalk dolomites. The thickness of the lower Muschelkalk evaporite formation, however, is not well constrained because both Courtion and Essertines stopped within this formation. Furthermore, in all three of them (Courtion, Buez and Essertines), tectonic complications seem to be present within the lower Muschelkalk evaporite formation. In summary, the total thickness of the Mesozoic below the Val de Ruz from top Cretaceous to the base of Muschelkalk appears to be about 2000 m with an estimated uncertainty of about ± 200 m.

7.1.2.2 Identification and comparison of reflectors

Due to the above presented summary knowledge of the local stratigraphy, and given the absence of any direct ties with logs from a nearby drillhole, the identification even of excellent seismic reflectors as seen on the longitudinal seismic sections SW 88-17 and SW 88-04 E (Figure 7.1-13) is not as straightforward as it might seem. A tentative identification of reflectors is presented in Figure 7.1-4. This correlation is based on the known stratigraphic thicknesses above the top Liassic as discussed in the previous paragraph. In Figure 7.1-4, layer thicknesses in meters and two way travel time (TWT) in seconds or "apparent thickness" of major reflectors on a seismic line are compared. This correlation diagram has been established in a trial and error procedure, using interval velocities as determined for comparable formations by direct methods in NAGRA drill holes from the eastern Jura (Sprecher & Müller 1986; Naef & Diebold 1990; Diebold et al 1991). In order to fit major reflectors with expected stratigraphic marker horizons (top Malm, base Argovian, base Aalenian, Muschelkalk dolomites), thicknesses had to be slightly modified from those known from the surface geology. It appears that the Dogger limestones are either slightly thicker than previously thought (ca. 400 m, as in Courtion, rather than only 350 m) or, alternatively, that these limestones might have lower velocities than those determined by Diebold et al (1991). The thickness of the Aalenian seems to be about 150 m, closer to the thickness known from Courtion than that estimated in the La Vue des Alpes area (90 m). The following major reflectors have been identified and labelled in Figure 7.1-4 (this labelling will be the same in all the following figures): a first series of closely spaced but laterally irregular reflectors between A and B corresponds to the Cretaceous. The major unconformity between the top Cretaceous and the base Tertiary (=A?) is not easily recognized on these seismic sections. Some minor obliquities (onlaps?) in line SW 88-04E (Figure 7.1-5 above A) could be interpreted as this discordancy. The Early Cretaceous, between reflectors A and B, consits of a layered series of limestones and marls. The underlying thick upper Malm limestones are represented by a homogeneous, massive structure. The strong reflector B corresponds to the top of the upper Malm limestones, a transparent zone without reflectors on the seismic line. The progressive transition from pure, massive limestones to the underlying, increasingly marl-rich Argovian marls, does not appear as a strong reflector (C). The pronounced reflector D, one of the most prominent marker horizons, is characterized by a very good lateral continuity. It corresponds to the top of the Dogger series. The "Aalenian" black shales corresponding to the Opalinus Ton of the Eastern Jura, contrast strongly with the overlying Dogger limestones. This is the oldest formation outcropping in this area. It appears very likely, that the strong reflector labelled F corresponds to the top Liassic (base "Aalenian"), whereas the top "Aalenian" may not show very clearly on seismic lines. The contrast between "Aalenian" and underlying Liassic, may not be as important as farther east, where this is one of the most important seismic marker horizons (Diebold et al. 1991) and as farther west respectively (Jordi 1993). Between 0.6 and 0.7 s TWT, a series of layered reflectors, labelled G, are interpreted as Liassic

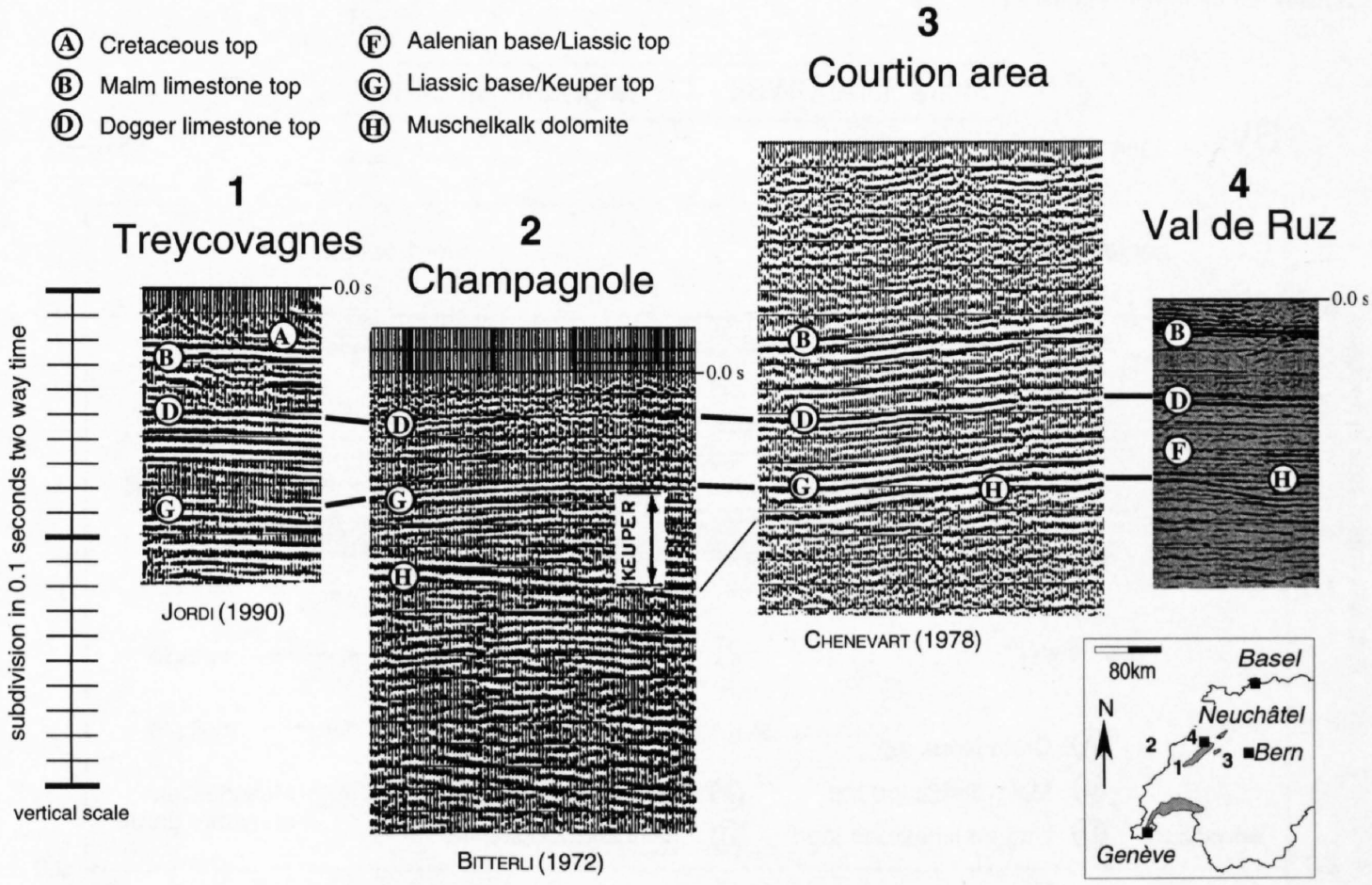

Figure 7.1-3
Main reflectors and their identification in strike parallel seismic line SW88-17 from the Val de Ruz is compared with parts of published lines from the Courtion, Champagnole and Treycovagnes areas respectively. Compare also with drill hole data as shown in Figure 7.1-2. For identification of reflectors A through H compare Figure 7.1-4.

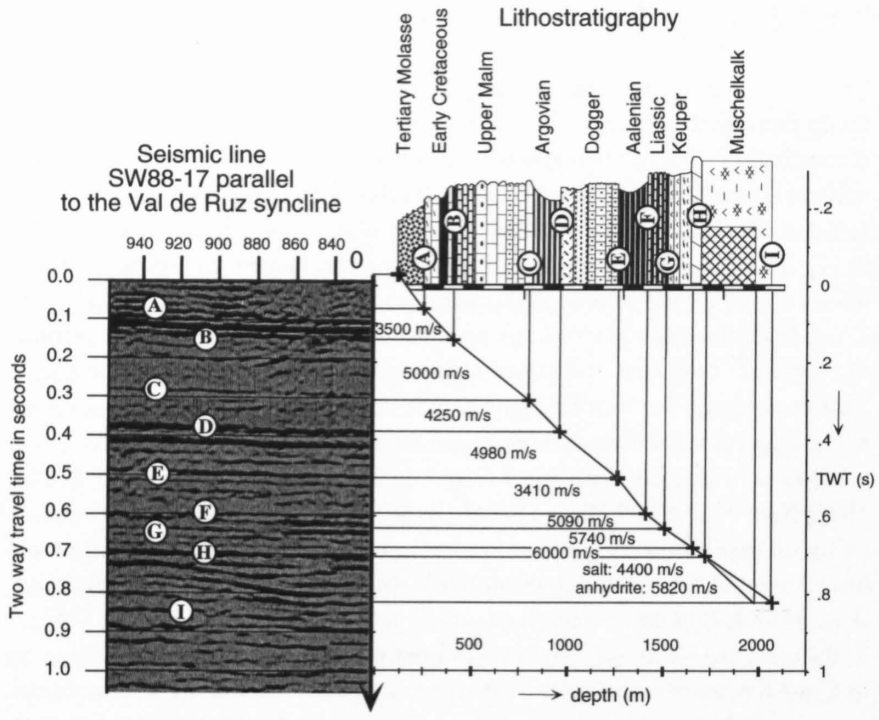

Figure 7.1-4
Tentative correlation of seismic reflectors in line SW88-17W (vertical scale in s TWT) with known and inferred stratigraphic thicknesses (horizontal scale in m). Seismic velocities are graphically represented in the depth-time diagram by the thick line: steep slopes correspond to low velocities, flat slopes indicate high velocities. Most velocities (with the exception of Malm) are calculated using depth/velocity relationships as determined by NAGRA for the same formations (Naef & Diebold 1990). For discussion see text.

limestones underlain by Keuper anhydrites and shales. The underlying strong, continuous reflector H most probably corresponds to the top of Muschelkalk dolomites. Below this formation, oblique reflectors, between 0.73 and 0.85 s TWT, constitute a prominent feature in the strike lines. They could represent duplexes within the major basal décollement horizon in comparison with the signature of the Keuper evaporites in seismic lines from the Courtion (Chenevart 1978) and the Champagnole (Bitterli 1972) areas (Figure 7.1-3). In order to estimate the poorly constrained thickness of the lower Muschelkalk evaporite formation (between reflectors H and I) the velocity of pure salt and anhydrite from Nagra data (Diebold et al. 1991) have been used. The calculated thickness is about 270 m for a salt-dominated and about 350 m for an anhydrite dominated lithology (Figure 7.1-4). These values seem to be high when compared with the Muschelkalk thickness observed in the Buez drill hole. However, the interval of about 0.12 to 0.20 seconds TWT in the seismic lines from the vicinity of Courtion (Figure 7.1-3) is comparable with that observed in the Val de Ruz area. The top basement (I ?) does not appear as a strong continuous reflector. The position of this top could well be somewhat lower (+0.1 s) than the position as indicated in Figure 7.1-4. This would again augment the total thickness of the lowermost Triassic thereby increasing the total thickness of the Mesozoic series to almost 2 km. Alternatively, reflectors below I, could represent Permo-Carboniferous; the deepest reflectors (below 1s) however, almost certainly are multiples (Figure 7.1-5).

Figure 7.1-3 presents a comparison of the seismic stratigraphy signature of the Neuchâtel Jura, Courtion, Champagnole and Treycovagnes areas. A very good correlation of all major reflectors exists with the seismic line published by Chenevart (1978) from an unspecified area of the Plateau Molasse some 20 km south of the study area. The summary identification of reflectors as given by Chenevart (1978) may have been tied with the Courtion drill hole. Seismic sections from the canton Vaud, in particular lines 79 SAdH 27, 78 SAdH 21 and an interpreted line 73 VD 7, all deposited at the Musée de Géologie at Lausanne, permit to follow individual reflectors from the Courtion area toward Essertines and Treycovagnes. Comparisons with Buez are not as direct. The Keuper interval in the Champagnole area for instance, as indicated by Bitterli (1972), seems to be rather thick – over 0.3 s corresponding to maybe as much as 700 m – a thickness which is in bad agreement with data from the nearby Buez drill hole. According to the two lines presented by Bitterli (1972, Figure 4), important lateral thickness variations seem to exist within the Keuper evaporite formation, an effect usually attributed to "salt tectonics". A similar effect of quite variable thicknesses within the lower Muschelkalk formation is also shown on the section published by Chenevart (1978) as well as on all sections from the Vaud (Essertines) area (e. g. Jordi 1990 & 1993).
Figures 7.1-5 and 7.1-6 show the stratigraphic interpretation of the lines parallel to the Val de Ruz "syncline". These line drawings highlight the good quality of the strike lines.

7.1.2.3 Structures

The dip line SW 88-14 (Figure 7.1-8 and Figure 7.1-14) permits to study the geometry of the subsurface structures below two major anticlines bordering the Val de Ruz. This line (Figure 7.1-1) runs sub-parallel to the Chaumont anticline in its southernmost part, crosses the Val de Ruz "syncline" (with lines SW 88-17 and SW 88-04 E), climbs to the Vue des Alpes to end shortly south of the town of La Chaux de Fonds where it crosses the strike parallel line SW 88-12 (Figure 7.1-7). In Figure 7.1-8, a compilation of dip measurements along a cross section parallel to the seismic line SW 88-14 (Figure 7.1-1) are combined with a line drawing of this seismic section. Below La Vue des Alpes, the quality of the seismic section is rather poor but knowledge of surface structures is excellent. This relation is reversed within the Val de Ruz syncline due to Quaternary cover but the quality of seismic sections is excellent. A good correlation between surface dips and apparent dips of reflectors at depth exists in the area north of La Vue des Alpes where surface dips extend over more than one km to the SSE below the major anticline visible at the surface. Below the Val de Ruz basin, seismic reflectors cover the entire stratigraphic succession already recognized on the longitudinal seismic lines. The apparent overall dip of 15° to the SSE, visible on the southern half of seismic section SW 88-14 is almost certainly too high, however. On account of a strongly increasing thicknesses of Tertiary and Quaternary sediments from NNW to SSE within the Val de Ruz (Mornod 1970; Schnegg pers. comm. 1992), reflectors are "pulled down" in the southern part of the Val de Ruz. Converting this section from time to depth shows that the overall true dip within the Mesozoic is about 4° to 6° to the SSE (Figure 7.1-9).

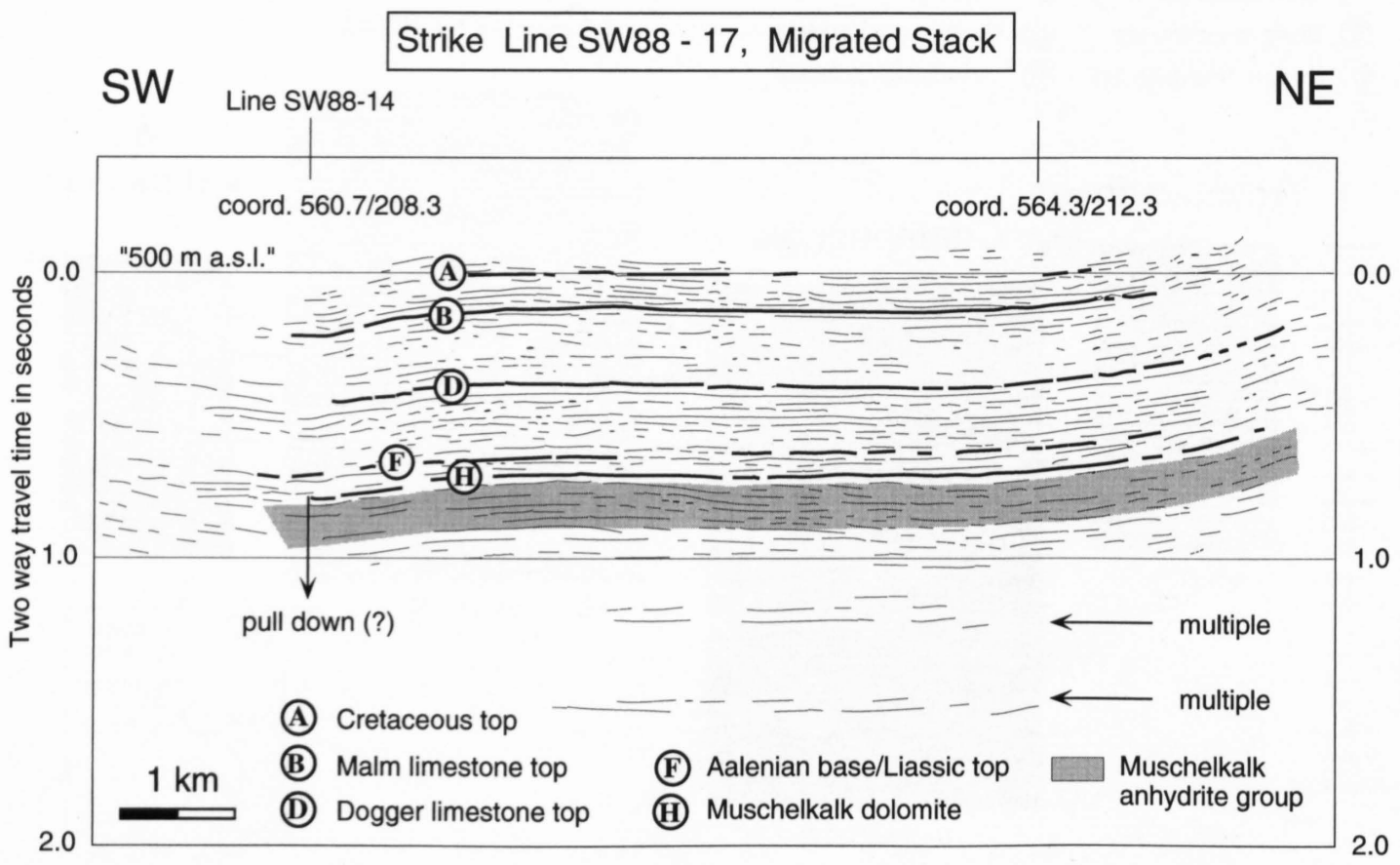

Figure 7.1-5
Line drawing of strike line SW88-17 in the southern Val de Ruz and identification of major reflectors (compare with Figures 7.1-3 and 7.1-4). Datum line 0s corresponds to an altitude of 500 m above sea level (a.s.l.).

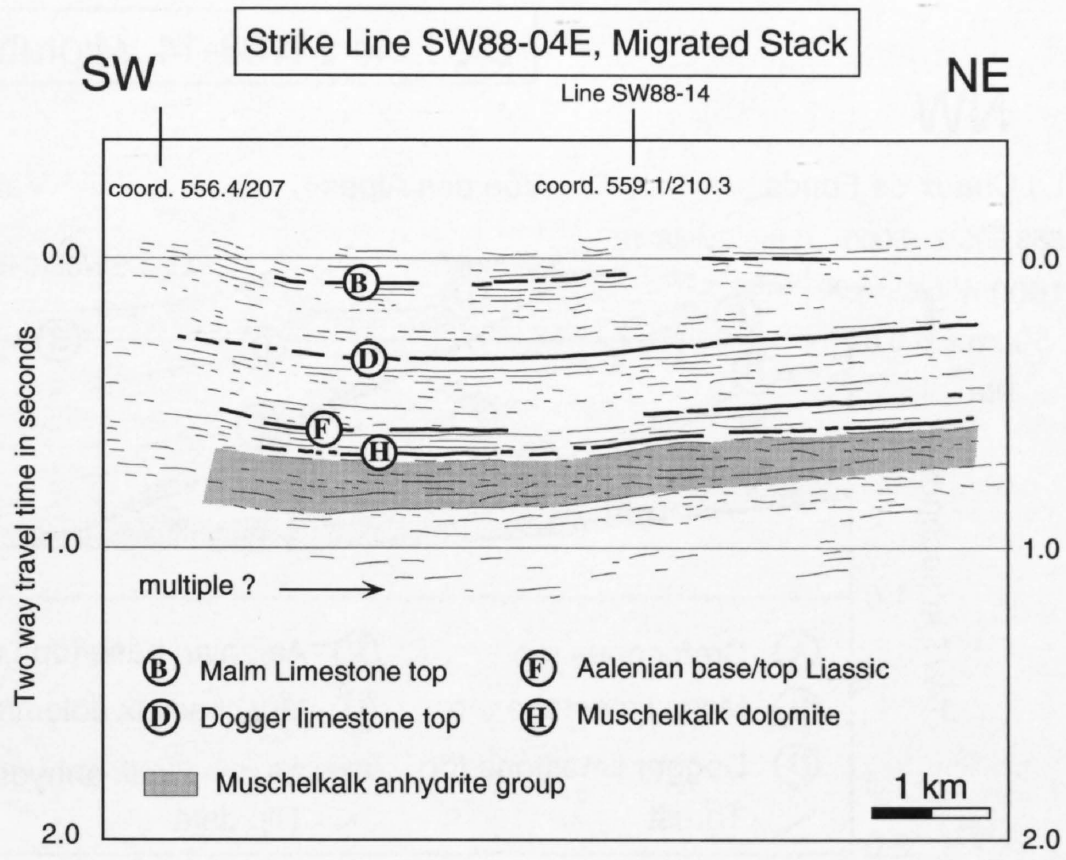

Figure 7.1-6
Line drawing of strike line SW88-04E in the northern Val de Ruz and identification of major seismic reflectors – compare with Figures 7.1-4 and 7.1-5. Datum plane: O s = 500m a.s.l.

Line SW 88-12 (Figure 7.1-7 and 7.1-13) runs almost parallel to and on top of a minor anticline north of la Vue des Alpes (compare Figure 7.1-1 and 7.1-9). This section lies within the "combe Argovienne" or right on the top of Dogger limestones. Accordingly the topmost major reflectors seen in the western part of this section most probably correspond to Triassic Muschelkalk, thrust here to an altitude of around 500 m a.s.l. Below, a coherent package of reflectors could be identified as Malm to Triassic. Laterally (eastward) most reflectors are lost within a disturbed (noisy) area but extrapolations allow to confirm the identification of reflector D at ca. 0.1 s and H (Triassic) at ca. 0.5 s in agreement with the strike perpendicular line SW 88-14. Most important, however, quite well defined but unidentified reflectors (H?) are present both to the right and to the left of the intersection with line SW 88-14. This makes it plausible that the base Mesozoic at this intersection lies at ca. 0.8 to 0.9 s, almost as deep as below the Val de Ruz. Accordingly there would be only a very week overall slope of this base Mesozoic/top basement between the northern Val de Ruz and La Chaux de Fonds.

From the south-east to the north-west, the geological section presented in Figure 7.1-9 crosses two major anticlines. The first anticline (Chaumont) is interpreted as a complicated fault propagation fold with a later "high-angle breakthrough" of the thrust to the surface (Suppe & Medwedeff 1990, Figure 11e). Unfortunately, seismic line SW 88-14 does not cross the entire structure. Comparison of surface geology with reflectors at depth, however, show clearly that the northern steeper limb of the Chaumont anticline cannot be directly connected with the underlying, subhorizontal Malm limestones (compare Suter & Lüthi 1969). A NNW vergent thrust has thus to be present. Such a structure has to be postulated for balancing reasons (Laubscher 1965) and has been identified by a magnetotelluric survey (Schnegg et al. 1983). The precise geometry within this anticline, however, in particular the southern footwall branch point in the competent Malm limestone and the presence or absence of a syncline in the footwall and/or duplexes are not constrained by the available seismic data.

The second major anticline near la Vue des Alpes is a more complex structure. Our interpretation of the seismic lines suggests the presence of a rather smooth thrust, separating a relatively uniform dip domain with gently SSE dipping layers in the footwall, and a more strongly folded and/or faulted hangingwall. A very good correlation between SSE-vergent kink folds at the surface ("genoux à regard suisse") and SSE vergent (blind?) thrustfaults at depth is observed. The southernmost of these backthrusts seems to be located above the area where the NNW thrust branches off from the major basal décollement. Other backthrusts are unrelated with bends in the main thrust. Two more major NNW vergent thrusts have been postulated based on surface geology in combination with interpretations of seismic lines.

The cross section shown in Figure 7.1-9 is crossed by the Ferrière fault which adds to the complexity of the broken up anticline near la Vue des Alpes (compare Figure 7.1-1). This fault zone is indicated on Figure 7.1-9 in its vertically projected position. If it was purely a late feature, its overall apparent sinistral offset of ca. 500 m could be compensated by a stretching of the section by a similar amount. On seismic line SW 88-14, however, reflectors on either side of the supposed fault trace at depth could be correlated without major offset suggesting that the Ferriere fault could be a superficial tear fault.

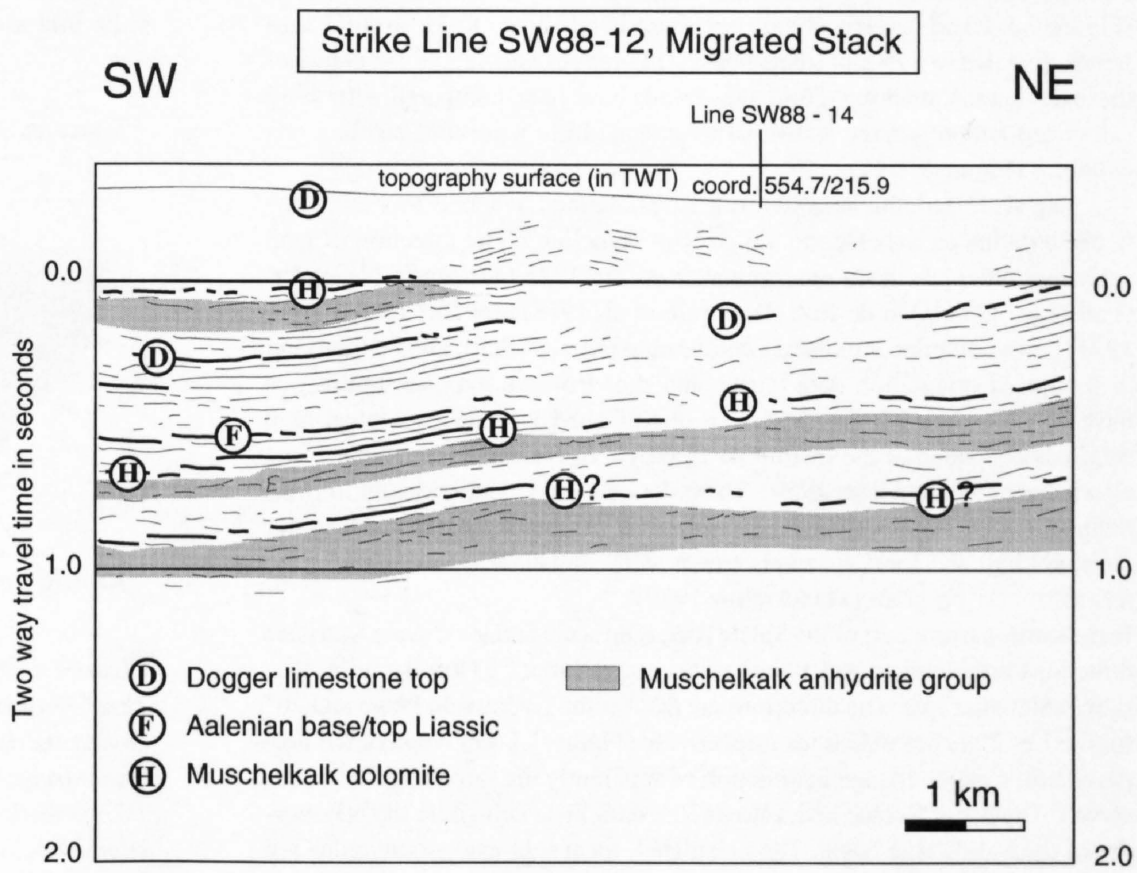

Figure 7.1-7
Line drawing of strike line SW88-12 (north of La Vue des Alpes), running on top of an anticline within the "combe argovienne" i.e. practically on top of Dogger limestones. Topography (1110 m to 1210 m a.s.l.) is indicated in TWT (s), 0.0 s datum corresponds to 500 m a.s.l. Note the twofold repetition of Triassic (H) and Dogger (D).

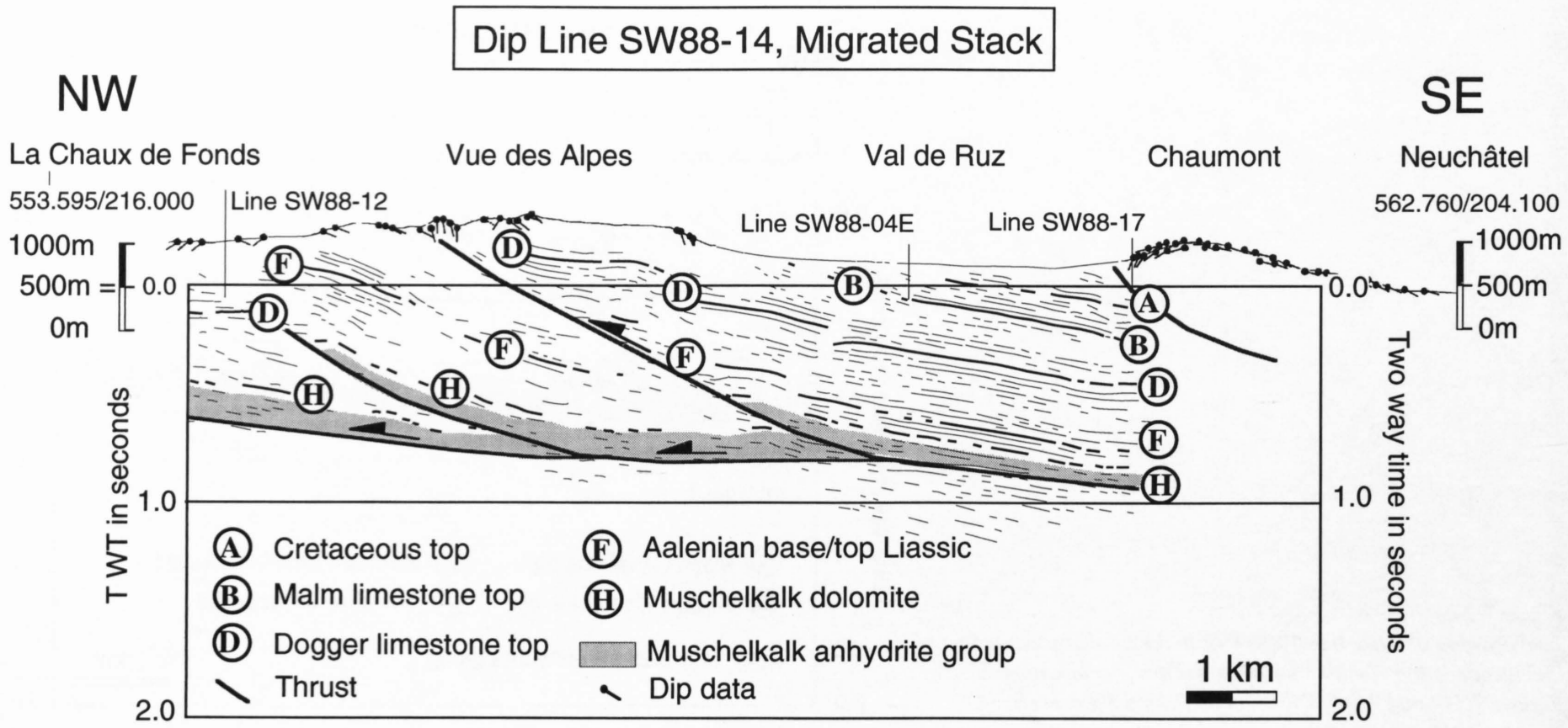

Figure 7.1-8
Line drawing of dip line SW88-14 with additional information about bedding plane dips as measured at the surface along this profile. The 0.0s datum line corresponds to an altitude of 500m a.s.l. Topography is drawn on a metric scale whereas reflectors are in TWT. Intersections with strike lines are indicated with thin vertical lines labelled SW88-17, compare with Figures 7.1-4, 7.1-5, 7.1-6.

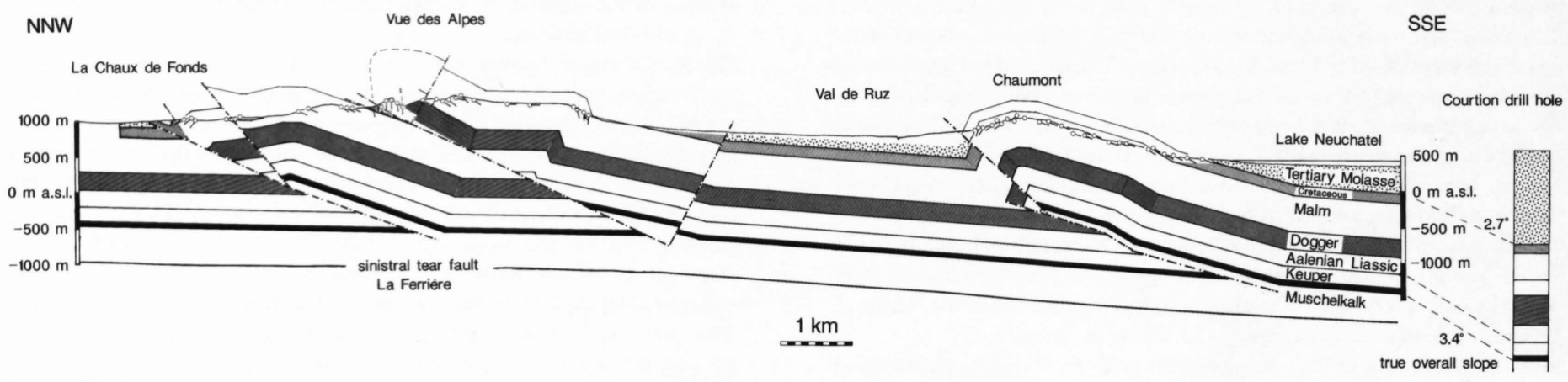

Figure 7.1-9
Geological cross-section based on surface data, completed at depth with information from seismic line SW88 – 14. This section is approximately line length balanced. The La Ferrière tear fault is located on the cross-section. The extension of this fault at depth is unknown. In constructing/balancing, this fault has been ignored. The statigraphy of the Val de Ruz area is correlated with the Courtion drill hole located 18km toward SSE from the town of Neuchatel.

7.1.3 Structural geology at regional scale

At the map scale, anticlines and synclines are the most obvious expressions of a generally NW–SE shortening of the sedimentary cover. The Val de Ruz basin is bordered by four anticlines oriented WSW–ENE and SSW–NNE (Figure 7.1-1 and 7.1-10). Relatively sharp bends of up to 35° in fold axes trends give rise to a rhomb shaped basin. In order to understand the nature of these deviations, map scale fold axes trends have been compared with those calculated (stereographic statistical treatment) from measured bedding orientations (Figure 7.1-11).
The map scale anticline axis trends are well defined, whereas it is more difficult to define an axis for the Val de Ruz "syncline". The direction of map scale anticlines has been determined from the 1:25'000 sheets Neuchâtel (Frei et al. 1974), Val de Ruz (Bourquin et al. 1968) and Biel (Schär et al. 1971) and a compiled structural contour map (Kiraly 1969). Over a thousand of measured orientation data (strike and dip) from all exposed lithologies have been compiled from a series of unpublished 1:5'000 geological map originals deposited at the Institut de Géologie of Neuchâtel University (see also Schaer 1956 and Baer 1959). These data, processed individually for well defined anticline sectors, have been reported on stereograms in order to determine "best fit" local fold axis trends with statistical methods using the STEREOPLOT program (Mancktelow 1989)
In the north-eastern part of the Val de Ruz, map scale and local scale fold axes directions are identical and rather constant over about 13 km from the Ferrière fault to the east. The directions are 60° for the La Joux du Plane and 70° for the Les Planches anticlines respectively (Figure 7.1-11). West of the Ferrière fault, a major change in direction of apparently the same anticline is observed. The Mont Racine and Tête de Ran anticlines constitute the NW border of the Val de Ruz basin. The calculated, local fold axes orientations are 212° for Mont Racine, 223° for Tête de Ran and 233° for an area inbetween the two faults Tête de Ran and Ferrière. Calculated (local) fold axial plunges to the SW are very gentle: 8, 2 and 0° respectively
To the south and south-east, the Val de Ruz basin is bordered by the Serroue-Chaumont anticline. This anticline forms a pronounced "dog leg" with map scale fold axes varying from 240° in its western to 205° in its eastern part.

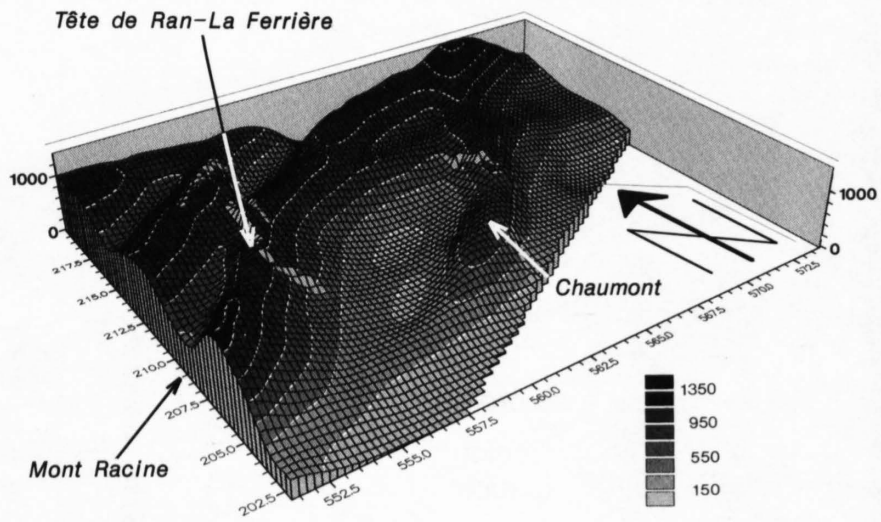

Figure 7.1-10
Three-dimensional view representing the base of Malm limestone (top of Argovian marls respectively) in the Val de Ruz area according to Tschanz & Sommaruga (1993), based on data from a structural contour map (Kiraly 1969). Vertical axes is in meters above sea level and horizontal axes are in kilometers (Swiss coordinate grid).

Stereographically determined, local fold axes indicate a relatively constant direction of 242° at both extremities with axial plunges from 5° to 13° to the SSW and WSW respectively.

For Mont d'Amin, La Joux du Plane, Les Planches and Chaumont-Serroue (sector W) anticlines oriented N70°, the bedding plane poles plotted on a stereogram are located on a great circle and define the same fold axis direction as the one of the map scale fold axes. On the other hand, the bedding plane poles plotted on a of Tête de Ran – La Ferrière, Mont-Racine and Chaumont (sector E) anticlines oriented N35° show much larger scatter around a calculated "best fit" great circle. In addition to the larger scatter, the calculated orientations (from the outcrop scale bedding plane orientations) are systematically different by 10° to 30° from the map scale direction. Map scale anticlinal axes are invariably offset in an anti-clockwise direction with respect to the locally determined fold axes.

In summary, map scale bends in major anticlines bordering the Val de Ruz, of about 20° to 35°, are not as pronounced in the orientation of layers measurable at the outcrop scale. SSW–NNE oriented parts of these anticlines show important discrepancies of 10° to 30° between local and map scale fold axes directions. The latter are invariably offset in an anticlockwise sense with respect to the former.

These structural observations are interpreted in terms of ramp geometry of major (hidden) thrust surfaces below these anticlines and overall transport direction (Figure 7.1-12). It appears that the WSW–ENE oriented anticlines are relatively cylindrical, "well behaved". We interpret these as being formed above frontal ramps and infer an overall transport direction to the

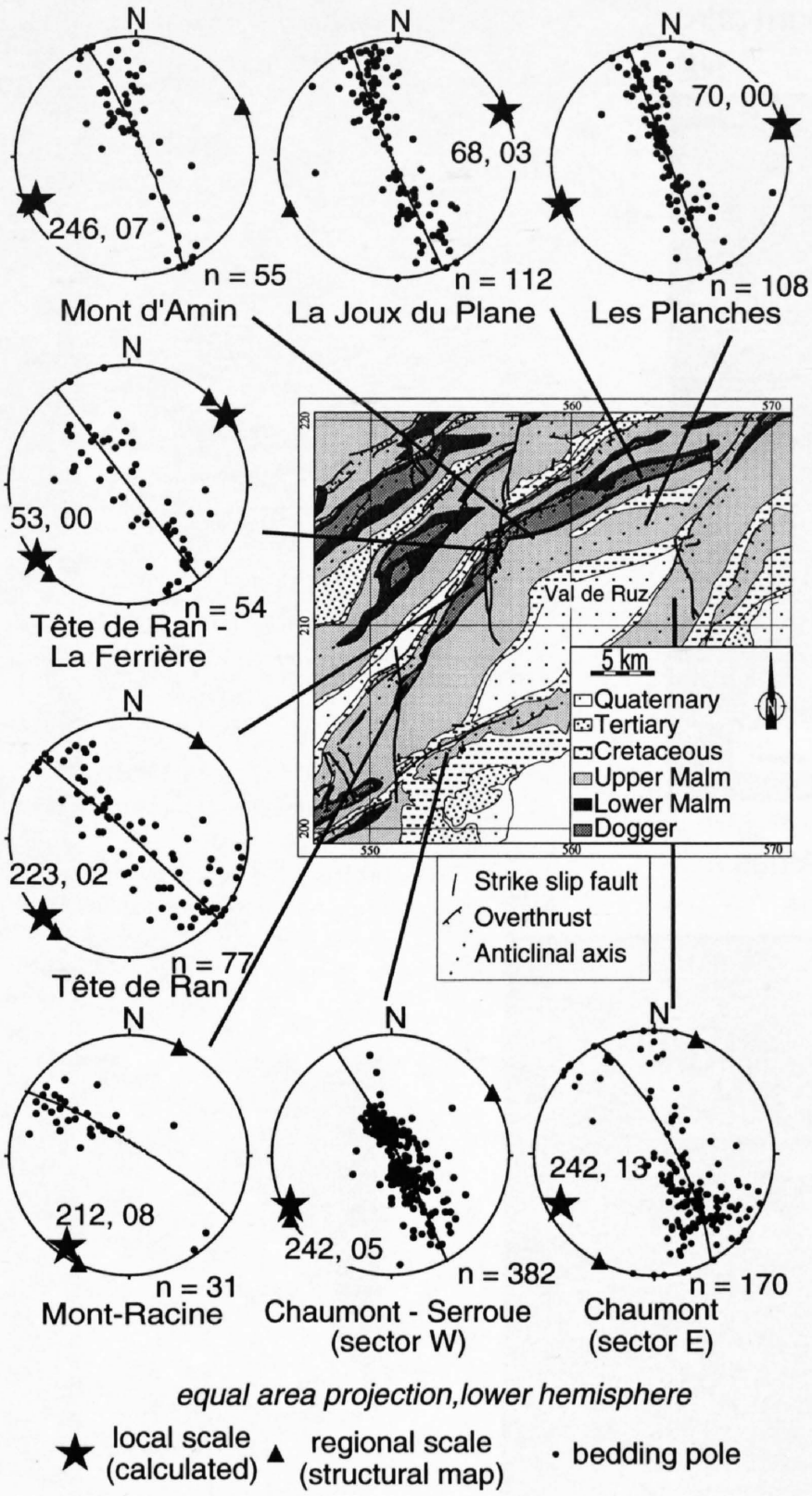

Figure 7.1-11
Local and regional scale fold axes trends are compared for different major anticlines bordering the Val de Ruz. Local scale fold axes trends are determined using to pole to "best fit great circle" as calculated with STEREOPLOT *program (Mancktelow 1989). Map scale fold axes trends are determined from the structural contour map and geologic maps.*

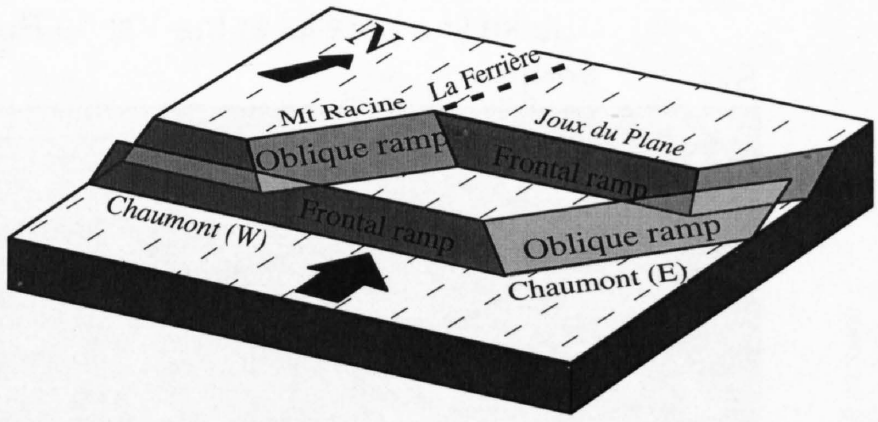

Figure 7.1-12
Simplified 3-D ramp geometry at depth in the Val de Ruz area (compare with the Figure 7.1-1, 7.1-9, and 7.1-10). The overall transport direction to the NNW is indicated by the big black arrow and dashed lines. The white floor corresponds to a major basal detachment within the lower Muschelkalk anhydrite group.

NNW. SSW–NNE oriented anticlines, on the other hand, in particular the NE part of Chaumont, are interpreted as non-cylindrical, "wrench fold" type anticlines which formed in an orientation oblique to the overall transport direction. The location of these anticlines is thought to be predetermined by the oblique orientation of ramps, probably due to preexisting faultzones in this general direction. Candidates for this structural trend, observed in many parts of the central and eastern Jura, are so called rhenish (Oligocene) faults (Aubert 1959; Lloyd 1964; Laubscher 1972, 1985; Illies 1981; Bergerat 1987).

As a consequence of this interpretation, if follows that cross sections which are to be balanced, should be drawn in a general NNW–SSE direction. The seismic line SW 88-14 (Figure 7.1-8) nearly fulfills this condition.

7.1.4 Summary and conclusions

35 km of industry seismic lines from the Neuchâtel Jura have contributed to greatly increase the knowledge about the regional geology. For the first time in this part of the central Jura, the thickness of the entire Mesozoic could be established using the excellent quality strike parallel lines from the Val de Ruz. Identification of reflectors relies on comparisons with the well known local stratigraphy for formations younger than Liassic and drill hole data from Courtion, Essertines and Buez. Since logs combined with seismic lines are available only from Essertines with quite a different stratigraphy, no direct ties with any drill hole could be established. Thus some ambiguities remain with the identification of the deeper reflectors. The total thickness between top Cretaceous and base Triassic appears to be 1800 ± 200 m (depending on interpretations of the lowermost reflections and on the assumed seismic velocities). Below the Val de Ruz syncline, the Keuper formation is estimated at ca. 180 m, above a strong, laterally continuous reflector interpreted as dolomitic Muschelkalk. Two thick Triassic evaporite series over- and underly a major marker-horizon, interpreted as Muschelkalk dolomites. Folds formed above major, NNW vergent thrusts with more than kilometric throw. North of La Vue des Alpes, such thrusts appear clearly on the strike perpendicular seismic line. Important thrusting is further evidenced by a doubling of the entire Mesozoic series (Triassic to middle Malm) as seen on a strike parallel seismic section a few km west of La Vue des Alpes. The depth converted "base Mesozoic" is relatively smooth and has an overall slope of ca 4° toward the SSE in the southern part and is flat lying in the North. Anticlines formed above NNW verging thrusts of at least kilometric throw. The importance of these thrusts has been largely underestimated in previous cross sections. Folds are interpreted as fault-propagation folds (FPF) with steep, broken-through frontal limbs. Since Muschelkalk dolomites are involved in thrusting, a major décollement must be present within the lower Muschelkalk evaporites.

Relatively sharp bends of up to 35° of the regional, map scale fold axes trends control the geometry of the rhomb shaped Val de Ruz basin. A compilation of thousands of strike/dip measurements around the Val de Ruz basin permit to distinguish frontal, cylindrical from acylindrical portions of major anticlines. WSW–ENE trending anticlines formed as cylindrical "frontal" folds, whereas NNE–SSW trending anticlines are interpreted as wrench folds, formed above oblique ramps. The origin of the latter could be related with preexisting fracture zones (Oligocene rhenish trend) of approximately N-S orientation. Such faults are present as map scale, sinistral tear faults e. g. in the Vue des Alpes area. This La Ferrière fault-system, however, appears to be unimportant on a strike perpendicular line which leads us to the interpretation as a tear-fault rather than a deep-reaching strike slip fault.

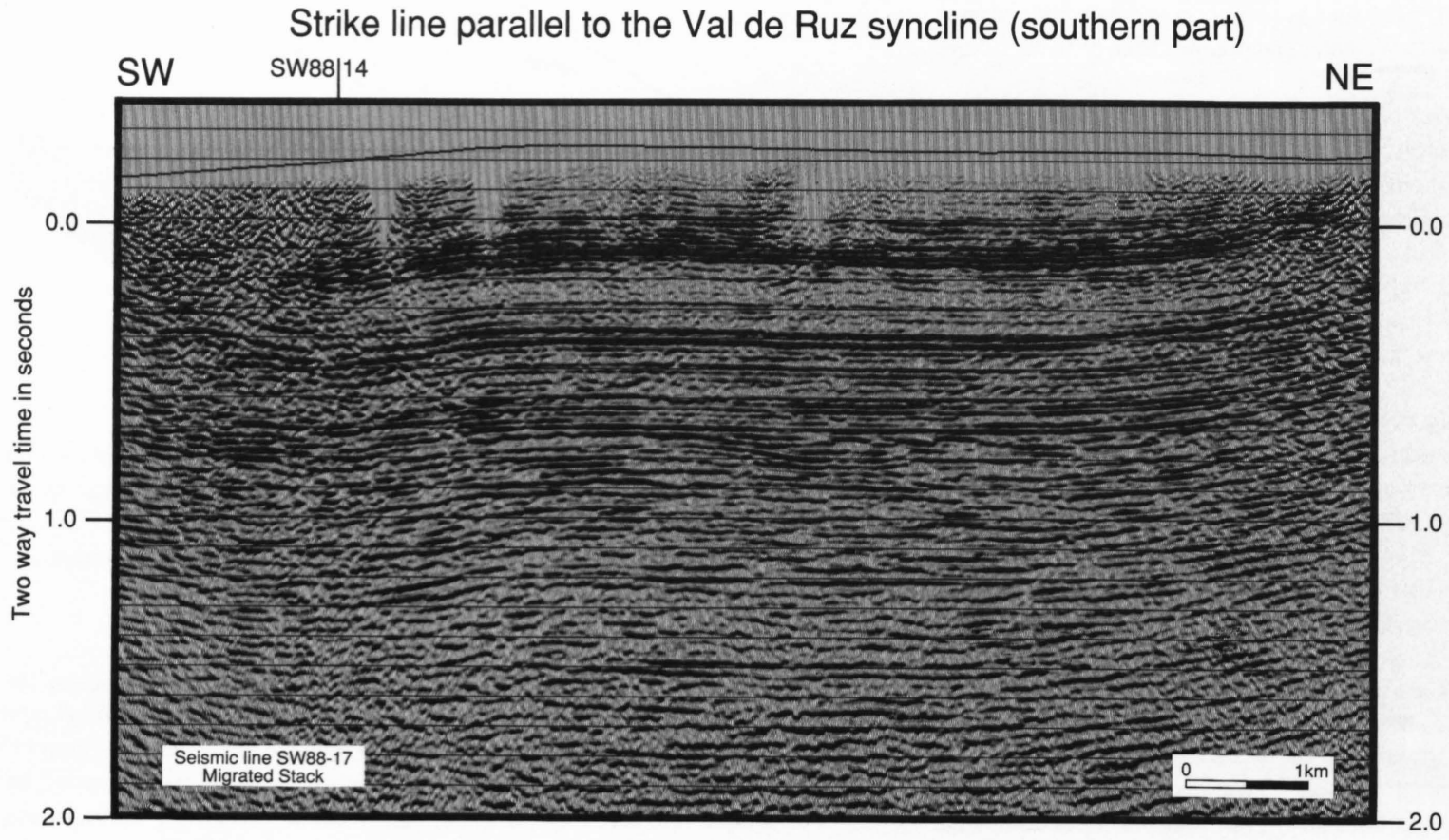

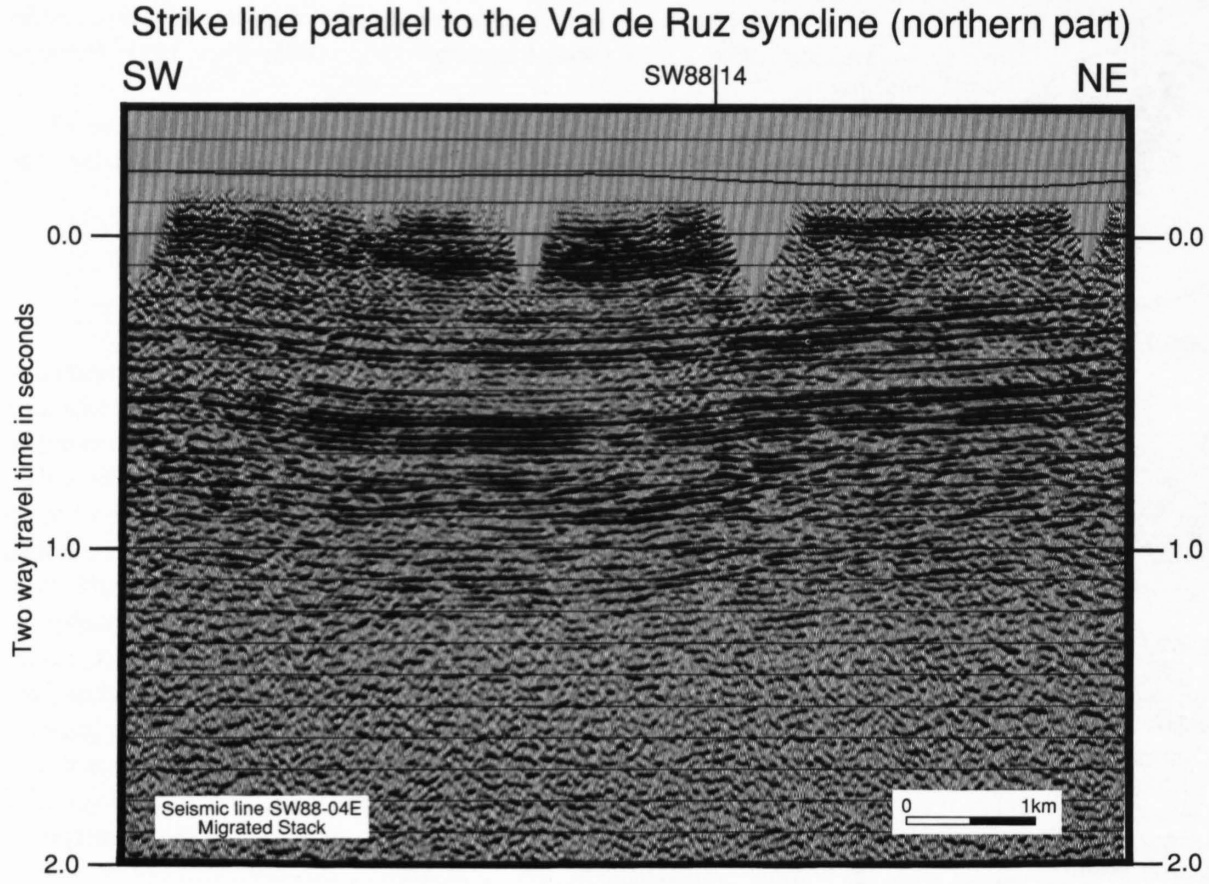

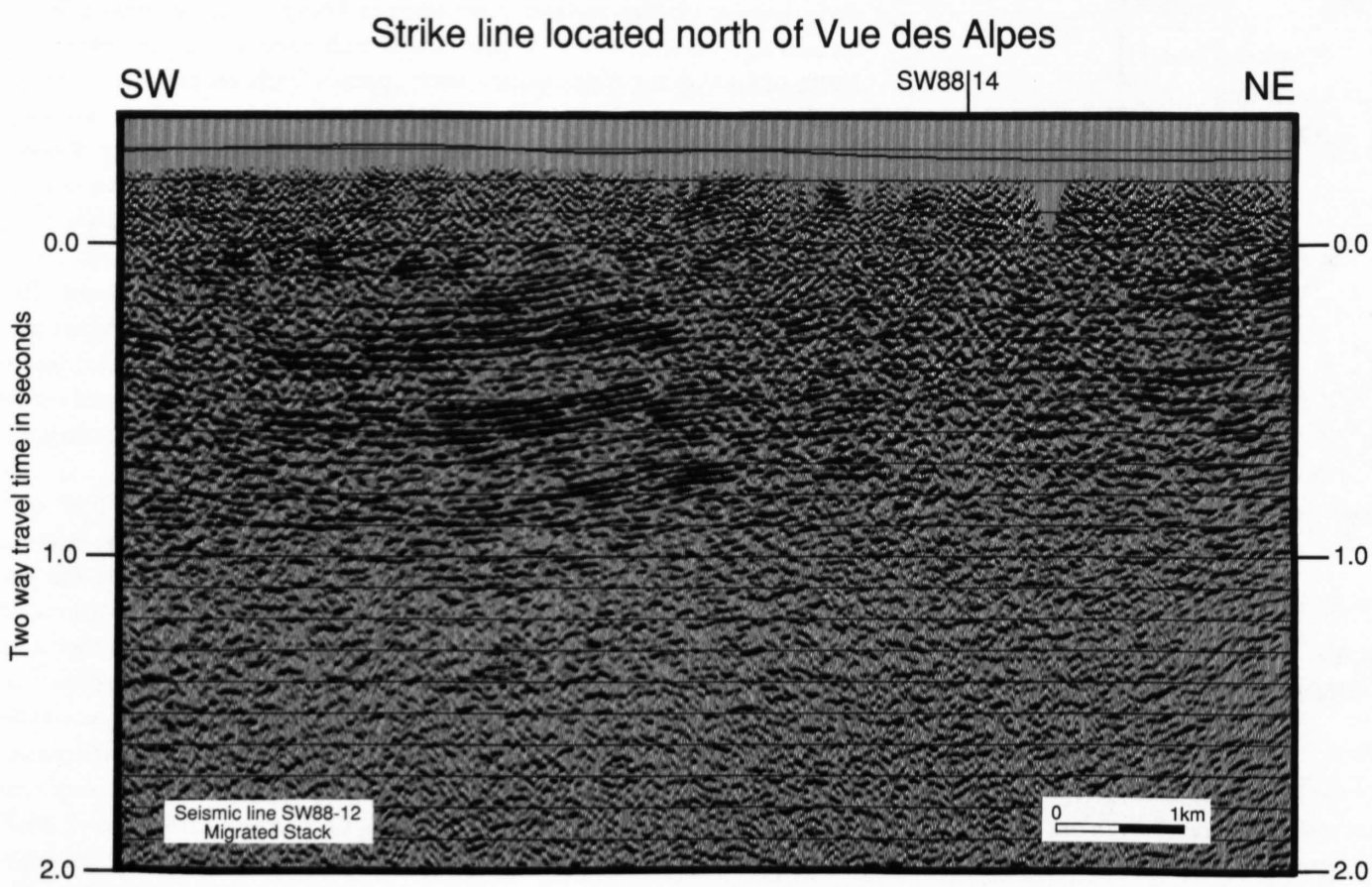

Figure 7.1-13
Migrated seismic strike lines SW 88-17, SW 88-04E, and SW 88-12. For location see Figure 7.1-1.

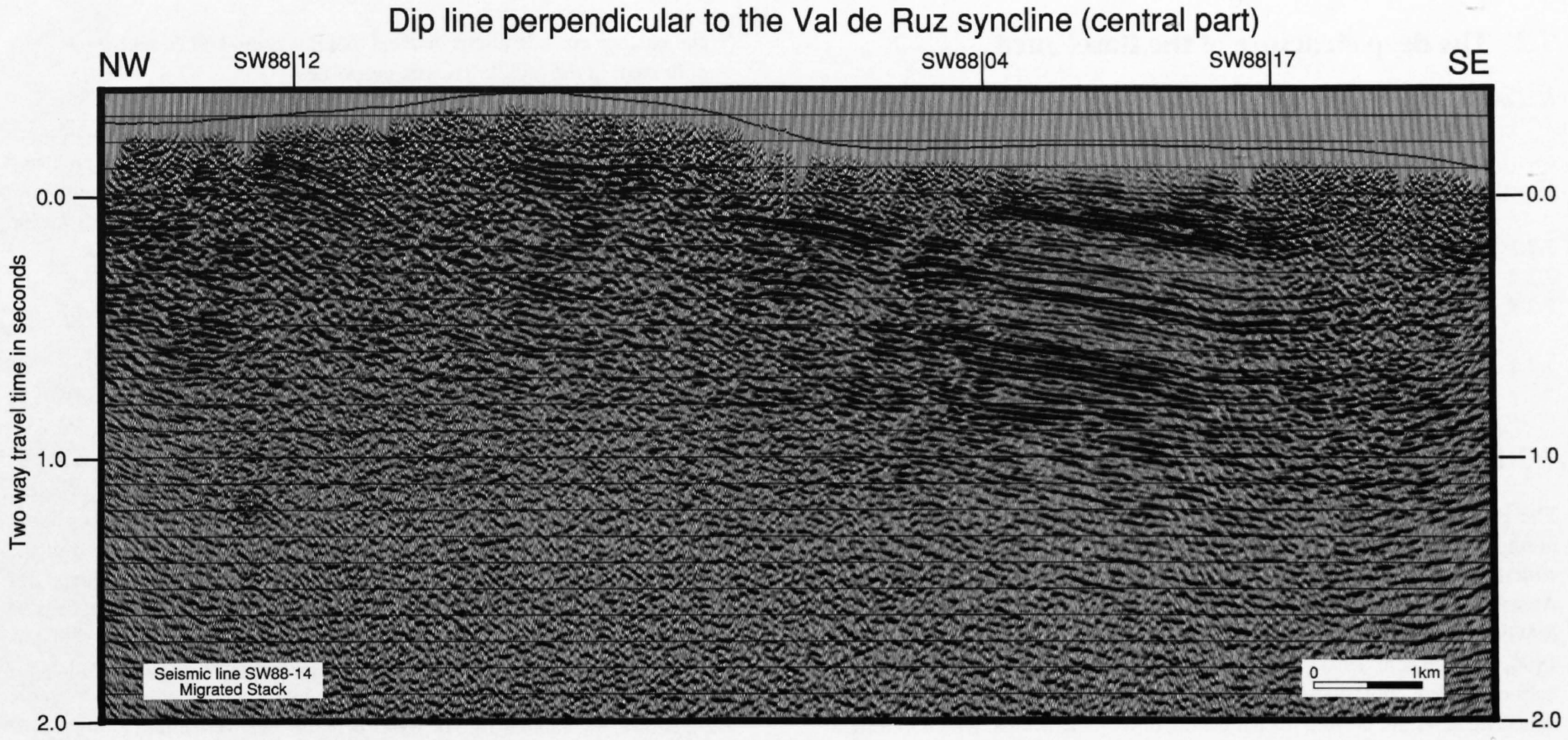

Figure 7.1-14
Migrated seismic dip line SW88-14. For location see Figure 7.1-1

Acknowledgements

This work has been possible only thanks to **BP** (British Petroleum England) and **FMN** (Force Motrice Neuchâteloise) who made some of their seismic lines available for reasearch and who kindly permit their publication. We owe special thanks to J. ROSSAT, P. LEHNER and V. MCCUTCHEON for arranging this agreement. This study has greatly benefited from the help by and many discussions with A.W. BALLY, C. CRAMEZ, G. GORIN, L. KIRALY, B. KÜBLER, P. LEHNER, J. MEIA, J. MOSAR, R. OLIVIER, F. PERSOZ, O. A. PFIFFNER, J. P. SCHAER. A. BAUD, Director of the Geological Museum of Lausanne, kindly provided access to the seismic sections of canton Vaud. The authors thank particulary H. A. JORDI and R.W. SCHOOP for the review and the fruitful discussions. This paper represents part of A. SOMMARUGA's PhD thesis. Support by the University of Neuchâtel and the SWISS NATIONAL SCIENCE FOUNDATION is gratefully acknowledged (grants No. 4020-031533, 81 NE-33478 and 21-37'366.93).

7.2 The deep structure of the Basel Jura

H. Laubscher & Th. Noack

Contents

7.2.1 Introduction

The Basel region straddles the southern end of the Rhine graben and the northeastern part of the folded Jura (Figure 7.2-1). Information on its deep structure has recently been provided by the seismic profile Jura-1 (see Ansorge et al., this volume). In addition, the results of the exploration of NAGRA farther east (Sprecher & Müller 1986, Laubscher 1986, Diebold 1990, Diebold et al. 1991) may be extrapolated into the Basel region with the help of surface geology which offers a wealth of tectonic and stratigraphic data. The latter are needed for the timing of tectonic events, which in turn is essential for the interpretation of the seismic data. For that reason a series of projects flanking the main efforts of NFP 20 were carried out at the University of Basel, partly under the guidance of P. Diebold, particularly by Noack (1989); Bitterli (Diebold et al. 1991); Meyer (1990); and Gonzalez (1989); and Laubscher (unpublished maps) spent a number of summers mapping in the region. All of this information has been used for this paper.
Deep crustal data were also obtained by Finck et al. (1984) from the originally shallow reflection line NAGRA 82-NS-70 (Sprecher & Müller 1986, Laubscher 1986, Diebold et al. 1991). Although the line does not intersect Jura-1 (see Figures 7.2-1, 7.2-2), it seemed worthwhile to redraw it to the scale of Jura-1 in Figure 7.2-6 and attempt some correlations (Figure 7.2-7). For comparison with the ECORS deep reflection survey in the southwestern Jura, see Bergerat et al. (1990), Guellec et al. (1990), Mugnier et al. (1990), Roure et al. (1994).
No attempt is made in this article to address the wider regional problems of Jura tectonics. For one of the more recent elaborations of this aspect see Laubscher (1992).

7.2.2 The tectonic situation as gathered from surface information

Figure 7.2-2 shows the location of seismic line Jura-1 within its geographical and tectonic framework; the western end of NAGRA 82-NS-70 appears at the eastern margin of the figure. Also shown is the location of 5 profiles (Figure 7.2-3), based on surface geology and tunnel data, that flank the seismic profile and serve as illustrations for what surface geology has to offer for the assessment of deep crustal structure.
The tectonic situation in Figure 7.2-2 is characterized by the following main units (for more detailed information see Laubscher 1986, 1987, 1992; Diebold 1990; Diebold et al. 1991) :

1 the Black Forest, entering the picture at the Eggberg fault in the northeastern corner;

2 the Dinkelberg and Buus plateaus. They represent an eastward embayment of the southern end of the Rhine graben, characterized by tabular outcrops of Triassic separated from the crystalline rocks of the Black Forest by the large Kandern and Wehratal faults;

3 the Tabular Jura of Basel, consisting mainly of Jurassic sediments that are dissected by numerous normal faults. Transgressively and discordantly overlying the peneplained fault blocks are remainders of Upper Marine Molasse (OMM) of probably late Burdigalian age and more extensive masses of middle Miocene fluviatile to lacustrine rocks (about 15 to 11 MA: Naef et al. 1985; Kälin 1993). They date the fault mosaic as essentially Paleogene, coeval with the Rhine graben system. Some elements – faults and flexures-connect with the hinge line of the early Miocene Molasse basin as dated farther east (Von Braun 1953; Naef et al. 1985).

4 the folded Jura with its frontal imbrications and main frontal thrust, overriding the Miocene sediments and therefore younger than 11 MA. Material balance considerations demand that it is thin-skinned with a basal décollement in the middle Triassic evaporites.

Important additional information is contained in the cross-sections Figure 7.2-3. The faults of the **Tabular Jura** have effected very little overall displacement except for the Zeiningen fault, which is the southern continuation of the Wehratal fault. Figures 7.2-2 and 7.2-4 show that the fault distribution is not uniform but may be roughly subdivided into 3 domains:
- an eastern domain that is virtually free of faults (Profile 1);
- a central domain, where a series of rather narrow grabens separated by unbroken tableland appear (Profile 2);
- a western, intensely faulted domain (Profile 3).

The grabens of domains 2 and 3 are often composed of severely tilted blocks that imply a listric fault geometry. The bounding faults of the grabens seem to converge at a comparatively shallow depth, and this, together with the lack of important overall displacements, suggest a décollement of some kind at that depth. The sum total of these characteristics suggests sliding of the detached slab westward into the Rhine graben with break-up of the sliding masses. The main problem is the identification of the décollement horizon. It seems to be located several hundred meters below the Triassic, and as it is difficult to assume an intracrystalline décollement interval at this shallow depth (where brittle behavior is expected because of low temperature), the presence of Paleozoic sediments may be conjectured. As Figure 7.2-2 shows, the Tabular Jura of Basel is in the westward continuation of the main Permo-Carboniferous trough of Northern Switzerland (or Constance-Frick; compare Sprecher & Müller 1986; Laubscher 1986, 1987; Diebold et al. 1991), although so far this conjecture is unsupported by wells or seismic data.

The geometry of the **Folded Jura**, although thin-skinned, exhibits tale-telling irregularities obviously due to irregularities at the décollement level. These suggest further complications in the basement (Profiles 4 and 5). Unfortunately, the localization and definition of these irregularities demands time-consuming construction of balanced cross-sections and kinematic inversion or backstripping (compare Bitterli 1992). It appears that the position of the main frontal thrust is due to a basement flexure comparable to that un-

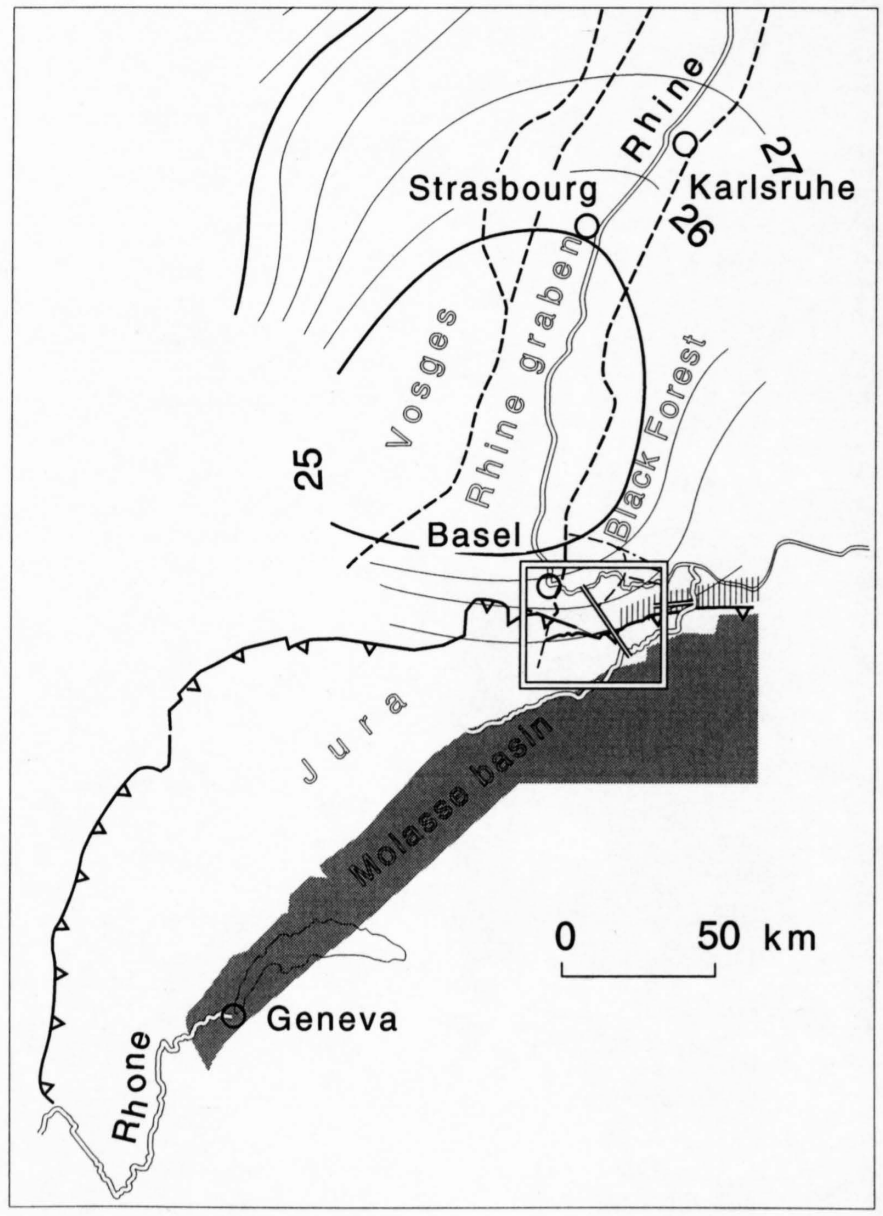

Figure 7.2-1
Location map of the Basel region, showing the main tectonic elements and the outlines of Figure 7.2-4 (quadrangle) with the deep reflection profile Jura-1 (double line). Vertically ruled: Late Paleozoic trough. Contours are depth of Moho (from Müller & Lowrie 1980).

earthed farther east by Nagra exploration (e. g. Laubscher 1987). This eastern basement flexure not only nucleated the main Jura thrusts, it also turns out to be the southern margin of the Permo-Carboniferous trough reactivated (though weakly) in the Tertiary. These findings due to the seismic prospection of NAGRA (Sprecher & Müller 1986) are projected into Profiles 4 and 5. The northern border of the trough has been placed where there is a slight hinge or break in gradient, similar to that found at the weakly pronounced Mandach flexure at the northern margin of the Permo-Carboniferous Constance-Frick trough (Figure 7.2-2, 7.2-5; Laubscher 1986; Bitterli & Matousek 1991).

To complicate matters, unfortunately, the boundary flexures of this conjectured late Paleozoic trough change direction somewhat and split up at interfering lineaments (Figures 7.2-2, 7.2-5); it seems probable that the trough disintegrates into a series of branch troughs (Figure 7.2-3, Profiles 2, 4, 5). These complications, however, may only be surmised on the basis of surface information, and their true dimension may well exceed that shown in Figure 7.2-3. For the southern boundary, e. g. the staggered appearance of the frontal Jura thrusts (Figure 7.2-4) possibly indicates junction with subsidiary troughs such as those indicated farther south by seismic information (Figure 7.2-4; Laubscher 1986).

At Eptingen (E in Figure 7.2-2) the Jura front swings around from a generally northeastern trend in the east to the WNW, thus forming what is usually referred to as the "Eptingen embayment". Adhering to the assumption that in this region too the Jura front is nucleated at a system of north-dipping flexures – an assumption so far borne out by the few balanced sections across the front –, and that these flexures are the expression of Tertiary reactivation of Paleozoic troughs, an important WNW-striking element in deep basement tectonics here enters the picture. It heads towards the Landskron flexure that terminates the Rhine graben proper in the south (Figures 7.2-4 and 7.2-5). The WNW-direction plays an important role in the tectonics of the Constance-Frick trough, as well as in its northern foreland: both the Eggberg fault (Figure 7.2-2) and the Vorwald fault identified in the southern Black Forest are found to deeply influence the structure of the Constance-Frick trough in impressive ways (Laubscher 1986; Diebold 1990; Diebold et al. 1991).

The **Dinkelberg** and **Buus plateaus** (Figure 7.2-2) are dominated by the essentially flat-lying limestone layer of the middle Triassic Muschelkalk. This layer is interrupted by occasional narrow grabens filled with upper Triassic and Lias. These grabens are much narrower than those of the Tabular Jura proper and seem to converge in the Middle Triassic evaporites underlying the limestones. As the plateaus flanking the grabens are hardly displaced at all (Figure 7.2-3, Profile 2), the conjecture again is hard to avoid that there is a décollement under the plateaus – in this case a very shallow one in the middle Triassic evaporites (compare Laubscher 1982). The frontal shortening of the strata gliding on the Triassic evaporites is possibly represented by parts of the flexures bordering the plateaus in the W (the Rheingraben flexure at the western border of the Dinkelberg plateau, the Zeiningen flexure (Figure 7.2-3, Profile 2) delimiting the Buus plateau). If the plateaus had been able to slide in the indicated directions, even by minimal amounts, there must have been a possibly very slight paleoslope in that direction, now not present any more or even inverted (Laubscher 1982).

A rollover of the Dinkelberg plateau at the Wehratal fault suggests a listric geometry of that fault flattening out at a depth of several kilometers in the crystalline crust, suggesting décollement at that level. No weak sediments can be imagined at that level, and its incompetence may be the result of thermal influence, such as high pore pressure, e. g. due to dewatering reactions, or high ductility of such minerals as quartz. In a rather vague way the level may be referred to as "tectonically defined brittle-ductile transition".

Thus, in the domain of the southeastern flank of the Rhine graben, décollement-bounded extension penetrating to various levels of the crust played a role:

- the Dinkelberg and Buus plateaus with very narrow grabens suggesting décollement in the middle Triassic evaporites;
- the Tabular Jura of Basel with rather narrow grabens suggesting décollement in Paleozoic beds;
- the composite block west of the Wehratal-Zeiningen fault, suggesting décollement in the brittle-ductile transition.

7.2.3 A summary of the timing of events and their possible documentation in the Jura-1 section

The foregoing discussion implies the following timing of tectonic events that should find its repercussion in the deep structure of the Jura-1 profile (compare Laubscher 1992, Figure 6; Diebold et al. 1991):

1. The first stratigraphically recognizable event in the domain of Jura-1 is the late Paleozoic dissection of the crystalline basement by deep troughs of kinematically varying functions; they probably were dextrally transtensive during some intervals, dextrally transpressive during others. As the crustal roots formed by Variscan orogenic processes have vanished almost com-

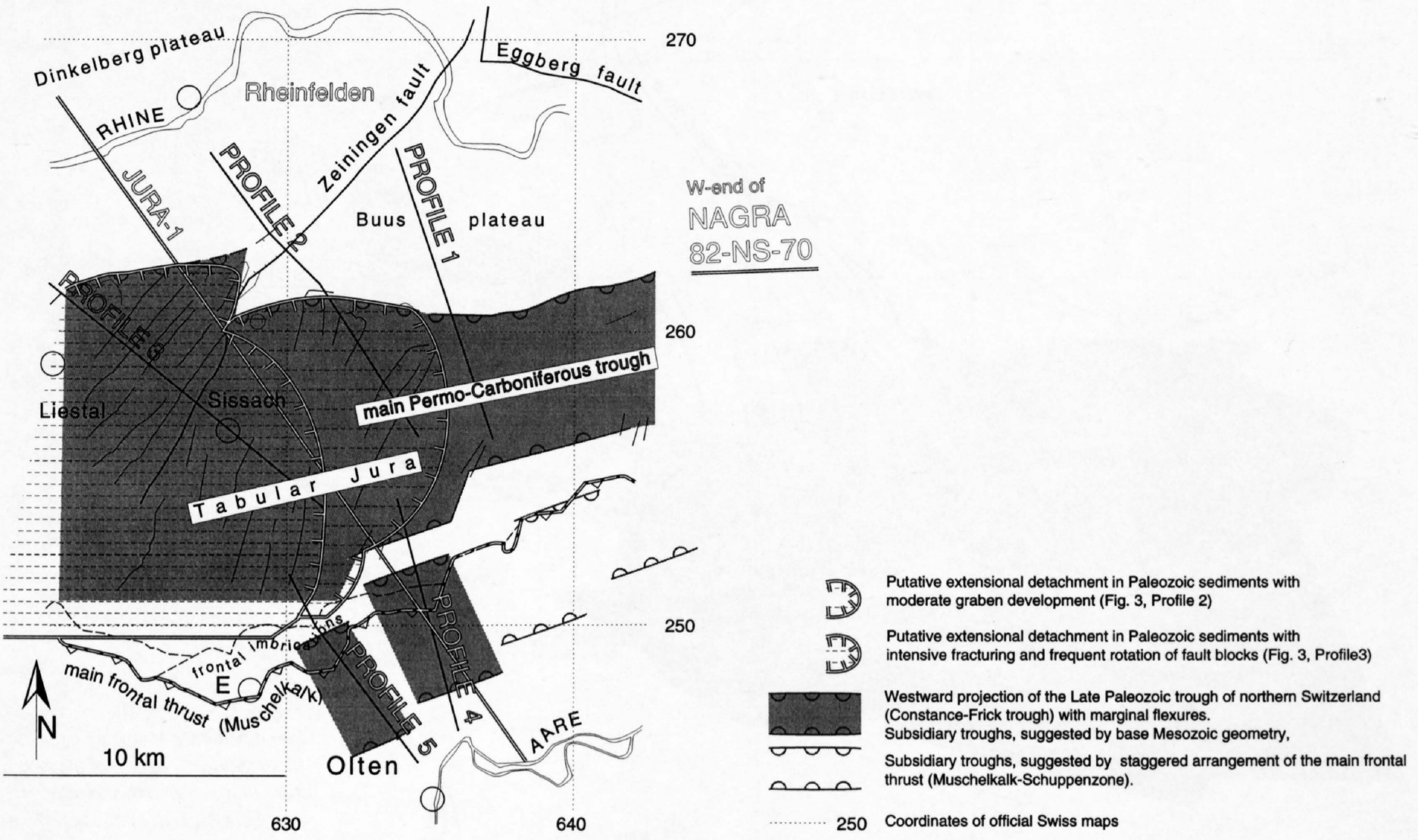

Figure 7.2-2
Tectonic elements of the Jura of Basel between Rheinfelden and Olten with the location of the profiles 1–5 of Figure 7.2-3 and Jura-1 (Figure 7.2-6 and Ansorge & Baumann, Chapter 5.1).

pletely in western Europe, it is to this subsequent, pervasive event, coupled with extensive magmatism, that a large part of the formation of the present lower crust of western Europe may be attributed. This impression is enhanced by the composition and timing of various mafic intrusions in the Ivrea body, which apparently represents the lower crust of a trough of similar age belonging to the same system of troughs (compare Bürgi & Klötzli 1990; Arthaud & Matte 1977; Schumacher et al., this volume). It would appear that the excellent curved reflexions in the lower crust of Jura-1 (Figure 7.2-6), which after migration would shrink to narrow bulbs, fit best into this scenario of widespread late Paleozoic mafic intrusions into an extensive system of troughs.

Sediment-filled troughs of that age are suggested by the conjectured décollement of the Tabular Jura of Basel, as shown in Figure 7.2-3. There are dipping reflections in the corresponding depth interval in the profile Jura-1,

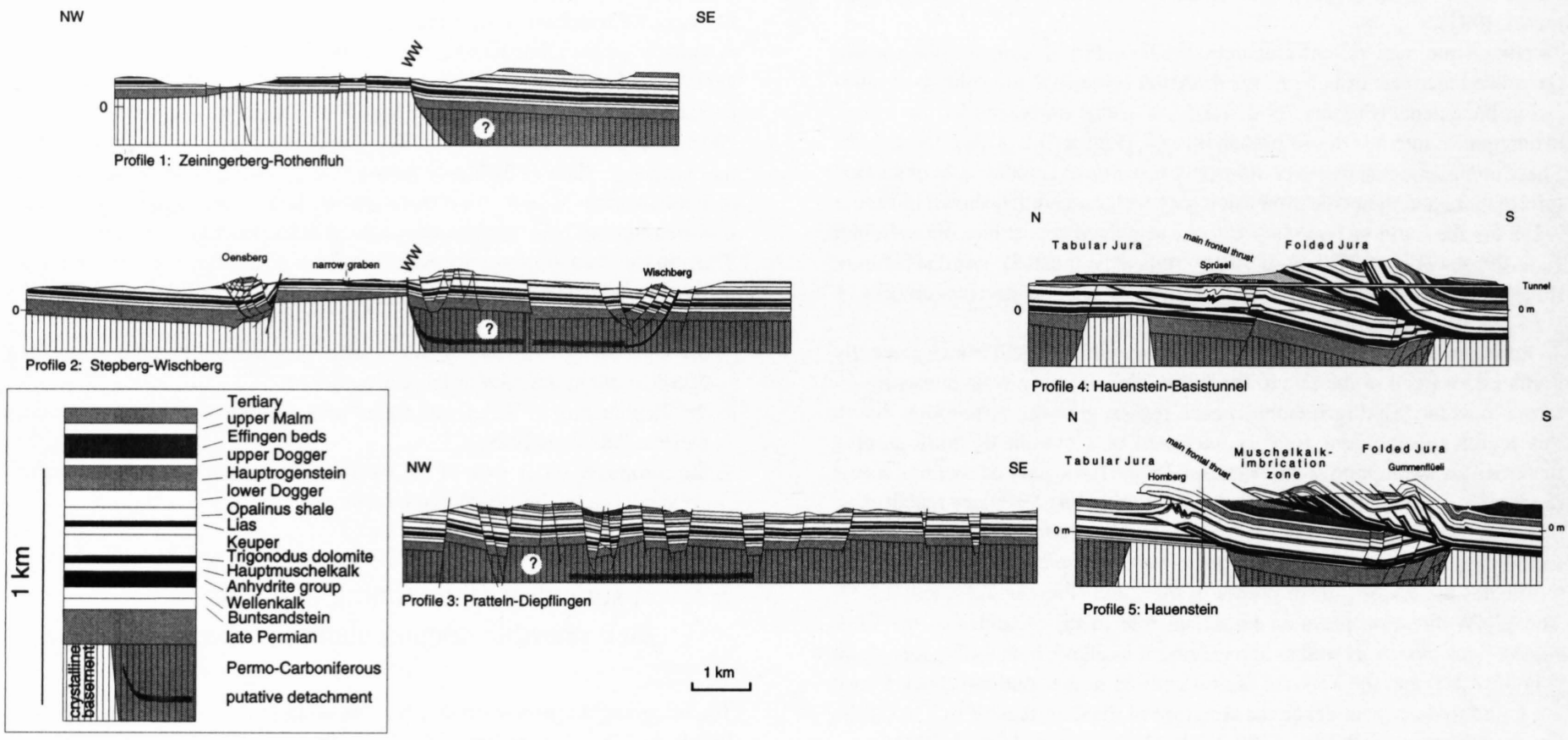

Figure 7.2-3
Cross-sections through the Jura of Basel. For location see Figure 7.2-2. The Late Permian sediments are more widespread than the Carboniferous-Early Permian ones; however, scant information permits only schematic representation (compare Gürler et al. 1887; Gonzalez 1990). The stratigraphic units are those traditionally used in maps and other publications on the geology of the region, although they are not defined with the rigor now required for the definition of formations.

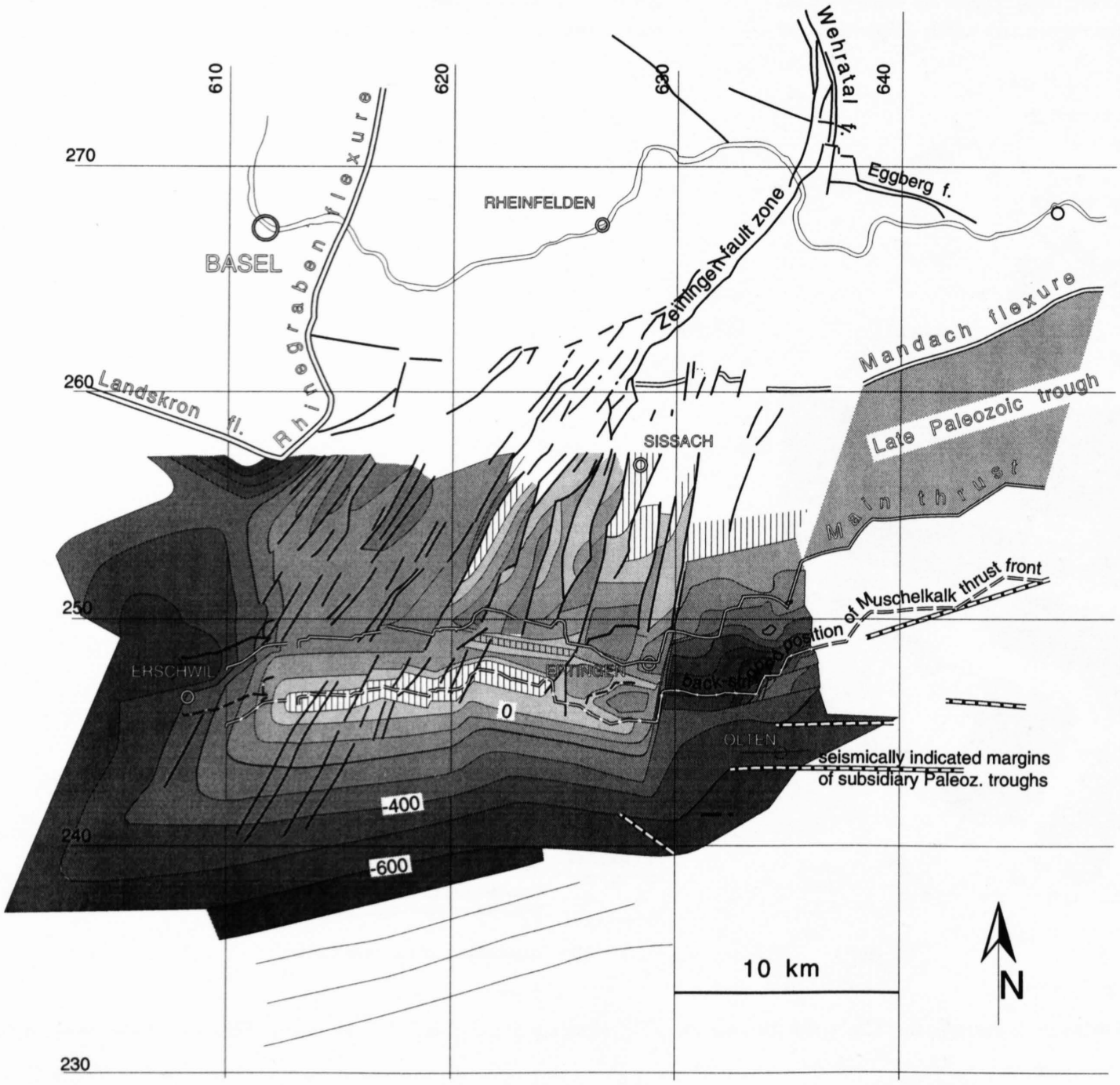

Figure 7.2-4
Simplified base Mesozoic geometry of the southern part of the Basel Jura between Erschwil and Eptingen, after Bitterli (1992); modified. No attempt has been made to show the influence of small Rheingraben faults south of the backstripped position of Muschelkalk thrust front.

reminiscent of those obtained by much more detailed seismic profiling in the Constance-Frick trough (Sprecher & Müller 1986). Their occurrence is generalized in figures 7.2-6 and 7.2-7 (shading in the shallow crust). The trough borders as suggested by surface geology are interpreted as converging in a late Paleozoic brittle-ductile transition overlying the late Paleozoic lower crust.

2. The second event – the most impressive at the surface – is the Eocene to Early Miocene Rhine graben formation. It involved extensional faulting with décollement at various levels and some uplift of the graben lips as evidenced by conglomerates attributable to that time. Possibly, the vaguely defined brittle-ductile transition in Jura-1 was placed at about the same position as in the late Paleozoic.

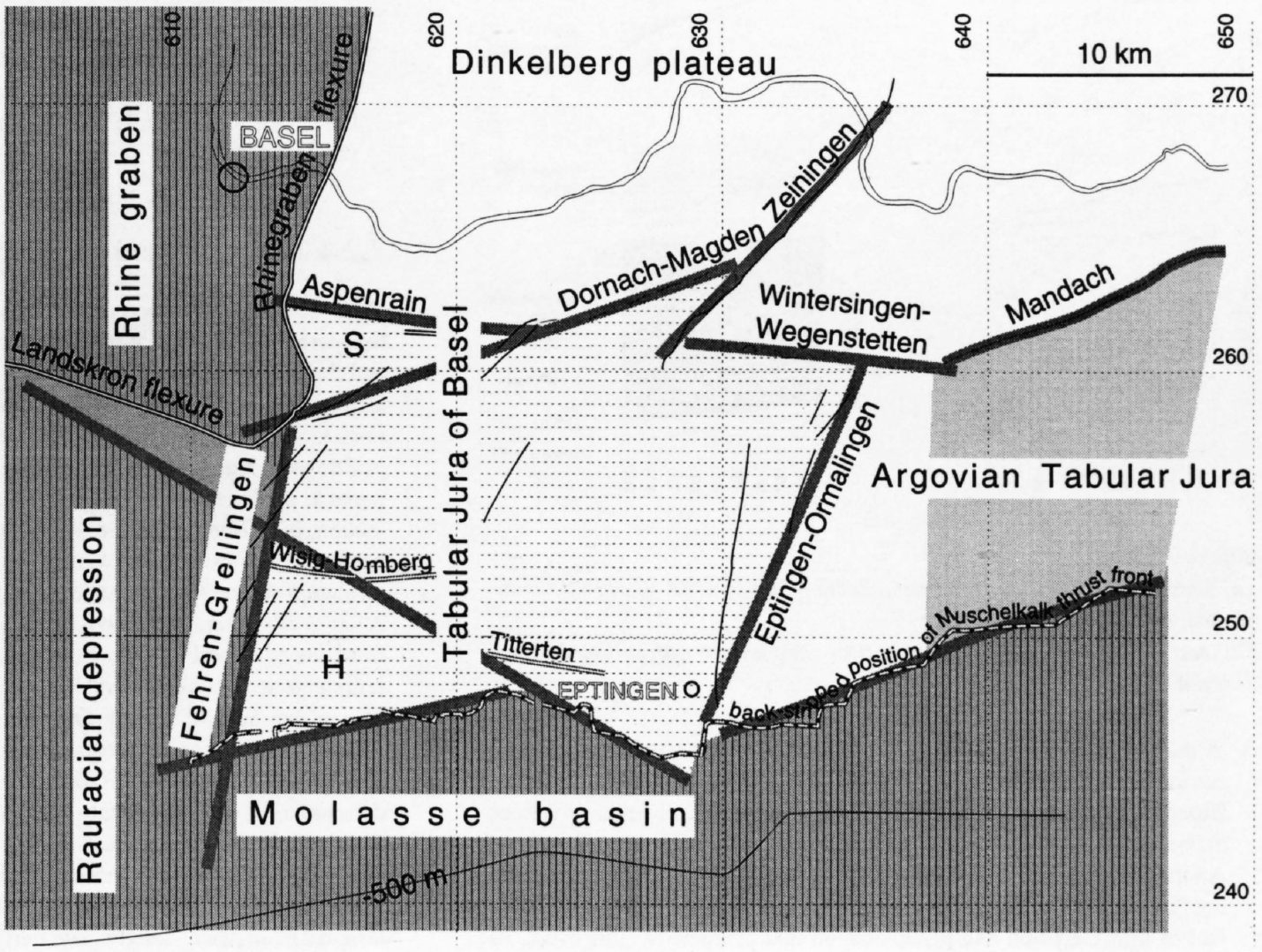

Figure 7.2-5
The principal basement lineaments of the Basel Jura. S = subplateau of Schönmatt, H = subplateau of Himmelried.

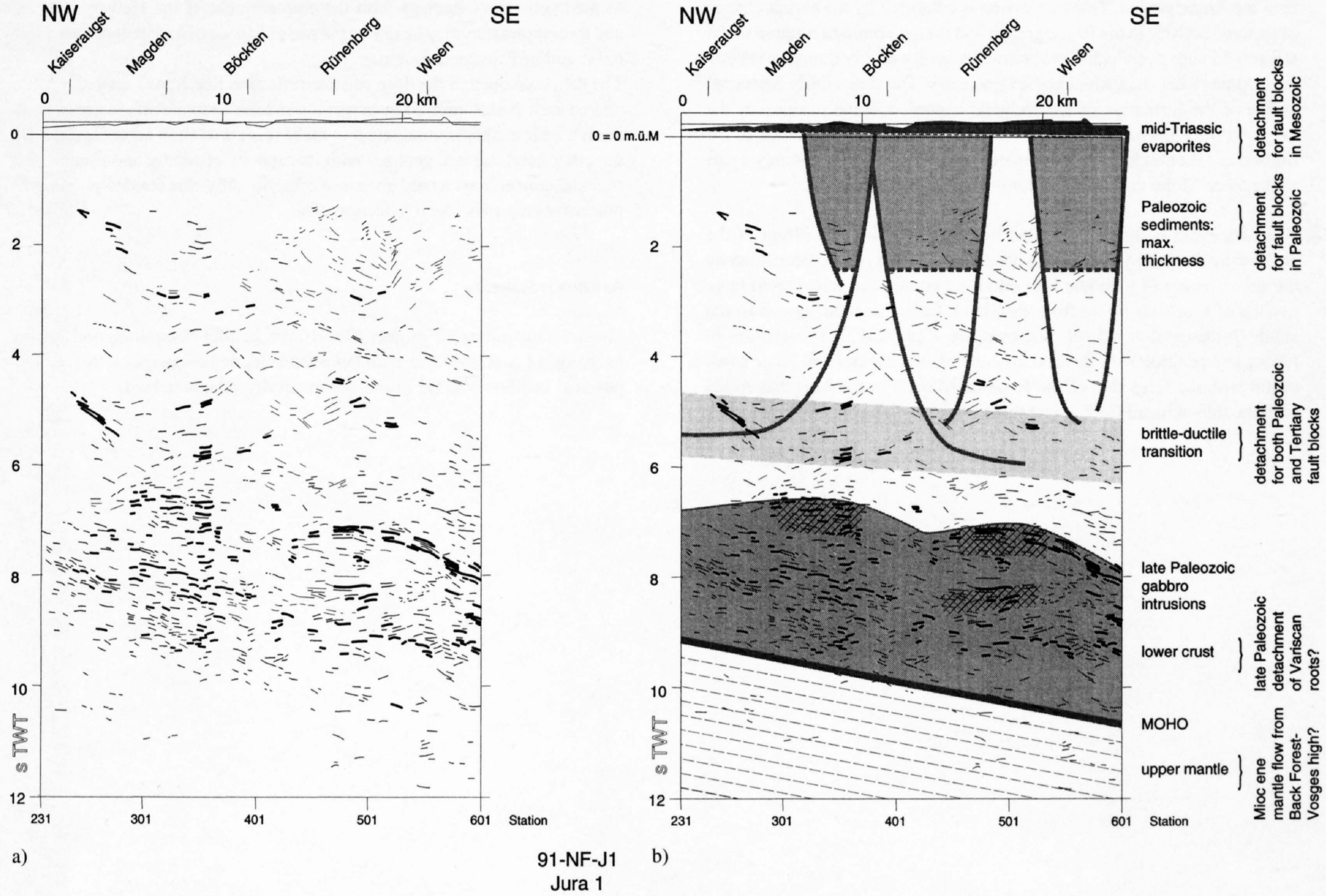

Figure 7.2-6
(a) Simplified line-drawing of deep reflection line Jura-1 (unmigrated; Ansorge & Baumann, Chapter 5.1);
(b) interpreted, with comments on possible correlations with surface geological data.

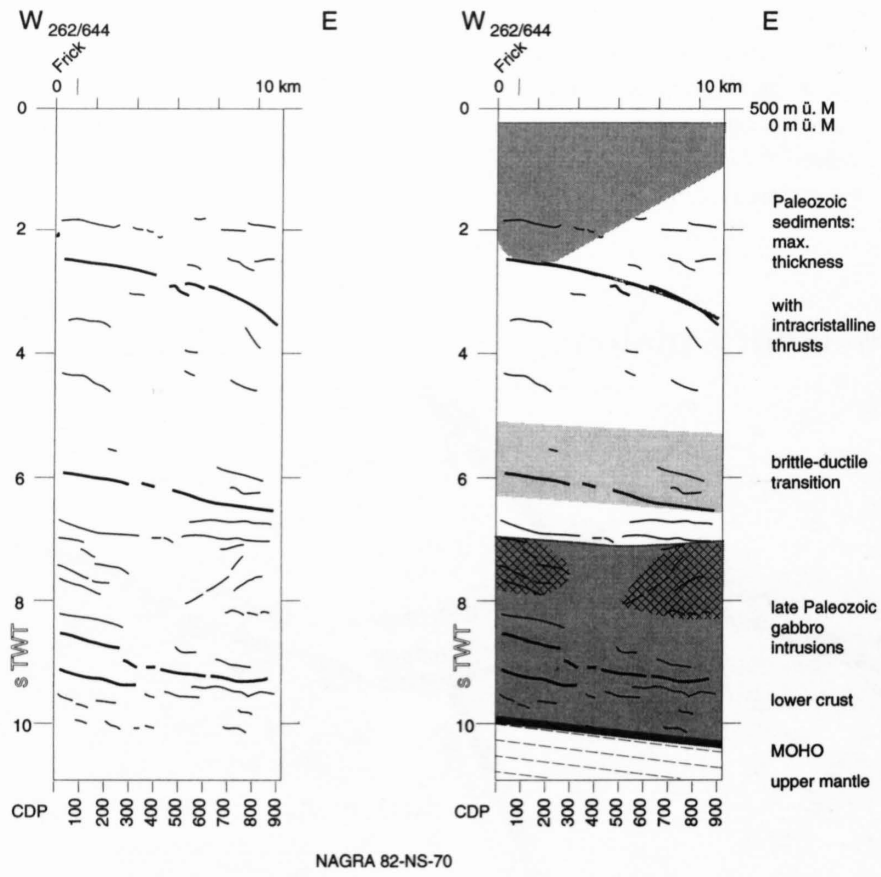

Figure 7.2-7
(a) Simplified line-drawing of deep reflection line NAGRA 82-NS-70 (unmigrated; after Finckh et al. 1984);
(b) interpreted, with comments on possible correlations with surface geological data.

3. A third event is documented by pre-Middle Miocene erosion and the unconformable deposition of the Middle Miocene (Upper Marine Molasse: Buxtorf 1901; Diebold et al. 1991). Its significance is intimated by various elements:
   An important feature that originated at that time is the roughly EW striking "northern hinge of the Molasse basin" (see Figures 7.2-4, 7.2-5). The fact of uplift, erosion and peneplanation that characterize this event, its trend and position suggest it to be an element of the Alpine foredeep rather than the Rhine graben. This impression is enhanced by the abrupt change of tectonic activity in the Rhine graben and the concomitant rotation of the stress field with σ_1 trajectories assuming a northwesterly direction reflecting Alpine rather than Rhinegraben geometry. The time (Early Miocene) is that of the formation of the Helvetic nappes, and the position of the hinge with its uplift and erosion is that expected for the forebulge of the lithosphere (Laubscher 1992; compare Sinclair et al.1991). Possibly a part of the steep Moho dip visible in Jura-1 is due to this event.

4. A fourth event is that documented by renewed uplift and tilting of the shallow marine beds covering the peneplain of event (3), accompanied by the development of a middle Miocene river system that transported large masses of erosional waste from the Black Forest and the Vosges to the south (Juranagelfluh, 15–11 Ma, compare Kälin 1993). It coincides in timing and position with the development of an outer flexural bulge associated with the formation of the External Massifs in the Alps that ended with the thin-skinned folding and thrusting in the Jura. It is this event that produced the major part of the uplift of the Black Forest and the Vosges, and consequently the upper mantle "asthenolith"- whatever its exact physical nature-supporting it (Werner & Kahle 1980; Villemin et al. 1986). For that reason, the main part of the steep dip of the Moho in Jura-1, which is located on the southern flank of the Black Forest–Vosges Moho dome (Figure 7.2-1), is attributed to event ??(4). The thinning of the crust in the dome is not associated with a recognizable amount of middle Miocene stretching at the surface, quite besides the fact that the circular geometry of the dome would make stretching a kinematic enigma, implies differential stretching in lower parts of the crust. Such differential stretching in turn leads to postulating some kind of differential flow in the upper mantle asthenolith – a suggestion noted at the margin of Figure 7.2-6.

7.2.4 Summary and conclusions

The recent deep reflection profile Jura-1 through the Jura east of Basel may be interpreted in terms of the geological development inferred from surface and shallow subsurface geology. The lower crust is characterized by comparatively steep south-dips of a band of distinct if rather discontinuous reflections as well as some curved bands of excellent reflections. The first are compatible with the steepened south flank of the Black Forest-Vosges Moho dome as predicted on the basis of refraction data, which, from surface information, is of Middle to Late Miocene age. The curved reflection bands are believed to be the results of mafic intrusions during Late Paleozoic trough formation analogous to those found in the equally Late Paleozoic Ivrea body. A series of inclined reflections in the shallow crust may represent sediments from one or several Paleozoic troughs. The presence in the area of Paleozoic sediments at depths of several kilometers is also conjectured from the geometry of the field of mostly Oligocene normal faults; the convergence of grabens at that depth and frequently pronounced rotation of fault blocks with little overall displacement of the tabular masses between the grabens suggest detachment of an extensional slab in an incompetent pre-Mesozoic interval. An approximate contour map of the base Mesozoic reveals several lineaments that are similar to those characterizing the Late Paleozoic trough of Frick-Constance farther east. In particular, the northern hinge-line of the Molasse basin, in places dated as late Early Miocene, forms a pronounced, albeit thoroughly dissected ridge. This ridge is believed a part of the forebulge that formed contemporaneously with the emplacement of the Helvetic nappes, and its complexities may be due to the pre-existence of a system of Late Paleozoic and/or Paleogene faults.
The data contained in the deep seismic reflection line Jura-1 may all be correlated with events inferred from surface and shallow subsurface geology, although their quality is insufficient to make this correlation unambiguous. On the other hand, surface geology with its capacity of timing and establishing regional connections would appear to offer the only clue for deciphering the otherwise enigmatic deep reflection data.

Acknowledgments

Financial support by NF project 4020-10893, helpful discussions and the free exchange of data and ideas with Peter Diebold, and cooperation by the Geophysical Institute of ETH Zurich are gratefully acknowledged.

7.3 Late Palaeozoic troughs and Tertiary Structures in the eastern Folded Jura

P. Diebold & Th. Noack

Contents

7.3.1 Introduction

This paper discusses methods and results of a project that, successfully attempted to map the basement surface in the area of the Jura south of Basel. The project was based on the relationship that could be established in the well-explored Eastern Jura, between Late Palaeozoic troughs, Palaeogene fault rejuvenation and the geometry of the Jura fold-belt.
On the basis of available geological surface- and isopach data the geometry of the Folded Basel Jura was modelled involving two- and three-dimensional approaches. The basement relief was then reconstructed by palinspastic restoration and subsequent stripping of the sedimentary cover. Results revealed the presence of several large scale basement features in the area. But, the resolving power of the iterative modelling was found to be restricted by limits inherent in the inversion process and also by ambiguities in available tectonic surface data and uncertain isopachs.
Laubscher & Noack (chapter 7, section 2) review in depth the regional geology of the area investigatigated by the project. Although not the subject of this paper, some relevant aspects are covered in the captions to Figures 7.3-2 to 7.3-5.

7.3.2 Geological Background

The discovery by NAGRA, some ten years ago, of deep Late Palaeozoic troughs in the subsurface of Northern Switzerland, has vastly increased our insight into the structure and geology of the region. Geophysical surveys (reflection seismic and gravity) indicate that these troughs are accompanied by major deep reaching fault zones and that their sedimentary fill could reach a thickness of up to 6 km.
The available data so far indicate the existence of two troughs in Northern Switzerland. The northern Konstanz-Frick Trough [KFT], (Laubscher, 1986), is relatively well explored by seismic, gravity and drilling. One of the deep exploratory wells drilled in the central part of the KFT (Weiach), furthermore, discovered bituminous shales and coal. The block diagram, Figure 7.3-3, provides a qualitative impression of the depth and structural complexities in parts of the KFT.
Another system of troughs may exist in an area south-west of the KFT; the Olten-Lenzburg Trough [OLT], (Laubscher, 1987) has been inferred on the basis of scattered indications on reflection seismic but it is not confirmed by drilling (see Figure 7.3-5). Noack (1995) has recently inferred the existence of a trough in the Hauenstein area. The latter, although being in an intermediate position between the KFT and OLT, could be seen as a possible westward extension of the KFT.
These discoveries are of considerable interest. From a scientific point of view these deep structures and their development are key links in our understanding of the regional structural/geological history. In addition, these troughs also present a practical dimension:

- The major fault zones are now considered to be the venue of ascending deep ground waters. The latter are responsible for the positive geothermal anomaly observed in the area of the KFT that offers prospects for geothermal energy (Rybach et al., 1987).
- Strong earthquakes in stable cratonic areas occur preferentially along dormant, pre- existing major fault zones (Johnston & Kanter, 1990). In Northern Switzerland, faults of just this type exist along the margins of the Late Palaeozoic troughs. The Basel earthquake of 1356 has been attributed by Mayer-Rosa & Cariot (1979) and also by Meyer et al. (1994) to an east-

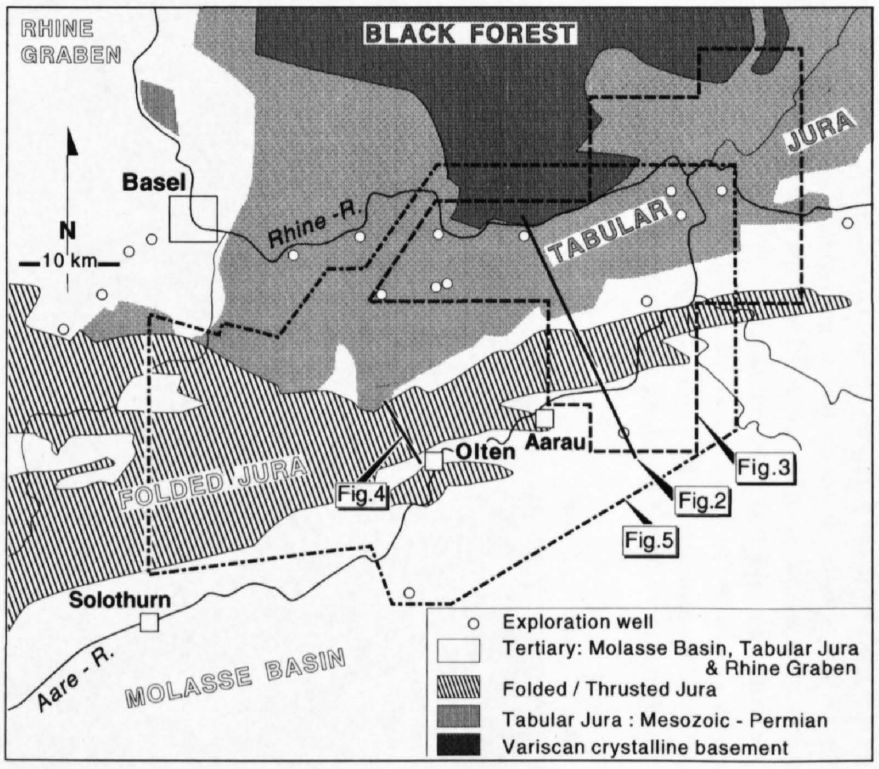

Figure 7.3-1
Location map for Figures 7.3-2 to 7.3-5

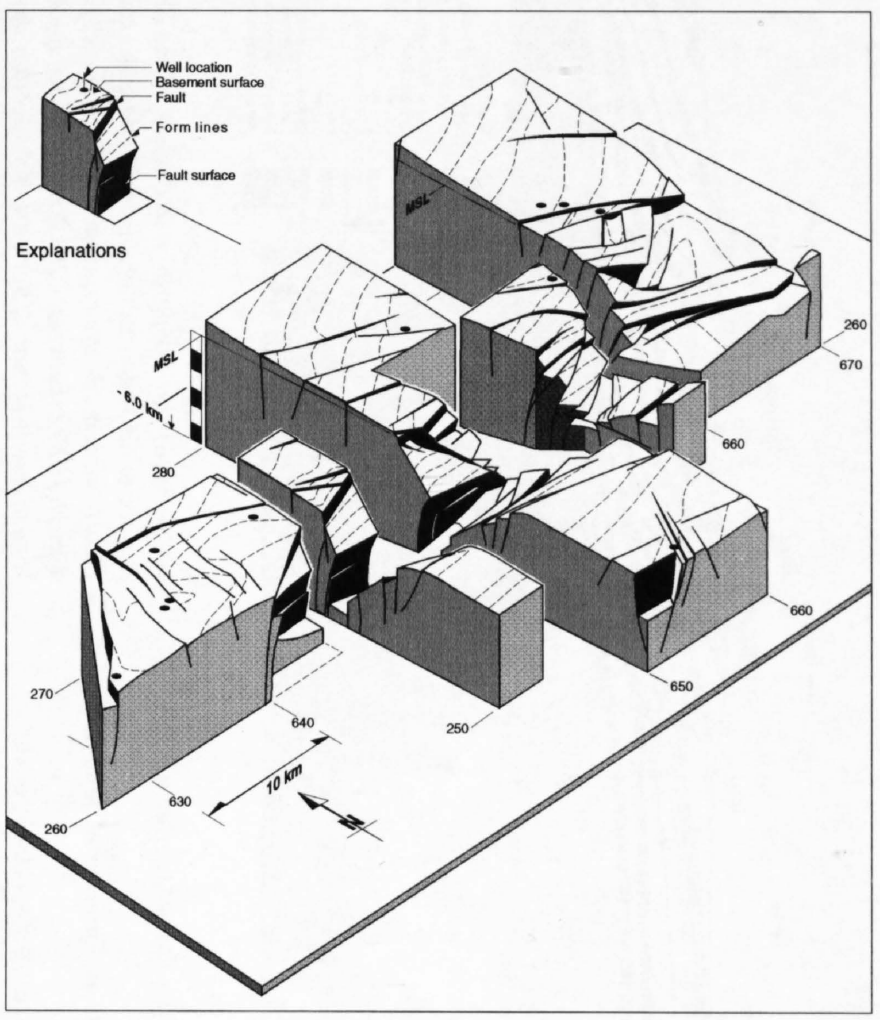

Figure 7.3-3
Late palaeozoic Konstanz-Frick trough
Simplified blockdiagramme of the western part, westward as far as explored by NAGRA, modified after Figure 17 in Diebold et al., 1991 (for location see Figure 7.3-1).
The diagram is intended to convey a qualitative impression of structural complexities in the Konstanz-Frick Trough (KFT). The interpretation is based on reflection seismic and well data (Laubscher 1987, Diebold et al., 1991) and has been inspired by data from analogous, well-explored late Palaeozoic coal-basins in the French Massif Central.
The stratigraphy and sedimentology of the Permo-Stephanian basin fill, based on four cored deep wells (Matter, 1987), provide a tenuous time frame for the multiphase tectonic development:

- *(? Westphalian) Stephanian and lower Permian (Autunian) subsidence, probably transtensional, with the deposition of coal beds and bituminous shales in a WSW-ENE trending intramontain basin;*
- *strong dextral transpressive deformation (Lower Permian, Saalian phase) involving major oblique fault systems (e.g. Eggberg-&Vorwald fault zones);*
- *during subsidence at the end of the Variscan orogenic cycle, the Upper Permian (Rotliegend) was deposited in a wide depression overlapping the pre-existing rims of the KFT.*
- *While tectonic quiescence prevailed during the Mesozoic, major fault zones of Variscan origin were reactivated as normal faults and/or flexures in the wake of both, the Rhine Graben rifting and the subsidence of the Molasse Basin during the Palaeogene – early Miocene. These rejuvenated fault-/ flexure zones vertically displace Mesozoic strata and are mostly discernible on reflection seismic profiles (e.g. Figure 7.3-2). These faults have been mapped on Figure 7.3-5 (eastern part).*

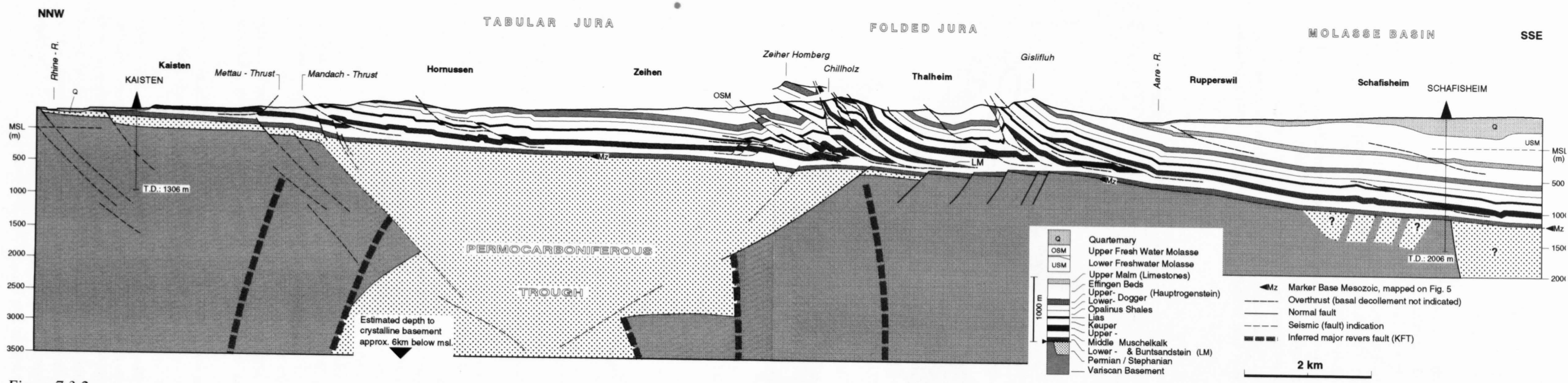

Figure 7.3-2
Eastern Folded Jura: reflection seismic and geological interpretation Line 82-NF-10 (NAGRA) Kaisten – Schafisheim, for location see Figure 7.3-1.
Reflection seismic: 36 fold stack, migration, Seismic reference datum: 500 m asl. for details see Sprecher & Müller, 1986.
Interpretation: velocity control: geophysical well surveys Kaisten and Schafisheim (Weber et al.1986); velocity model and reflector identification: Diebold et al. 1991.
The section serves mainly to illustrate the relationship prevailing in the Eastern Folded Jura between the geometry of the Basement surface and thin skinned fold/thrust tectonics in the detached sedimentary cover (Laubscher, 1986). Based on this paradigm, the geometry of observable Jura folds has been used to construct the relief of the Basement surface in the Basel Jura, an area where no geophysical data is available.
In 1986 reflection seismic section 82-NF-10 was the first published profile across the Eastern Folded Jura allowing a well-constrained geological interpretation of:

- *structural details of the Tabular Jura and the Jura thrust-belt, also revealing hitherto unknown tectonic details concealed in the subsurface. This allowed improved estimates of the total shortening in the detached sedimentary cover as being more than 6 km along the section and*
- *the geometry, i.e. the position and relief, of the Base Mesozoic surface and hence also of the basal decollement surface in the evaporites of the Middle Muschelkalk.*
- *clearly discernible are rejuvenated (Palaeozoic) faults in the flexure at the northern rim of the Konstanz – Frick Trough [KFT] (between CDP 2000 an 2100, approx. 200 ms), some three km south of the well Kaisten. The geological interpretation of this part of the section shows the relationship between the Mandach thrust and the underlying faulted flexure.*

Similar rejuvenated faults and flexures can also be inferred on the southern shoulder of the KFT, below the Folded Jura (approximately CDP 950 – 1250, at some 500 ms). However, the interpretation of seismic data which is ambiguous in this area, remains somewhat speculative. While the possibility of reverse faulting (e.g. a basin inversion cf. Roure et al., 1994) cannot be ruled out entirely, surface geology and regional considerations are constraining the timing of such events in the eastern Jura as pre-dating the Jura folding.
A complex pattern of reflections from below Mesozoic sediments (sub-Mesozoic reflections) can be gleaned between approx. CDP 1200 – 2150. This originates in the sedimentary fill and/or on major fault zones of the Palaeozoic Konstanz – Frick Trough. The geological interpretation of these reflections, although highly tentative, has been attempted by Laubscher (1987) and Diebold et al. (1991). The Blockdiagramme Figure 7.3-3 is based on these interpretations.

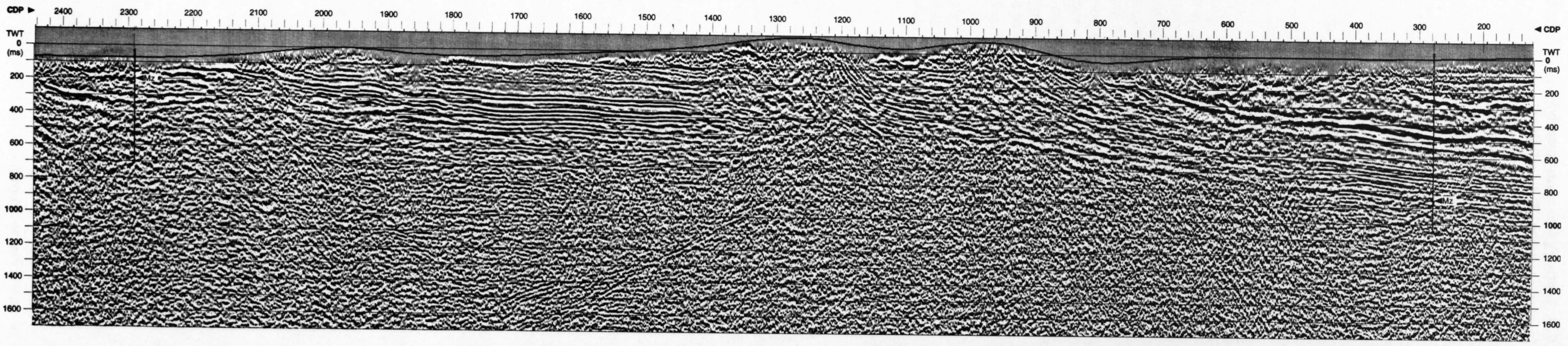

west striking fault zone, probably of Palaeozoic origin and not to one associated with the Tertiary Rhine Graben as hitherto assumed on the basis of the observed local seismic activity (Deichmann, 1990).
- Coal and oil shales found in the sedimentary fill are source rocks for natural gas (and oil). Although coal is too deep for conventional mining, both coal-bed methane or possible future underground coal gasification offer prospects.
- Ground waters with both high Chloride and Sulphate concentrations have been found to adversely affect road- and railway tunnels in the area of the Eastern Jura (Hauber, 1994). Some of these concrete-aggressive ground waters might possibly originate in the KFT.
- The scrutiny of NAGRA's reflection seismic data clearly revealed that fault-zones of Palaeozoic origin, preferentially the main trough boundaries of the KFT, have been rejuvenated as normal faults and/or flexures during the Palaeogene (Laubscher, 1986 and 1987; Sprecher & Müller, 1986). The timing of this rejuvenation can be linked to subsidence in the Rhine Graben and the Molasse Basin (Laubscher, 1987; Naef & Diebold, 1990).

The effect of this early Tertiary fault rejuvenation is discernible on Figure 7.3-2 (Tabular Jura, northern part of seismic line 82 NF 10) where Mesozoic sediments are vertically displaced at the northern rim of the KFT.
Laubscher (1986) has investigated the relationship between these basement structures and the geometry of the overlying thin-skinned decollement foldbelt for the eastern Folded Jura: of importance is the fact, that the reactivation of the fault/flexure pattern is essentially of Palaeogene age and clearly predates the late Miocene Jura Folding.
This regional fault pattern, mapped on the basis of available reflection seismic, is shown in the eastern part of the map Base Mesozoic on Figure 7.3-5.
In the area of the late Miocene decollement thrusting, but most conspicuously in the Folded Jura, these structures have acted as important boundary conditions for the nucleation of folds and thrusts.
In view of the scientific and practical importance of such deep seated basement structures, it appeared warranted to investigate ways and means to extrapolate the knowledge gained in the Eastern Jura towards the West, to the Jura south of Basel (Figure 7.3-1), where, so far, no equivalent geophysical and/or well data is available. The project was carried out within the framework of NRP 20, at the Geological Institute, University of Basel, between 1986 and 1991, involving an effort of some eight man years.

7.3.3 Methodology

In the areas of the Tabular Jura, not affected by decollement and folding, the process of mapping the basement surface is relatively straight forward and depends primarily on an accurate knowledge of the overburden thickness.
The attempt to map the relief and discontinuities of the basement surface under the Folded Jura, however, involves a two steps geometrical construction, which strips off the overburden by
- an inversion of the tectonic processes of the late Miocene folding (retrodeformation) in order to place the stack of sediments into its original, unfolded pre-decollement position and
- with a knowledge of sediment thicknesses, the position and relief of the basement surface can then be estimated by downward extrapolation.

Fold/thrust geometries have been investigated by means of an array of densely spaced balanced cross sections, running as far as possible perpendicular to the fold axes. For the construction of such cross sections powerful and elegant computer programmes are now available, taking two-dimensional material balance fully into account, e. g. Kligfield et al., 1986. Figure 7.3-4 provides an example of such a construction from the Hauenstein area (Noack, 1989, 1995).
However, the palinspastic reconstruction for parts of the Folded Jura is basically a three-dimensional geometrical problem. In view of many known and/or suspected strike slip faults, lateral material transfer with respect to cross sections must be expected; therefore in a purely two-dimensional approach to retrodeformation some minor misfits have to be accepted.
For the purpose of investigating the third dimension a computer assisted method of "Block Mosaics" was developed:
The method is based on the fact that stratigraphic horizons have been deposited as continuous surfaces (layers), which after tectonic deformation could be disrupted along discontinuities, e. g. layers are broken up by faults into individual pieces (= blocks); overlapping blocks are indicative for reverse faulting (thrusts).
The method aims to restore a layer to its original state: For a given stratigraphic key horizon, the inventory of blocks and faults is projected onto a map. The resulting mosaic is then rearranged by shifting and/or rotating individual blocks into contiguous, non overlapping positions (for details see Bitterli, 1988 and 1990).
The "Block Mosaic" proved invaluable for the detection of unrecognised and/or suspected strike slip fault and allowed for an evaluation of lateral material transfer with respect to cross sections.
The basic data required for the construction of these cross sections included the available inventory of mapped surface structures that had to be supplemented by selective additional mapping and checks in the field. Also a new, up to date set of isopach maps for stratigraphic intervals has been compiled for the region of Central-Northern Switzerland.

7.3.4 Results and Discussion

It was possible to reconstruct the Basement surface in the area underlying the Folded Jura south of Basel on the basis of available surface geological data and applying the method of retrodeformation and downward extrapolation.
The original results have been compiled in structural contour maps (Figure 101–103 in Bitterli, 1992). They are incorporated in Figure 7.3-5 and the regional synopsis, i. e. Figures 7.2-4 and 7.2-5 by Laubscher & Noack (section 7.2).

Figure 7.3-4
Balanced profile and palinspastic restoration Hauenstein Section (Noack, 1989, 1995), for location see Figure 7.3-1.
Upper part: balanced section of the deformed (folded/thrusted) Mesozoic sediments;
Lower part: palinspastic restoration of the same section (scale is 50% of the upper section).
By means of an array of densely spaced balanced cross sections, running as far as possible perpendicular to the fold axes, geometries of the detached sediments have been investigated. This section is retrodeformable, i.e. it complies with the criterion of two-dimensional material balance and is kinematically admissible. Here, it serves as one example to demonstrate that by a careful construction of the geometries and kinematic relationships of the deformed Mesozoic sediments of the Folded Jura the relief of the underlying basement can be inferred.

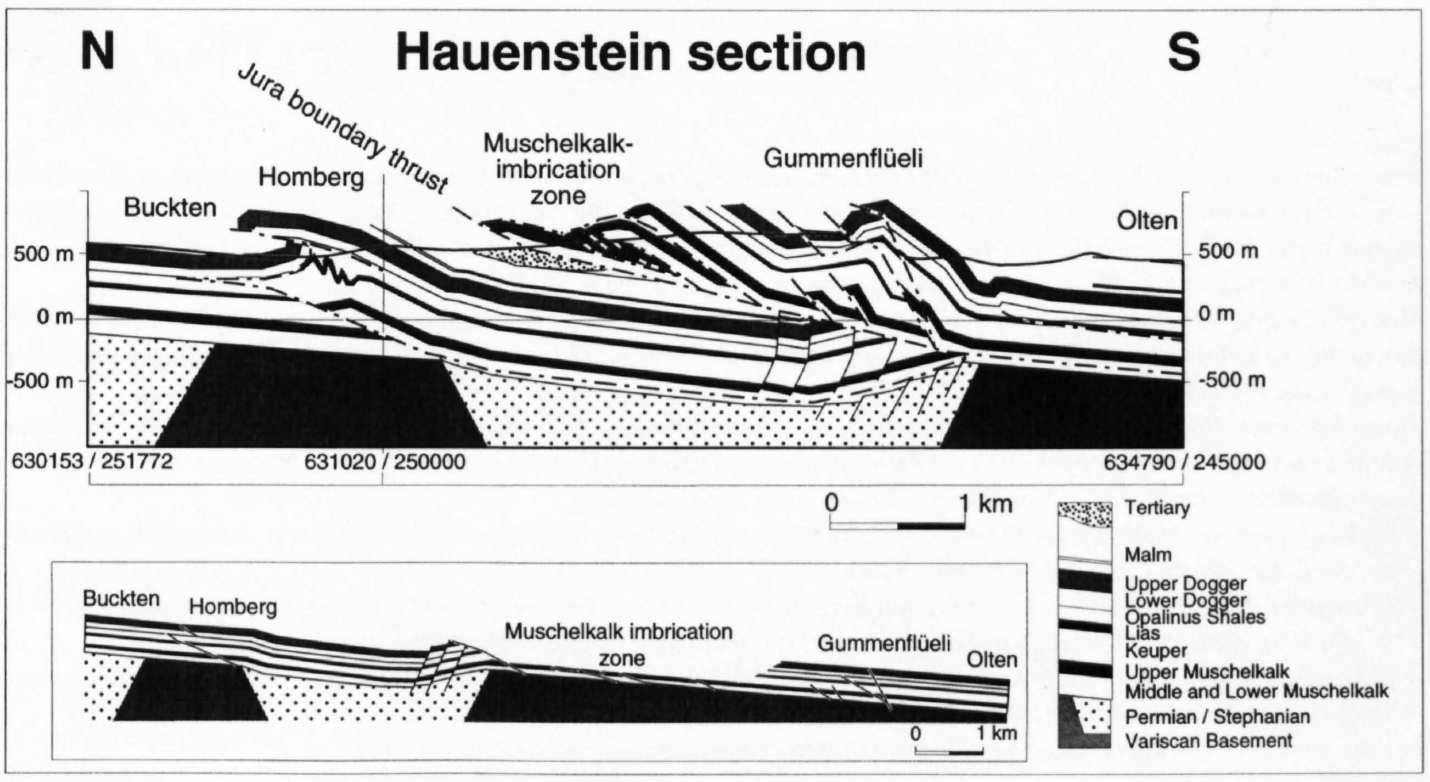

However, a number of problems and limitations were experienced:

- Bedrock exposure in the area is far from ideal; this leads to an incomplete structural inventory and often impedes the unambiguous identification of key tectonic elements, e. g. strike slip faults.
- Decollement- and thrust surfaces are tectonic discontinuities which separate levels of differing geometries. Deeper levels are generally not accessible to observations from the surface and extrapolation downward, across such discontinuities is fraught with problems.

For the construction of cross sections, from the surface down to basement, it was therefore necessary to resort to the application of tectonic models.
The methodical application to the Folded Jura of geometric models of fault bend folds and fault propagation folds, developed by Suppe, 1983; Mitra, 1986; Mitra & Namson, 1986 and others, has been quite successful. By definition, these models meet the criteria of two-dimensional material balance and inconsistencies have not been found in the course of the project.

Cross sections of the modelled geometry of the Folded Jura, such as the one shown in Figure 7.3-4 (Noack, 1989, 1995), are internally consistent as they satisfy the conditions of two-dimensional material balance and are kinematically admissible (Geiser, 1988). We have ruled out models, such as the involvement of an inverted basement (e. g. Roure et al., 1994), as we could not conceive a corresponding geometrical and kinematically viable model, that fits the data. This does not mean that there is no alternative model. However, for any other proposed model to be valid, it also has to comply with the criteria of material balance and kinematic admissibility.
Two-dimensional material balance often provides the only control, although without guarantee for a correct tectonic interpretation of available data. It is valid with the caveat that lateral material transfer has not taken place across the plain of sections. The "Block Mosaic" for control in the third dimension was, therefore, also required.
Mapping the basement surface under the detached and folded/thrusted stack of sediments is an iterative process. The first iteration of basement recon-

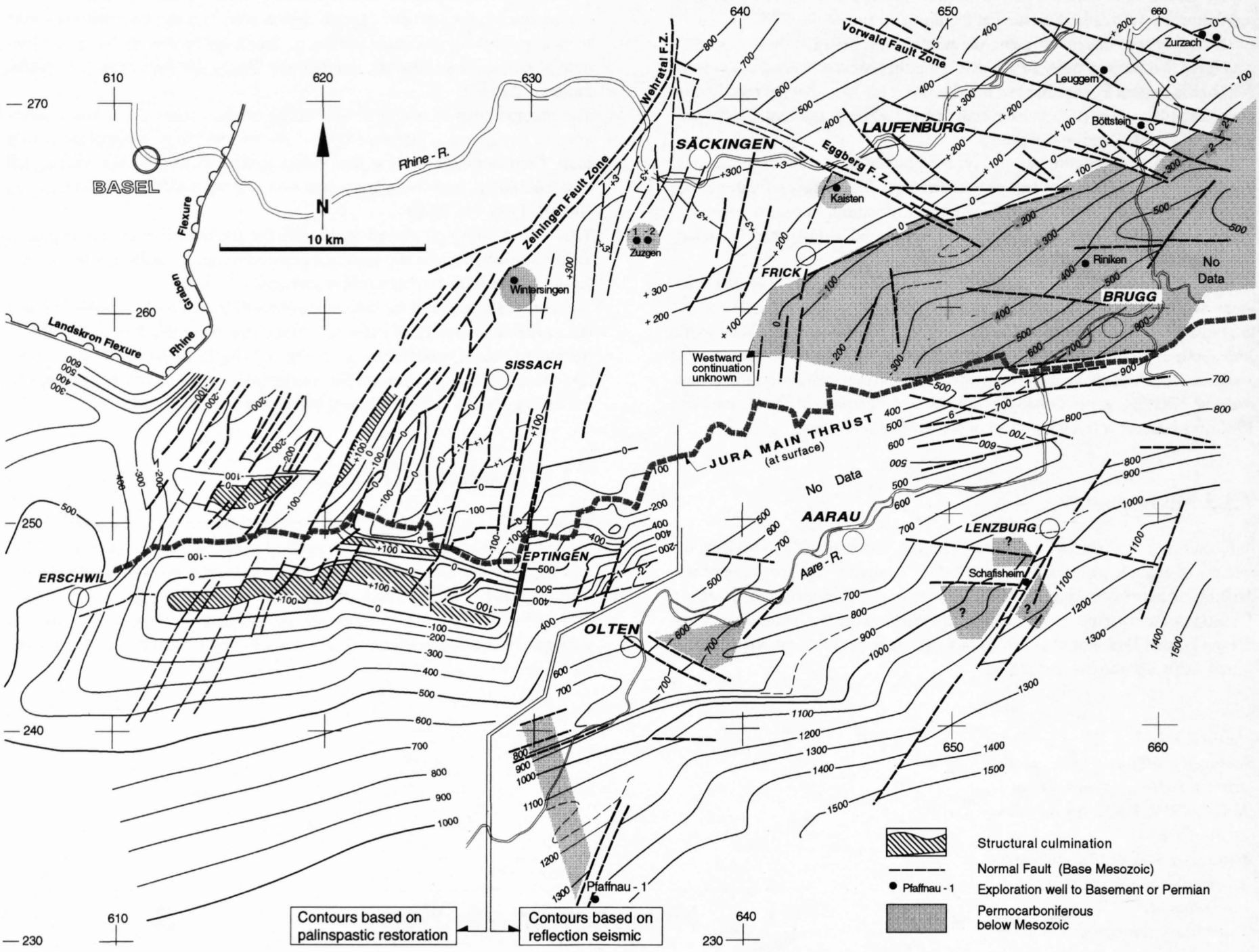

Figure 7.3-5

Structural contour map, base Mesozoic. The map compiles reflection seismic data and structural contours that are based on a palinspastic restoration of the Folded Jura in the area south of Basel. The eastern part, i.e. approx. east of a line Säckingen – Olten – Pfaffnau, is based on reflection seismic as available by end 1990, modified after Encl. 35 in Diebold et al., 1991. The western part of the map is based on Figure 7.2-4 by Laubscher & Noack (Section 7.2); the latter incorporates results of our project, i.e. the basement reconstruction (e.g. Figures 101 – 103 in Bitterli, 1992).

Mesozoic sediments (Buntsandstein, Lower Muschelkalk) are thought to overlay Permian and /or the Variscan Basement on a fairly smooth peneplain. The departure of the present day geometry of this peneplain (i.e. the Base Mesozoic) from an approximately horizontal surface represents the total (vertical) crustal deformation after the Permian.

Minor Mesozoic differential warping and local normal faulting, thought to be mainly related to late differential compaction in underlying Permo Carboniferous sediments are reflected in isopachs and the facies pattern of Mesozoic strata (e.g. Bitterli, 1992, Jordan, 1994). However, the main part of the deformation must be attributed to tectonic activities during the Tertiary:

- *Reflection seismic in the area of the eastern Folded Jura revealed that the mapped faults/flexures in many parts represent rejuvenated Palaeozoic fault zones of the KFT, e.g. Figure 7.3-2, below Mandach thrust.*
- *In the area shown on Figure 7.3-5 faults and flexures have been dated essentially as Palaeogene to Lower Miocene by analogy (Laubscher, 1987; Naef & Diebold, 1990); direct local geological evidence constrains the timing as pre Upper Fresh Water Molasse.*
- *The conspicuous regional tilt of the entire area to the SSE is a phenomenon related to subsidence of the Molasse Basin and the uplift of a foreland bulge in the Vosges – Black Forest area (Miocene, c.f. Laubscher & Noack, section 7.2).*

For the project it is of importance that this tectonic deformation phase pre-dates the Jura Folding.

struction lead to a rough outline of the geometry of the basal detachment surface, indicating major flexure- and fault zones only. Improvements have been achieved by adapting and readapting the tectonic model to successively "better" basement geometries. However, the detection of small scale faults is generally beyond the resolving power of the method. Furthermore, using a densely spaced set of approx. N–S running cross sections for basement mapping, preferentially reveals cross trending, i. e. E–W striking structural features.

The Hauenstein section (Figure 7.3-4) is an example of the result of this iterative process. It shows how the relief of the underlying basement can be inferred by careful construction of the deformed Mesozoic sediments (Noack, 1989, 1995).

In the Tabular- and Folded Jura south of the Rhine Graben a number of approx. N–S striking normal faults of Palaeogene age have been mapped (Laubscher & Noack, section 7.2). These basement faults also affect the sedimentary cover; but, in the Folded Jura they have been detached from basement and were dislocated during the folding. Palinspastic restoration of such fault traces in the sedimentary cover reveals the location of their "roots" in the basement. The unambiguous identification as being of Palaeogene origin and not merely the result of the late Miocene Jura Folding remains, however, an intrinsic difficulty.

7.3.5 Conclusions

Experience has shown that it is feasible by means of iterative palinspastic reconstruction and back stripping to determine the relief and to locate major discontinuities of the basement surface under the Folded Jura south of Basel. However, limits are soon reached:

- Available surface geological data are inadequate for the unambiguous and complete geometric reconstruction of the Folded Jura; therefore the additional application of tectonic models is necessary. Elegant methods for a balanced three-dimensional retrodeformation of fold- and thrust geometries appear to be as yet unavailable.
- Our state of knowledge of the thickness of certain stratigraphic intervals is still insufficient for precise modelling and back stripping, and
- improvement, i. e. the gain in details and precision, from repeated iterations is marginal and a point of diminishing return is soon reached.
- Results of possible future geophysical surveys and/or deep drilling might verify the quality of our prognosis of basement structures under the Folded Jura south of Basel.

Acknowledgements

Financial support by NF project 4020-10893 and the co-operation by Geological Institute, University of Basel is acknowledged. Also NAGRA's permission to use their data is gratefully acknowledged.

8 Two cross sections through the Swiss Molasse Basin (lines E4–E6, W1, W7–W10)

O. A. Pfiffner, P.-F. Erard & M. Stäuble

Contents

NRP 20 acquired several lines within the Molasse Basin from industry (Swiss Petrol). These lines extend the Alpine lines E1 and W1 of NRP 20 to the north and define two transects through the entire Swiss Molasse Basin. They were completely reprocessed in the framework of NRP 20 by Stäuble (see Stäuble & Pfiffner 1991) and Erard (work in progress). This chapter intends to discuss the architecture of the Molasse Basin in the light of these two transects.

8.1 Geologic framework

The North-Alpine Molasse Basin is a peripheral foredeep which developed by flexural bending in response to thrust loading and compression of the European lithosphere in the later stage of the Alpine collision. The basin fill was, however, deformed by the latest orogenic movements. Owing to this, three distinct structural zones can be distinguished (see Figure 8-1).

The **Subalpine Molasse** comprizes the southernmost outcropping part of the basin; it forms a stack of imbricate thrust sheets which are in turn overridden by the Alpine, Helvetic and Penninic nappes. In the central part of the basin, the **Plateau Molasse**, the beds are generally subhorizontal, with a gentle dip of 3 to 4° in the lower part of the section. Some gentle folds of variable orientation tilt beds, with structural dips being in the order of 5°. Stronger tilts occur in the vicinity of the Subalpine Molasse. Towards the north several folds with axes subparallel to the ones in the adjacent Jura Mountains can be recognized in the **Subjurassic zone**. Some of these folds extend directly into the Jura Mountains. Within the latter Molasse sediments, preserved in some of the synclines, in some instances clearly overly their Mesozoic substratum discordantly.

The Molasse sediments comprize four major stratigraphic units (Figure 8-2). The lowermost, "Untere Meeresmolasse" or UMM, is composed of shallow marine sandstones and shales (see e. g. Diem 1986) known only from outcrops within the Subalpine Molasse. The following unit up, the "Untere Süsswasser, sandstones and great masses of gravel fan conglomerates derived from the Alpine orogen (Habicht 1945, Frei 1979). This clastic fluviatile series reaches its greatest thickness of over 4 km in the Subalpine Molasse. In this proximal part of the basin rapid lateral facies changes (conglomerates into yellow marls) influenced the structural style considerably, and led to truncations and lateral discontinuities. This must be kept in mind when interpreting seismic data. The USM represents a coarsening-upward megacycle

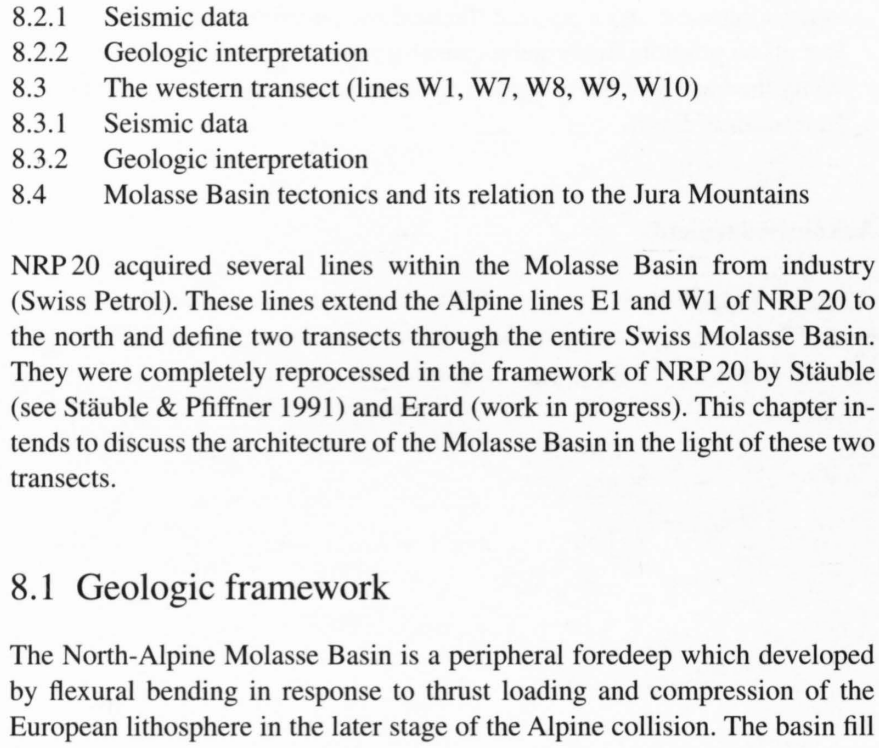

Figure 8-1
Tectonic map of the Swiss Molasse Basin and adjoining areas showing traces of seismic lines (thick) and geologic profiles (thin lines).

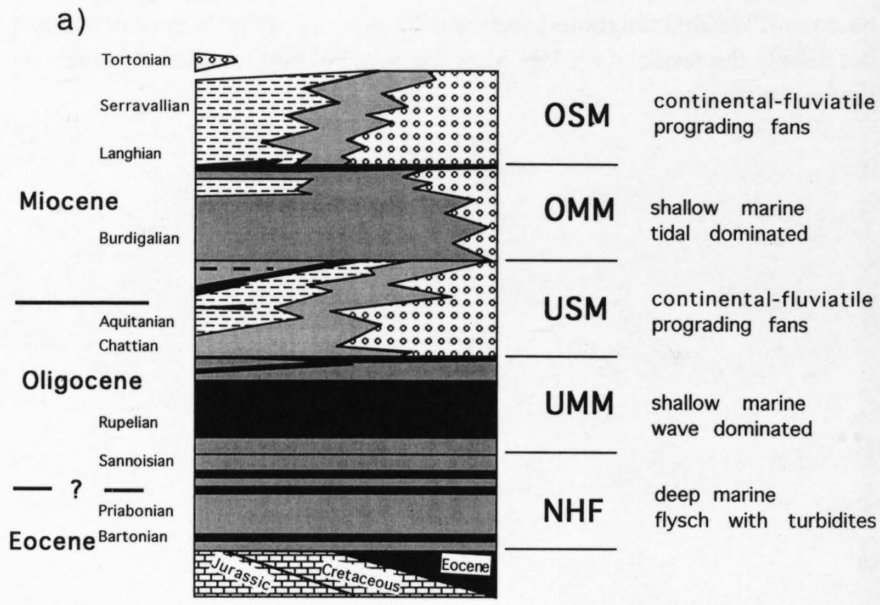

Figure 8-2
Summary stratigraphic section of the Swiss Molasse Basin.
a) Tertiary foreland basin sequence. NHF: North-Helvetic Flysch, UMM: Unterer Meeresmolasse (lower marine molasse), USM: Untere Süsswassermolasse (lower freshwater molasse), OMM: Obere Meeresmolasse (upper marine molasse), OSM: Obere Süsswassermolasse (upper freshwater molasse).
b) Mesozoic platform sequence as encountered in well Entlebuch 1 (Vollmayr & Wendt 1987, Herb 1990, unpubl.)

with deltas prograding northward into the basin. The USM is overlain by the "Obere Meeresmolasse" or OMM, which consists mainly of thick-bedded shallow marine sandstones (see Keller 1989). It attains a maximum thickness of 800 m in the south and tapers off towards the north. The youngest unit, the "Obere Süsswassermolasse" or OSM, contains conglomeratic fan deposits in the proximal part in the south, which are intercalated with shaly sandstones and marls (see Bürgisser 1981). To the north a furrow filled with micaceous sandstones straddles the Subjurassic zone. The gravel fans attain thicknesses of up to 1500 m in the centers which taper out northwards. In western Switzerland the OSM was subsequently eroded. The western limit of the occurrence of OSM sediments coincides more or less with the western transect studied here.

The Molasse sediments continue southward beneath the Alpine nappes (a southernmost inlier can be found in the tectonic window of the Val d'Illiez)

and overly the North Helvetic Flysch, NHF. This flysch is slightly older and represents an early stage of the foreland basin development (Pfiffner 1986). Its youngest strata, the Matt formation, are characterized by radial sediment transport from a source situated in the south. In the underlying Taveyannaz and Elm formations on the other hand, basin-axis parallel sediment transport prevailed and shedding of volcanic debris occurred occasionally as bombs thrown directly into turbidity currents (Siegenthaler 1972). The entire sequence is very often strongly folded and its maximum thickness can be estimated at 4–5 km. Although the North Helvetic Flysch now overlies the Mesozoic on the northern flank of the Aar and Aiguilles Rouges massifs, much of this flysch seems to be allochthonous with respect to its substratum (Siegenthaler 1972). This places constraints on the palinspastic reconstruction of this basin (Pfiffner 1986) and suggests that in eastern Switzerland the flysch basin developed on top of, rather than to the north of the Aar massif.
The Mesozoic sediments underlying the Molasse basin are known from wells (Büchi et al. 1965, Lemcke 1961, 1968, Diebold et al. 1991 and references therein). Their total thickness varies between 800–1000 m. The more important lithologies are sandstones, dolomites, evaporites and shales for the Triassic, shales, marls, sandstones and limestones for the Early to Middle Jurassic, and massive limestones for the Late Jurassic-Cretaceous. Facies changes affect more or less all the units and will be discussed in more detail in chapters 8.2 and 8.3. Eocene lateritic deposits cap the Mesozoic. During the erosional phase the land surface was karstified and Eocene and Early Oligocene laterites rest locally on strata as old as Oxfordian. This erosional phase which spans Paleocene to early Oligocene times corresponds to a phase of compressional deformation of the Alpine foreland (Ziegler 1990), as well as of the Alps themselves (Schmid et al., chapters 14 and 22).
The pre-Triassic basement consists of polymetamorphic gneisses and schists intruded by late-Variscan granites. The basement is transected by a system of Late Paleozoic grabens that are filled with Permo-Carboniferous clastics. These grabens formed in response to post-Variscan transtension and cross the area of today's Molasse basin in an ENE-WSW direction.

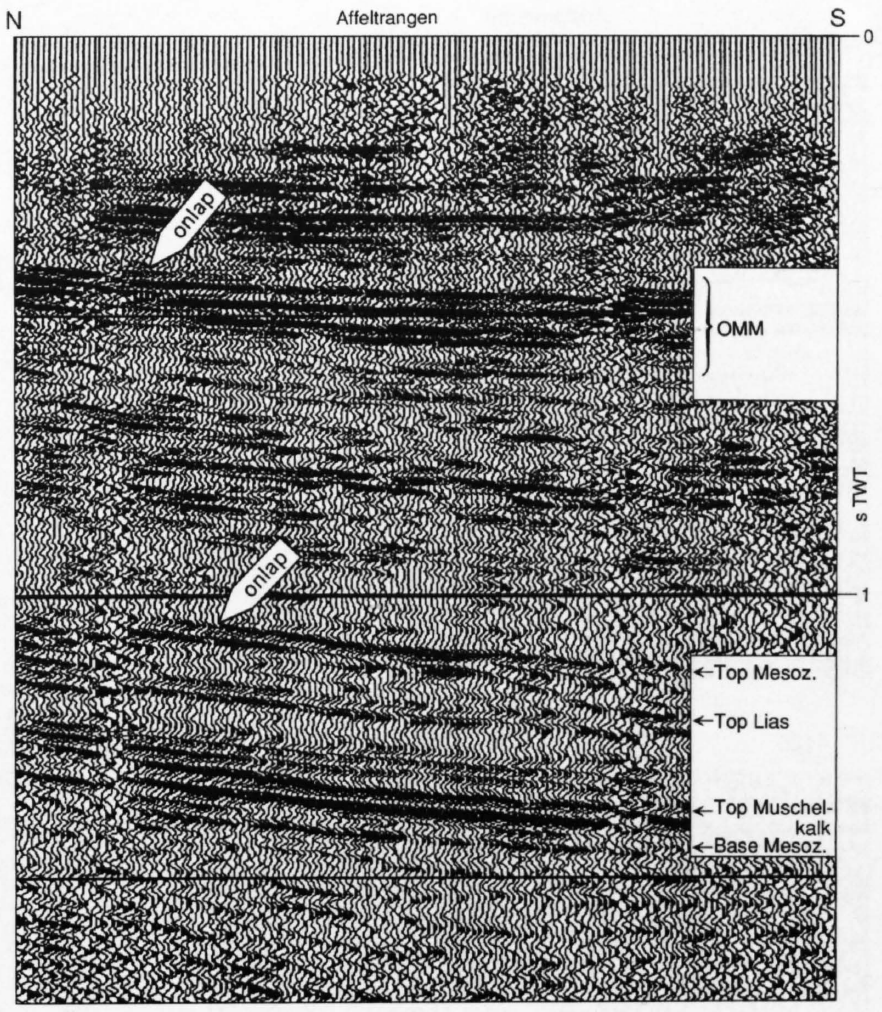

Figure 8-4
Detail of line E6 showing onlaps of USM onto Mesozoic and OSM onto OMM strata.

8.2 The eastern transect (lines E4, E5, E6)

O. A. Pfiffner & M. Stäuble

8.2.1 Seismic data

The seismic sections for lines E4 to E6 are shown in Plates 8-1 to 8-3. There are no wells in this transect to calibrate the observed seismic reflections. The closest published seismic line calibrated by a well is NAGRA line 84-NF-65neu (Diebold et al. 1991), the southern end of which is given in Figure 8-3. As is evident from Figure 8-3, a strong continuous reflection band is generated by the OMM sandstones, possibly by constructive interference of the thick bedded sandstones. The USM is characterized by a series of individual reflections of lower and varying amplitude. They might originate from individual layers of sandstones (and conglomerates in the proximal part) contained within shales. A strong, continuous reflection marks the top of the Mesozoic and corresponds to the interface between shales and Mesozoic carbonates. Within the Mesozoic the top of the Liassic (contact between Middle

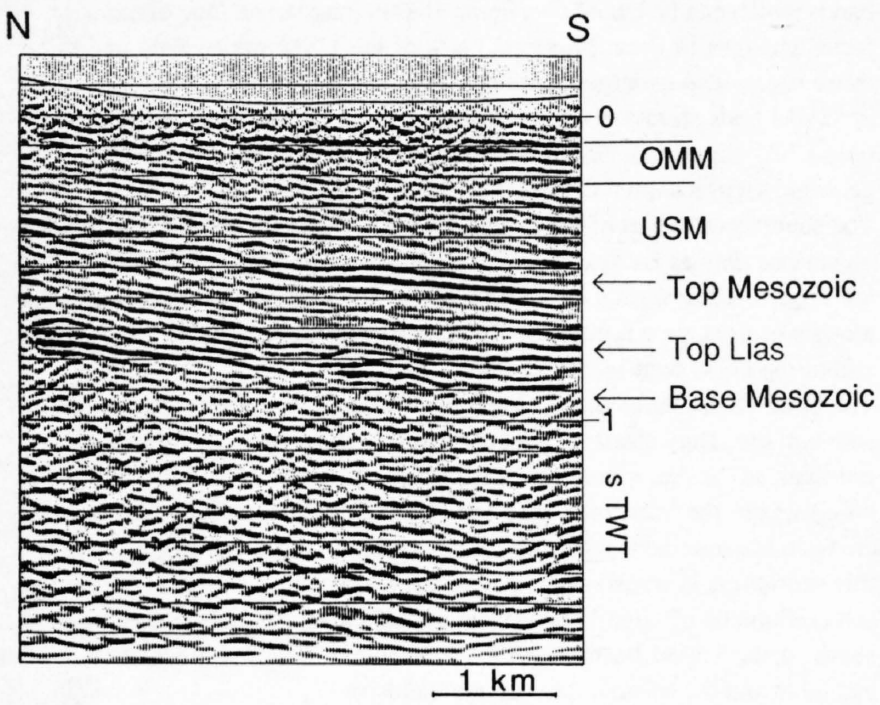

Figure 8-3
Seismic stratigraphy of southern end of NAGRA line 84-NF-65 neu (Embrach area, 20 km N of Zürich).

Jurassic shales and Early Jurassic limestones) and the Muschelkalk can be correlated with relatively strong and continuous reflections. Based on this seismic stratigraphy the observed reflections in lines E4, E5 and E6 were identified as shown in Figure 8-4. A comparison of figs. 8-3 and 8-4 shows a striking similarity in reflection character of the Mesozoic and Tertiary strata. The OMM reflection band can be followed relatively easily southward until the beds are tilted upward (line E5) upon approaching the Subalpine Molasse. The reflections from the Mesozoic strata can also easily be followed across line E6 and into E5. But within line E5 a change occurs somewhere beneath the Subalpine Molasse. In Figure 8-5 two detailed views of the Mesozoic from the north and the south show noteable differences in seismic reflection character. In the north the top Mesozoic reflection is a continuous strong double-cyclic band and several reflections stem from the top Liassic and the Muschelkalk. To the south, in contrast, the top Mesozoic reflection is weaker, but still continuous, reflections from the Lias disappear, and a strong reflection sets in, which derives probably from the top of the Triassic carbonates (Röti dolomite). This same seismic character can be traced southward into lines E4 and E1. Figure 8-6 gives two detailed views of the Mesozoic from line E1. The reflections beneath shotpoint Simmibach (located on the northern end of E1) are indistinguishable from the ones on line E5 beneath Krummenau. Beneath Ragaz the reflections are less continuous for reasons of the complexity of Alpine structures (see Pfiffner et al., chapter 13 for a detailed discussion). Because the Mesozoic strata outcrop a few km south of Bad Ragaz (in the Vättis inlier) the seismic character of the Mesozoic should be compared to that particular sequence. The latter is characterized by a ca. 50 m thick middle Triassic dolomite overlying directly crystalline basement (the Bundsandstein is probably missing). The Late Triassic to Middle Jurassic strata are very thin (30–60m) and in part shaly. They are overlain by thick (1200 m) and massive Late Jurassic-Cretaceous carbonates. Considering the high measured velocities in these carbonates and dolomites (Sellami et al. 1990, and Wagner & Sellami, chapter 6) it is proposed that the strong double-cyclic reflection originates from the top of the dolomite and the weaker, but continuous reflection above from the top-Mesozoic.
From a stratigraphic point of view the Vättis inlier was part of the Alemannic Land (Trümpy 1949), a horst bordered by synsedimentary faults in the Early Jurassic. The northern rim of this high is ill constrained, but must be located between the Aar massif and the southernmost boreholes in the Molasse Basin. It is suggested here that this rim is located beneath the triangle zone bordering the Subalpine Molasse in line E5. The exact orientation of the rim can obviously not be determined from a single seismic line. From a study of the Early Jurassic sediments Trümpy (1949) concluded that both, E-W and N-S oriented faults existed.
An additional feature that emerges from the seismic sections is an increase in thickness of the USM (and to some degree OMM and OSM) strata. For the

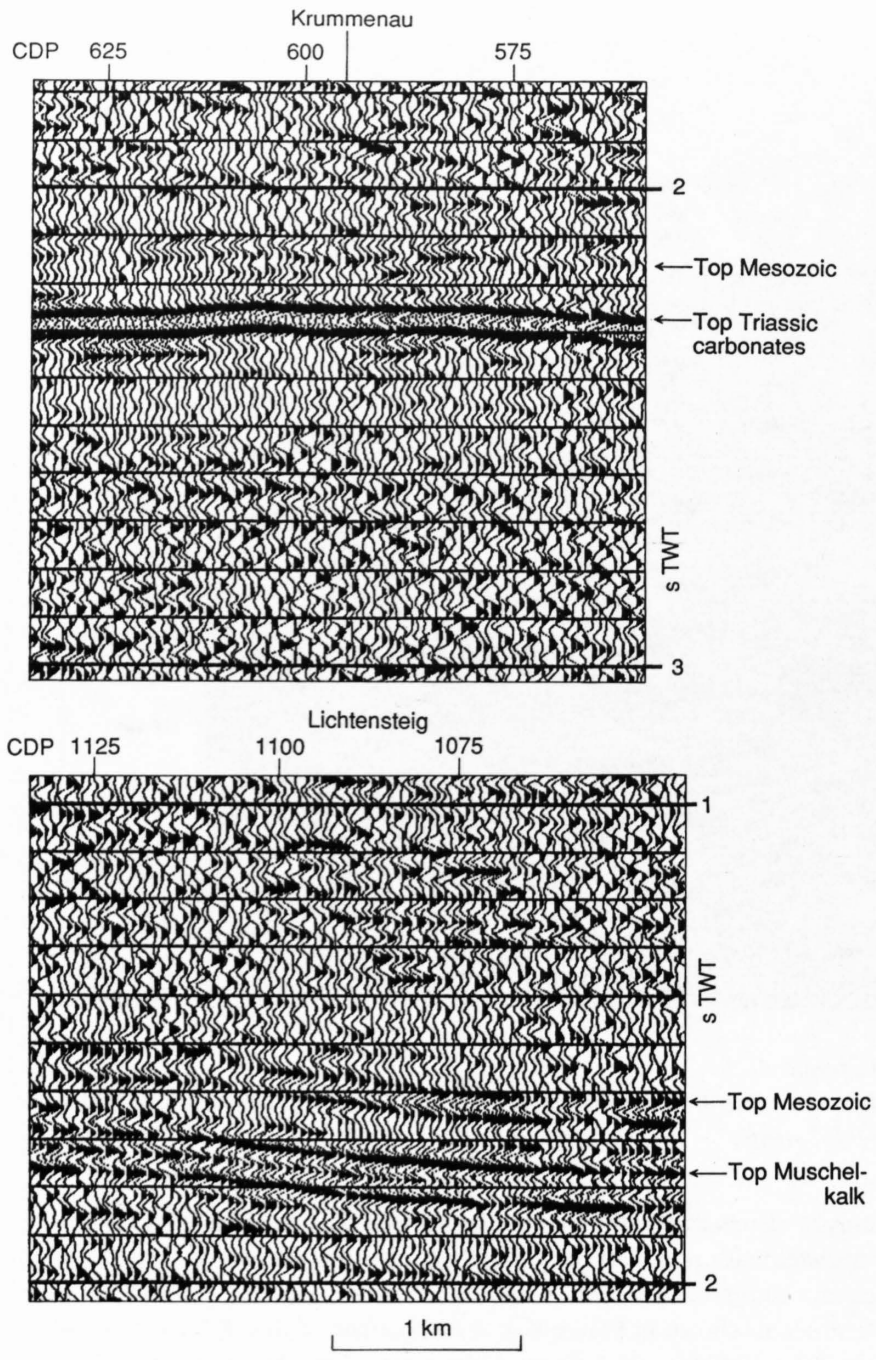

Figure 8-5
Details of line E5 showing differences in seismic stratigraphy of Mesozoic strata beneath Plateau (Lichtensteig) and Subalpine Molasse (Krummenau). Beneath the Subalpine Molasse the top Mesozoic corresponds to a weak reflection and a strong double-cyclic reflection derives from the top of the Triassic carbonates (Röti dolomite).

OSM and the USM this thickness increase is related to onlaps (see Figure 8-4). In the case of the UMM an important thickness change occurs beneath the triangle zone bordering the Subalpine Molasse in our interpretation. It is shown to coincide more or less with a discontinuity in the gentle southerly dip of the Mesozoic (see Figure 8-7). The transgression of the UMM beds following Eocene faulting and uplift of the North-Alpine foreland progressed from east to west (Bachmann et al. 1982, 1987, and Herb 1988) and the northwestern pinchout of the UMM is to be expected in the vicinity of the triangle zone proposed here. In our interpretation reactivated Tertiary faults (controlled by the presence of Early Jurassic faults?) are incorporated to constrain the kinematic evolution.
Figure 8-7 contains hand-made line drawings of the seismic sections E5 and E6, which highlight the principal seismic structures. Based on the preceeding discussion on the seismic stratigraphy the reflection groups a-f can be identifed as follows: a = top Mesozoic, b = top Muschelkalk, c = base Mesozoic, d = intra-USM, e = OMM, f = intra OSM.

8.2.2 Geologic interpretation

The geologic profile shown in Figure 8-8 is a straight section following the seismic lines as close as possible. The geologic interpretation was based on the seismic stratigraphy as discussed above (Figures 8-3 to 8-7), on migrated seismic sections and on 2D seismic modeling (see Stäuble & Pfiffner 1991). Several faults affecting the Mesozoic strata can be recognized along lines E5 and E6 (see Figure 8-8). Some of them seem to be restricted to the Mesozoic while others clearly dissect the Molasse sediments and even relate to faults mapped at the surface. These faults include both, reverse and normal faults and often border tilted blocks, suggesting that they are in part listric at depth. As most of the observed offsets are apparent offsets only, a structural interpretation based on a single seismic line is very difficult or maybe even misleading. The faults that can be matched with surface mapping mark the border of narrow, WSW-ENE trending grabens (Hoffmann 1988, Atlas sheet 1073 Wil).

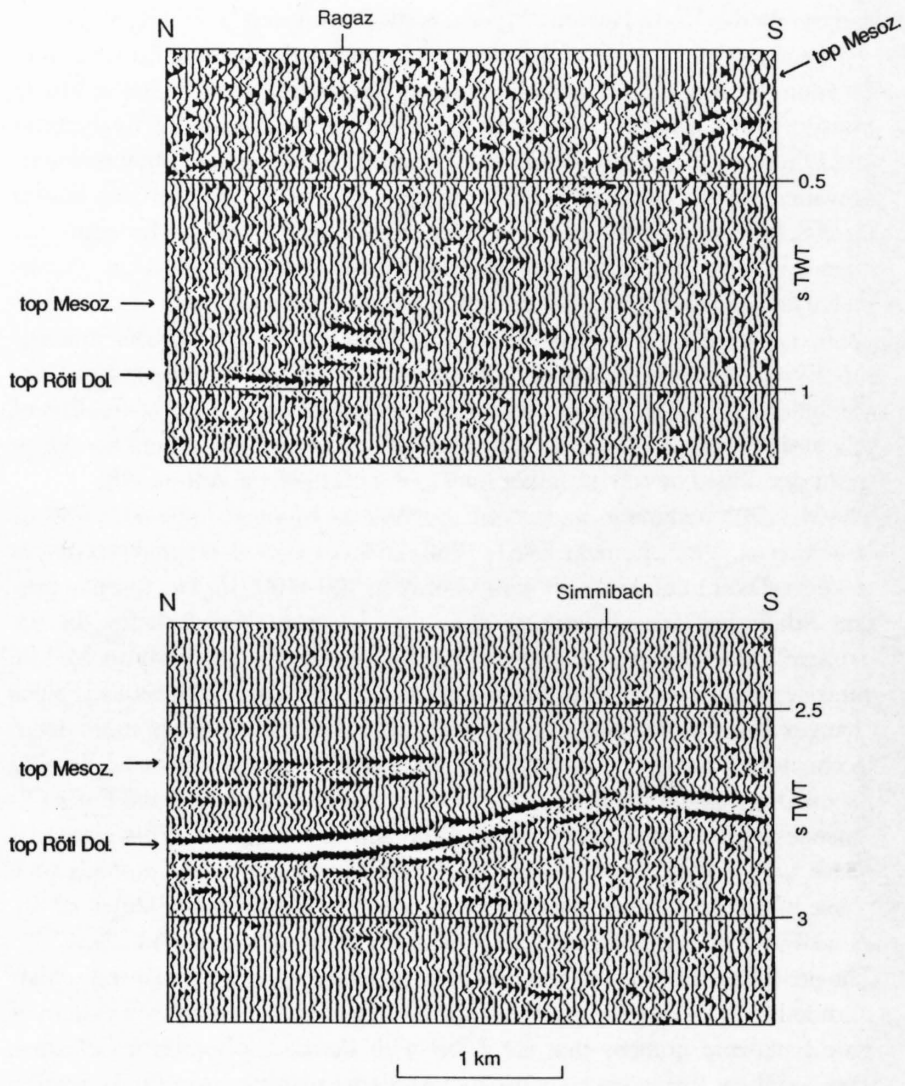

Figure 8-6
Detail of line E1 showing seismic stratigraphy of Mesozoic strata beneath Subalpine Molasse (Simmibach) and North-Helvetic Flysch (Ragaz). Similar to Figure 8-5 / Krummenau a weak reflection is likely to be correlated to the top Mesozoic and a strong double-cyclic band to the top Triassic carbonates (Röti dolomite). Reflections are less continuous beneath Ragaz – located on the northern flank of the Aar massif – due to scattering and defocussing of seismic energy.

The triangle zone between the Plateau and Subalpine Molasse shows up clearly in the seismic section (Figure 8-7) as sets of reflections with opposite dips. The structural interpretation based on surface data (namely Habicht 1945) shows a north dipping thrust fault underlying the tilted upper USM, OMM and OSM beds of the Plateau Molasse with a movement "top to the south" ("Randunterschiebung" in the older literature). An eastward continuation of this triangle zone has been documented in the Bavarian molasse (Müller et al. 1988).
Within the Subalpine Molasse several thrust sheets can be distinguished. The beds are dipping steeply at the surface and the corresponding reflections are seen to flatten out at depth. The thrust sheets were detached along the shaly middle UMM beds. In map view the latter outline the thrust faults as narrow bands which can be traced over some 10km along strike. Due to rapid lateral facies changes in these proximal parts of the USM gravel fans, individual thrust sheets also undergo lateral changes. e. g. the steep anticline with a core of UMM beds shown in Figure 8-8 appears as a thrust fault putting UMM onto USM slightly farther to the NE (on the actual trace of line E5 and the geologic section shown in Stäuble & Pfiffner 1991).
The southernmost part of the geologic section (Figure 8-8) is based primarily on surface data as far as the Helvetic nappes is concerned. The deeper parts are projections from lines E4 and E1 (the geologic profile was constructed along a straight trace rather than the slalom of the seismic line). The southern end of the USM beds is speculative.
The basal thrust faults of the Subalpine Molasse thrust sheets are shown to sole out, too. They clearly do not cut down into the basement until the northern flank of the Aar massif (see Pfiffner et al., chapter 13). Therefore shortening within the Subalpine Molasse must kinematically be linked to shortening in the basement within the northern flank of the Aar massif. The way this shortening is transferred through the UMM and the North-Helvetic flysch (sediments of slightly older age deposited in a trough situated slightly south of the UMM basin) is difficult to assess. There are no surface data available and the seismic data are inconclusive.

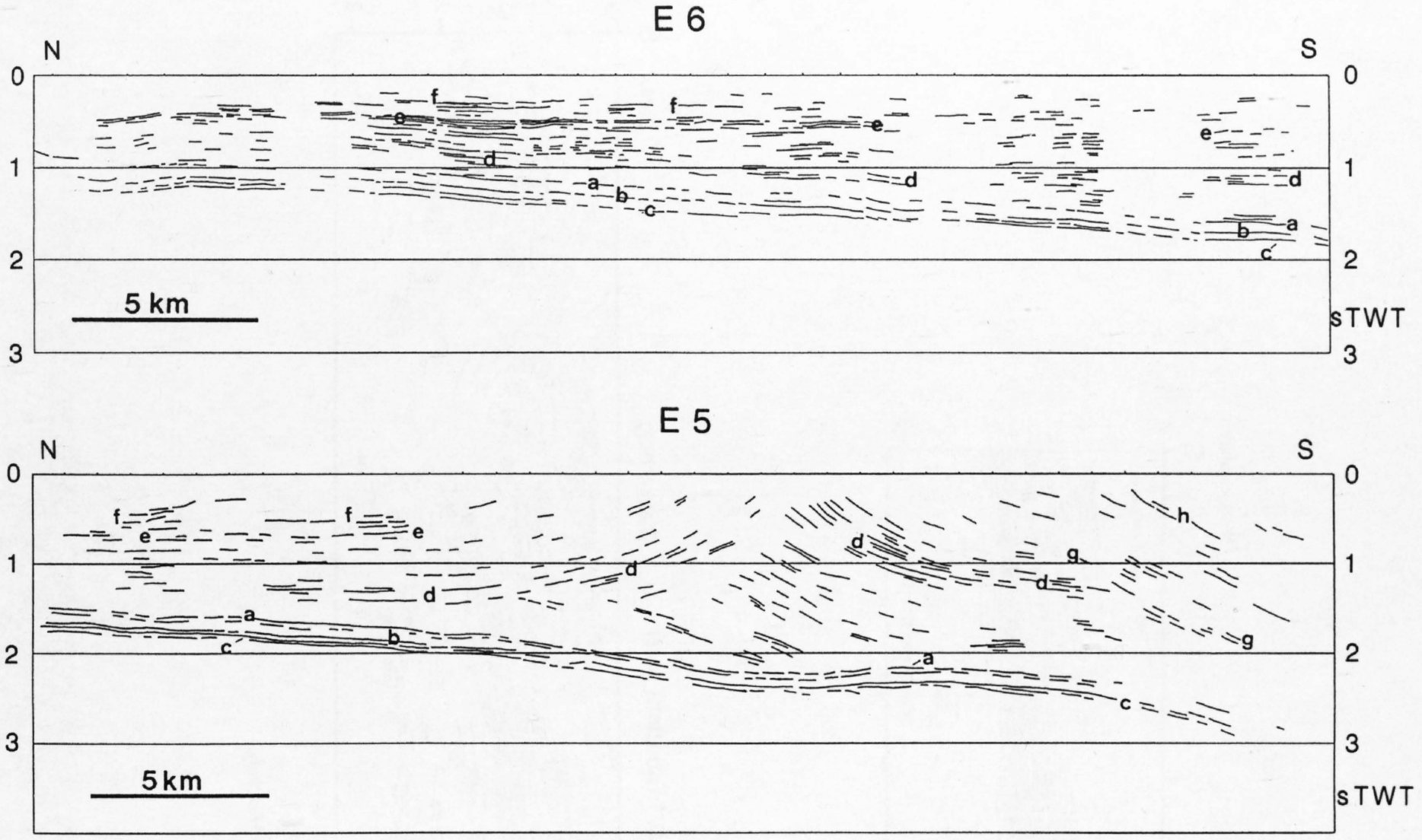

Figure 8-7
Line drawing of seismic lines E5 and E6 crossing the Molasse Basin of eastern Switzerland.
a = top Mesozoic, b = top Triassic Muschelkalk, c = base Mesozoic, d = intra-USM, e = OMM, f = intra-OSM, g = base of thrust sheet (USM), h = UMM

8.3 The western transect (lines W1, W7, W8, W9, W10)

O. A. Pfiffner & P. F. Erard

8.3.1 Seismic data

The western transect consists of a number of relatively short seismic lines which are in part considerably curved (see Figure 8-1). The seismic sections for lines W7 and W10 are shown in Plates 8-4 and 8-5. In contrast to the eastern transect a calibration of the seismic lines with well data is possible in this western transect. The most useful borehole, Hermrigen, is a short distance off line W10. The available markers (taken from a litholog from NEFF 1982) are shown on the reprocessed seismic line (see Figure 8-9). A well marked double-cyclic band can be correlated with the top of the Mesozoic. At this particular locality a few meters of Cretaceous overly the massive Late Jurassic limestones. As mentioned earlier, the Mesozoic is capped by Eocene and Early Oligocene lateritic deposits. Erosion with karstification removed much of the younger Mesozoic section. The Cretaceous, more complete in the outcrops to the north of line W10, disappears completely to the south of line W10. A series of prominent and continuous reflections correlate with the Middle Jurassic. The Middle Jurassic sections maintains ist great thickness towards the west (see Sommaruga & Burkhard, chapter 7.1), but thins out in the adjacent area to the east (NAGRA line 83-NS-22 in Diebold et al. 1991). The next deeper prominent reflection marks the top of the Lower Jurassic. This reflection can be observed throughout the Molasse Basin and seems to originate from the interface of Early Jurassic limestones and Middle Jurassic shales (see Diebold et al. 1991). A prominent reflection band correlates with the Middle Triassic, the uppermost loop corresponding to the top ot the Muschelkalk. The well Hermrigen did not penetrate the base of the Muschel-

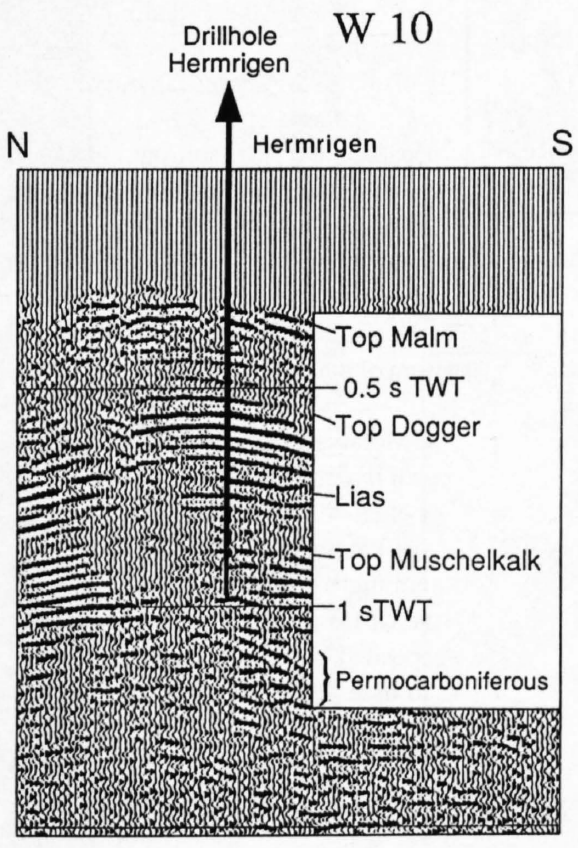

Figure 8-9
Seismic stratigraphy of line W10 correlated to borehole data of Hermrigen well (projected).

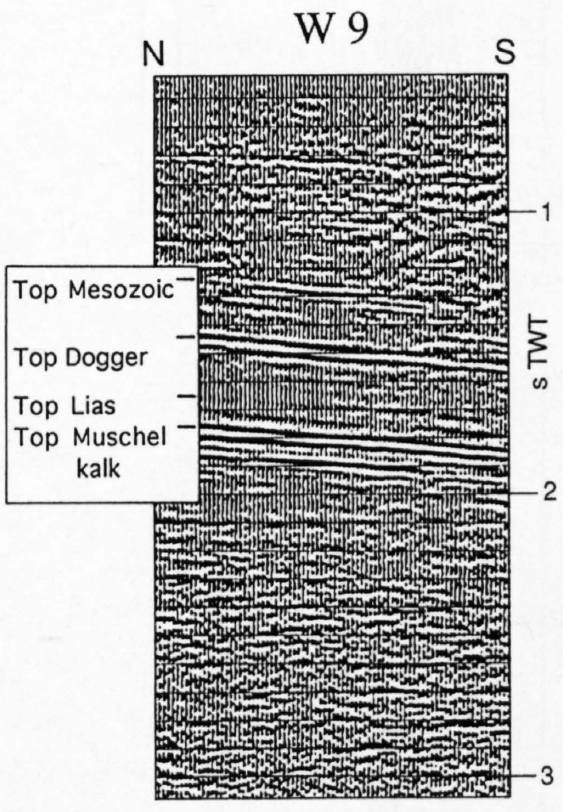

Figure 8-10
Detail of line W9 (southern end) showing seismic stratigraphy. The main difference to Figure 8-9 are strong continuous reflections from the lower part of the Malm.

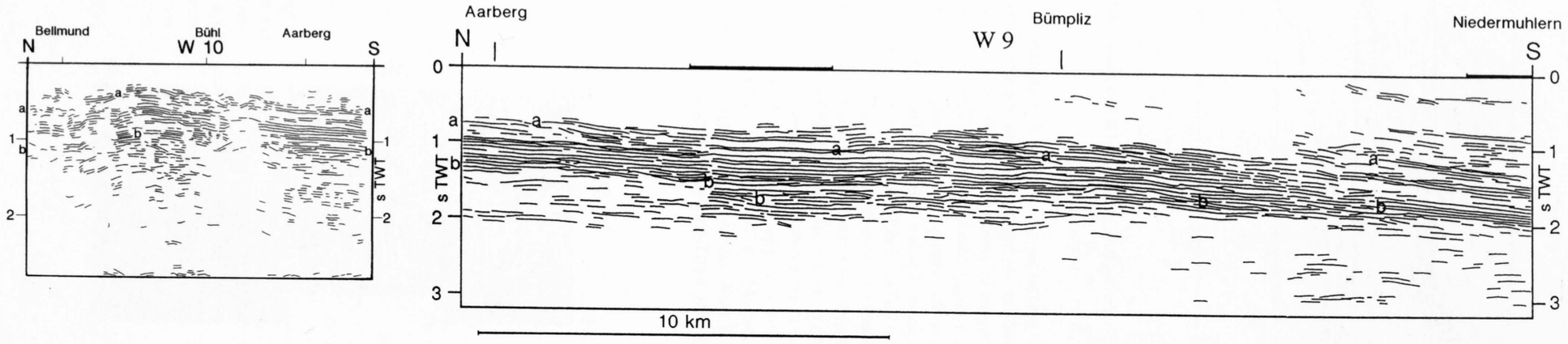

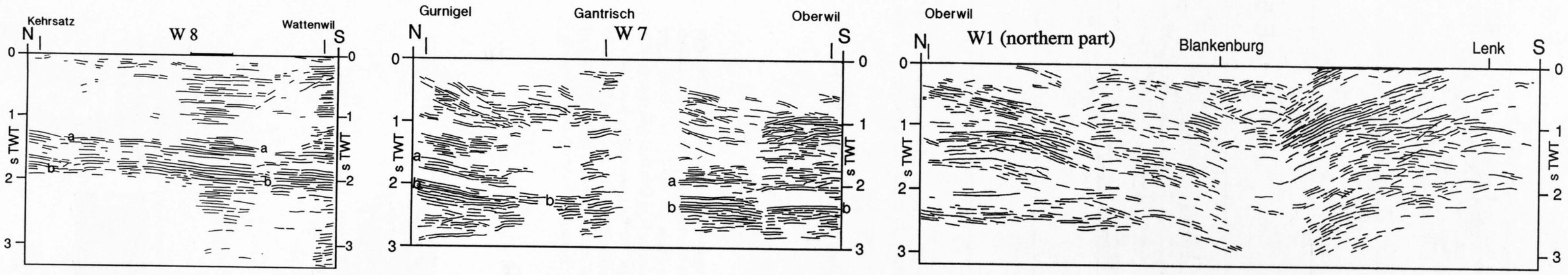

Figure 8-13
Line drawing of unmigrated seismic lines W1, W7, W8, W9 and W10 crossing the Molasse Basin of western Switzerland. a = top Mesozoic, b = top Triassic Muschelkalk. Position of Figures 8-10, 8-11 and 8-12 is given as thick line segment in lines W9 and W1

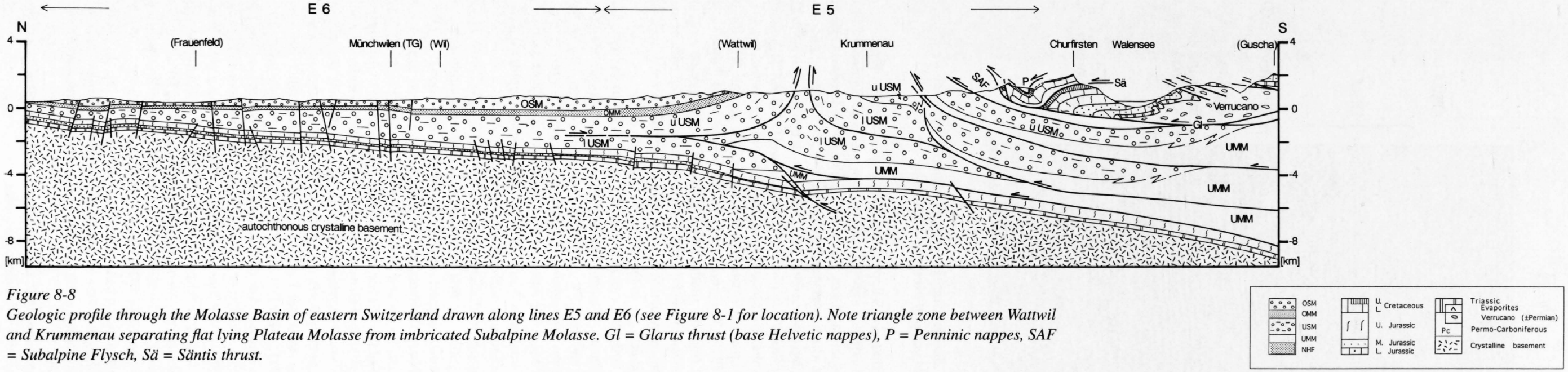

Figure 8-8
Geologic profile through the Molasse Basin of eastern Switzerland drawn along lines E5 and E6 (see Figure 8-1 for location). Note triangle zone between Wattwil and Krummenau separating flat lying Plateau Molasse from imbricated Subalpine Molasse. Gl = Glarus thrust (base Helvetic nappes), P = Penninic nappes, SAF = Subalpine Flysch, Sä = Säntis thrust.

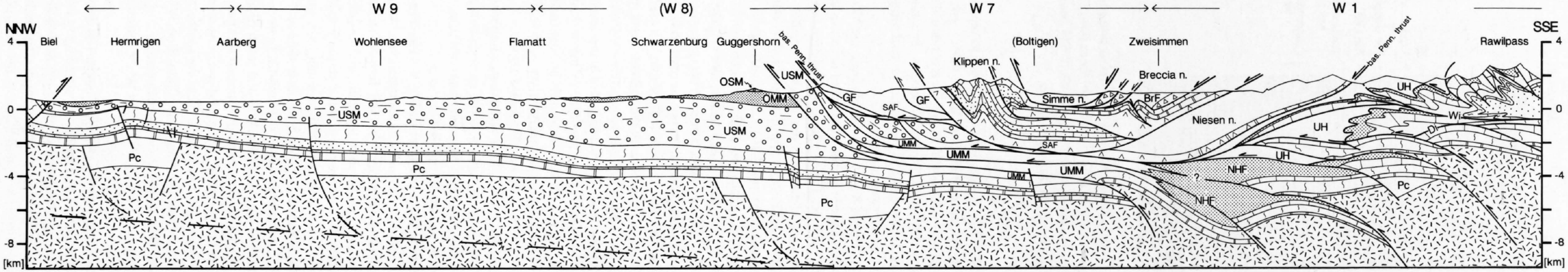

Figure 8-14
Geologic profile through the Molasse Basin of western Switzerland drawn along lines W1, W7, W8, W9 and W10 (see Figure 8-1 for location). Note decapitated thin imbricates within Subalpine Molasse thrust onto Plateau Molasse. OMM is at higher elevation compared to eastern Switzerland (Figure 8-8). BrF = Breccia nappe flysch, Di = Diablerets nappe, GF = Gurnigel Flysch, NHF = North-Helvetic Flysch, Pc = Permo-Carboniferous, SAF = Subalpine Flysch, Wi = Wildhorn thrust, UH = Ultrahelvetic nappes.

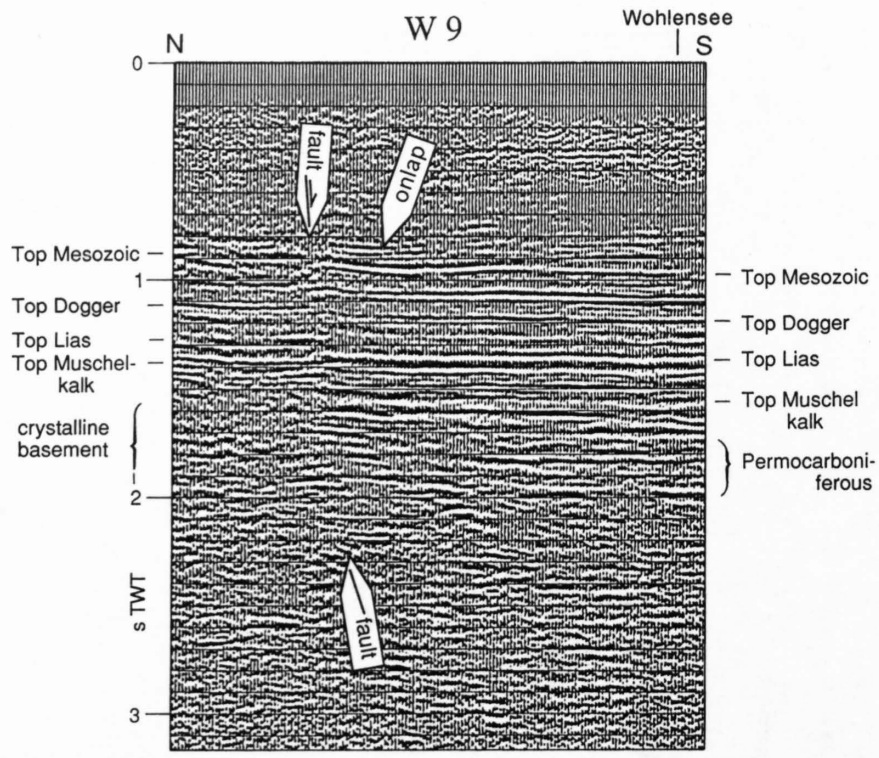

Figure 8-11
Detail of line W9 showing a long lived synsedimentary fault dissecting the Mesozoic (including Triassic evaporites). The fault is at the northern limit of reflections interpreted to stem from Permo-Carboniferous beds. USM beds show onlap onto the Mesozoic strata in the vicinity of the fault.

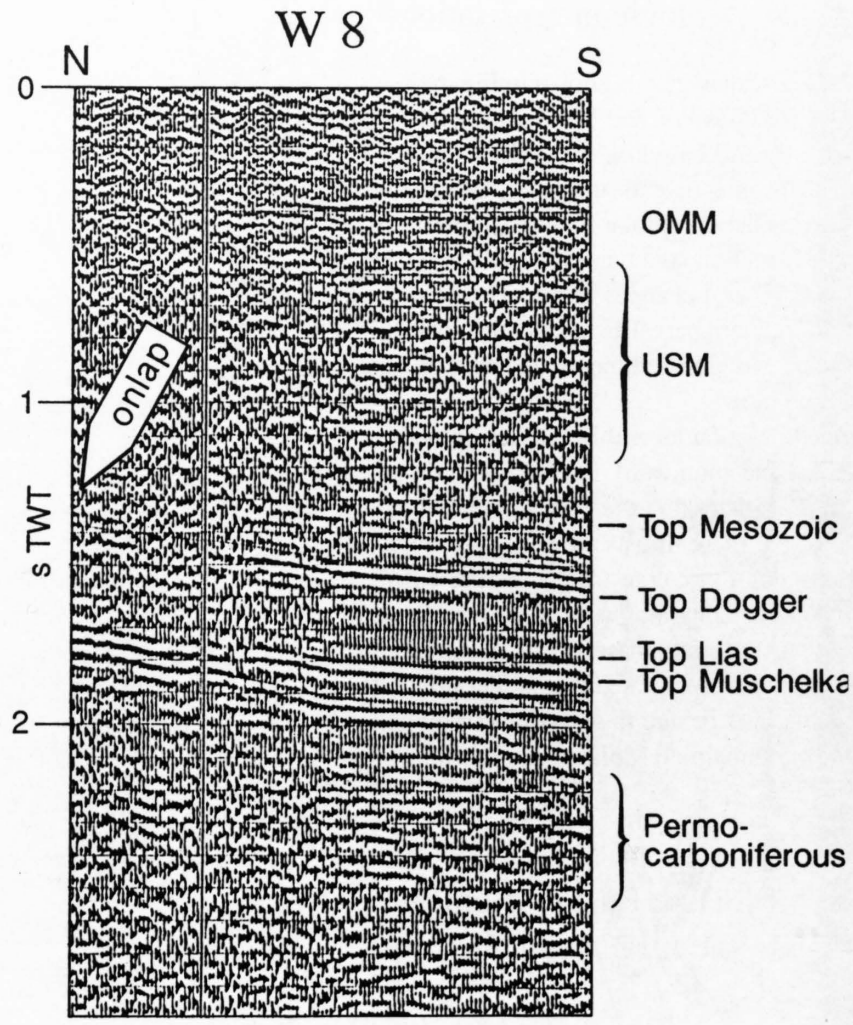

Figure 8-12
Detail of line W8 showing strongly dipping Mesozoic strata above Permo-Carboniferous, and onlap of overlying USM beds.

kalk. Several reflections below 1s TWT in Figure 8-9 do not seem to represent multiples but rather suggest the presence of Permo-Carboniferous sediments. The strongly S-dipping reflection beneath 1s TWT are possibly refractions from a thrust fault cross cutting the Mesozoic section. Seismic resolution of the Tertiary strata is rather poor due to the particular recording conditions. This is true for much of the western transect.

The seismic stratigraphy observed in Figure 8-9 can be traced across the Molasse Basin with some minor changes. Line W9 shows a marked decrease in thickness of the Lower and Middle Jurassic. The regularly spaced high amplitude reflections from the Middle Jurassic give way to a single strong double cyclic reflection above a band of weak, laterally discontinuous reflections (see e. g. southern end of line W9 shown in Figure 8-10). Likewise the reflections from the Lower Jurassic strata thin southward until only one double-cyclic high-amplitude band is left at the southern end of line W9 (Figure 8-10). Within the upper Jurassic strata a strong reflection band becomes successively more prominent. The Mesozoic succession is cut by a marked fault downthrowing the southern block within the northern half of line W9 (see Figures 8-11, 8-13 and 8-14). Reflections from beneath the Triassic strata in the southern block at 1.8-2 sTWT are slightly oblique to the Triassic strata and pinch out in the southern half of line W9. This is interpreted to represent a halfgraben containing Permo-Carboniferous strata bordered by the normal fault mentioned before. It is interesting to note that above this normal fault the upper-Jurassic sediments are overlain uncomformably by younger sediments. The onlap is particularly well visible following the high-frequency reflections on the southern block (Figure 8-11). These reflections disappear southward into the "noisy" transparent looking Tertiary strata; most probably they represent USM strata. It thus seems that this particular fault of Permo-Carboniferous age was reactivated during the Tertiary (?Oligocene).

The seismic character does not seem to change much across line W8 (see Figure 8-13). However, the Mesozoic in this line defines a broad monocline with a relatively steeply south dipping limb. Reflections from the Tertiary strata overlying this limb are subhorizontal, suggesting an onlap configuration (see Figure 8-12). This situation resembles the one observed in the northern half of line E5 in the eastern transect, which is also located at the southern margin of the Plateau Molasse. The reflections underlying the Mesozoic in the southern half reaching down to 2.5 sTWT are interpreted as a Permo-Carboniferous graben bordered by normal faults to the north (line W8) and south (line W7). Near the center of line W8 a high frequency band of continuous reflections between 0.3 and 0.7 sTWT could correlate to the OMM sandstones which are expected at that depth (Figures 8-12 and 8-13). Near the southern end (about above the two faults dissecting the Mesozoic strata) line W8 crosses into the Subalpine Molasse. The corresponding structures, the Seftigschwand and Fuchsegg imbricates (see Blau 1966) cannot be recognized in the seismic section.

Line W7 crosses the Gantrisch chain of the Penninic Klippen nappe. The data gap corresponds to an area of difficult access and moreover to an important bend (see Figure 8-1). Apart from the northernmost segment the Mesozoic section is flat. Near the southern end it is cut by an important normal fault with a throw down to the south (see Figures 8-13 and 8-14). In the shallow part in the north, both southdipping and horizontal reflections can be observed. They are interpreted as being derived from a stack of imbricate thrust sheets of the Subalpine Molasse, the floor thrust of which is taken to be at around 1s TWT (at which level the southdipping reflections become subhorizontal). The basal thrust of the Gurnigel Flysch, which outcrops just south of the northern end of line W7, is assumed to be at around 0.3 sTWT. It more or less truncates the Subalpine Molasse imbricates beneath it, a relationship that can be inferred from surface data east and west of the seismic line (Blau 1966, Caron et al. 1972). The prominent reflection band at 0.8 -1.3 sTWT extending northward from the southern end of line W7 is interpreted to stem from the Triassic evaporite and dolomite sequence marking the base of the Klippen nappe. This detachment horizon rises northward to break surface slightly north of the data gap in the seismic line (Figure 8-13).

The southernmost line, W1, contains data aquired by NRP 20 and industry (northernmost segment). The autochthonous Mesozoic strata can be traced from the northern end (at 1.5 to 2.5 sTWT) into the northern flank of the basement uplift of the external massifs discussed in detail by Pfiffner et al. in chapter 13. The Mesozoic dips southward and is at its greatest depth of 2.5-3 sTWT at the front of the basement uplift. This basement uplift itself occupies much of the southern half of line W1 and is associated with a rise of the Mesozoic sequence to shallower depths (ca. 0.8 -1.3 sTWT)by folding and imbricate thrusting. A first compressional structure within the autochthonous Mesozoic is suspected in the dome shaped reflections at 2 sTWT just north of shotpoint Blankenburg. The prominent reflection band at the northern end of line W1 located at 0.8-1.3 sTWT seems to represent the southern extension of the Triassic evaporites and dolomites from the base of the Klippen nappe described above (line W7). It is expected to rise southward and to break surface between shotpoints Blankenburg and Lenk. Some relatively faint northdipping reflections at 0-0.3 sTWT at that location could in fact represent these strata (see Figure 8-13). The prominent reflection band just beneath (at 0.8 -1.2 sTWT) is likely to represent an evaporite layer at the base of the Niesen nappe and/or the Ultrahelvetic thrust sheets (see Pfiffner et al., chapter 13). The shallower reflection band at the northern end of line W1 situated at 0.3-0.5 sTWT does not extend northward into line W7. Southward it disappears within the Klippen nappe and may well rejoin the evaporites at the base of this nappe. An important thrust fault putting Triassic strata onto Cretaceous strata and Flysch has been mapped north of Boltigen (see Rabowski 1912 or Plancherel 1979). Laterally this thrust fault links up with the Gastlosen thrust, a major fault (see Mosar 1991, Figure 2a). Its southward extension in the subsurface lines up with the upper reflection band just described which suggests that the Klippen nappe consists of two larger subunits in this transect.

Figure 8-13 contains hand-made line drawings of all of the seismic sections, which highlight the principal seismic structures.

8.3.2 Geologic interpretation

The geologic profile shown in Figure 8-14 is drawn along a straight line following lines W1 and W10 closely but avoiding the bend in line W8. It was constructed based on the seismic data discussed above and on surface data. The profile reveals that the Mesozoic strata generally dip southward to greater depths similar to the eastern transect (Figure 8-8). However, the Mesozoic section is not an even surface. Rather it is dissected by faults and contains several changes in dip. The deformed nature is particularly evident in the southern part. The age of this block-faulting is younger than the Miocene, tilted Molasse sediments and thus in part coeval with folding of the Jura Mountains.

The thrust faults within the Subalpine Molasse are shown to sole out downward and southward. Further south they must cut into the basement, similar to the situation in the eastern transect. However, in contrast to that transect, some of these thrusts are thought to rejoin the basal Penninic thrust at depth and then to diverge from it before cutting into basement. This solution reflects the comparatively thin zone of Molasse sediments available between the (deep lying) base of the Penninic nappes and the underlying autochthonous Mesozoic sediments. The comparatively small thickness of the USM strata may be due to scooping out by thrusting and/or to substantial erosion of the Subalpine Molasse prior to the arrival of the overlying Penninic nappes.

8.4 Molasse Basin tectonics and its relation to the Jura Mountains

O. A. Pfiffner

One of the pronounced differences between the eastern and western transect is today's elevetion of the youngest infill of the Molasse Basin. In western Switzerland much of the younger section (noteably OSM beds) are removed by erosion and the OMM beds, marking sea level in Burdigalian times, are at much higher altitudes (Lemcke 1974, Laubscher 1974, NAGRA 1988, Gorin et al. 1993). The top OMM is 800 to 1200 m above sealevel in the west, as compared to – 500 to +100 m in the east, the base OMM 600 to 800 m in the west and – 800 to – 200 m in the east. This component of vertical uplift, the **"Resthebung"** has been analyzed by Lemcke (1974) and Laubscher (1974) who postulated a vertical uplift of 1000 – 2500m in the western Swiss Molasse Basin. Laubscher (1974) tried to distinguish between effects of a south-dipping decollement horizon beneath the Molasse Basin on one hand, and a true regional basement uplift on this vertical component of uplift on the other hand. He concluded that true basement uplift contributed a few hundred meters only, and that most of the uplift was due to shortening related to **folding of the Jura Mountains**. For this Jura shortening the **"distant-push hypothesis"** (Fernschubhypothese) was advocated. This hypothesis was put forward by Buxtorf (1907) and Laubscher (1961) and postulates a transfer of the shortening within the crystalline basement (necessary to accomodate shortening within the Mesozoic cover) through the Molasse basin into the Alps (see Jordan 1992 for a review). It requires a major detachment along Triassic evaporites. However such a detachment can only occur along a somewhat smooth surface. The irregular surface dissected by normal faults and containing tilted blocks speaks against such a hypothesis. To overcome these difficulties a solution whereby the detachment branches towards the south beneath the Plateau Molasse was suggested by Jordan (1992). The upper fork of the detachment is thought to cut up-section, the lower one down into basement. In such a solution, only the northern half (north of the two forks) of the Mesozoic section beneath the Molasse Basin would be detached. In the case of a large displacement (as e. g. the 15 km in this transect estimated by Laubscher 1965, Figure 6), high amplitude anticlines above the lower fork and gaps in the Mesozoic in the upper fork would be the inevitable consequence. Both features are not observed in the western transect, rendering the explanation by a branching detachment unlikely. Thus additional possibilities for basement shortening associated with Jura folding must be explored (see below). Based on an analysis of reflection seismic data in the western Swiss Molasse Basin, Gorin et al. (1993) came to the conclusion, that a large-scale translation of the Mesozoic-Cenozoic strata is not supported by the data.

In Laubscher's model (1974) a decollement inclined at 5.3° and accomplishing a shortening of 15 km in a profile forming more or less the continuation of the western transect discussed here, results in 1300 m vertical uplift. The new seismic data suggest that the potential decollement horizon is inclined at 3.5° only and thus the vertical uplift in such a model would be 880 m only, far less than observed. Given the discrepancy between the observed and calculated vertical uplift on one side and the "bumpy" geometry of the potential detachment horizon discussed above, the "distant-push" hypothesis is questionable. An alternative hypothesis suggested here consists in having the **uppermost basement** involved in the Jura shortening. This uppermost basement would include the Permo-Carboniferous grabens, which in turn could be responsible for its involment (see below). As discussed earlier, inversion of such a graben might explain the Hermrigen anticline (line W10) and the Flamatt monocline (line W9). Similar inversions are also described from the North-Swiss Permo-Carboniferous Fricktal-Konstanz trough (NAGRA 1988, Fig 4-4, and Diebold et al. 1991). Also Ziegler (1990) evoked the possibility that the Jura Mountains represent a deeply inverted basin, with involvment of the underlying crystalline basement.

One of the key parameters that needs to be assessed for the postulated hypothesis of a basement involvement is the depth of detachment, i. e. the thickness of this basement. This is done using the following simple model combining area and bed-length balancing (see Figure 8-15): A wedge consisting of Mesozoic and Tertiary (Molasse) sediments of known thickness and bedlength, and of pre-Triassic basement of unknown thickness is pushed up an inclined basal detachment plane and internally shortened into the configuration observed today. Figure 8-15 shows a restored section of this wedge at the end of the OMM sedimentation. The (restored) width of the Jura Mountains (50 km) is based on the estimated shortening of 15 km by Laubscher (1965). For the Plateau Molasse a restored width of ~45 km (with 1 km of shortening) is inferred from the geologic cross section in Figure 8-14. Contracting this wedge by 16 km (15 km Jura shortening, 1 km Plateau Molasse shortening) and raising the southernmost OMM outcrop (Guggishorn) to its present elevation of 1200 m above sea level, corresponds to a dip of 3.1° for a planar SSE-dipping detachment horizon (which is very close to the 3.5° deduced for the Mesozoic strata from the seismic time sections and poorly constrained velocities).

In a next step the depth to detachment is calculated by equating curvimetric (16 km) and "volumetric" (areal) shortening. The areal shortening is deduced from the excess area defined by the shortened and uplifted top-OMM reference horizon (see Figure 8-15). In the Jura Mountains the top OMM is located at an average altitude of 2100 m above sea level in the southern chains (mostly eroded) and around 1100 m to the north, averaging 1600 m for the entire chain. In the Plateau Molasse this same horizon rises from 800 m above seal level at the northern margin to 1200 m at the southern margin. The total excess area can thus be estimated at ~100 km^2, which upon curvimetric balancing, gives a depth to detachment of 6.25 km. This depth, referred to the southern end of the wedge, is slightly more than 1 km beneath the top basement, i. e. significantly beneath the Triassic evaporites. A depth to detachment corresponding to the Triassic evaporites would require 20 km (instead of 15 km) curvimetric shortening or a smaller excess area. The 15 km shortening of Laubscher (1965, Figure 6) is on the high side, however, since this

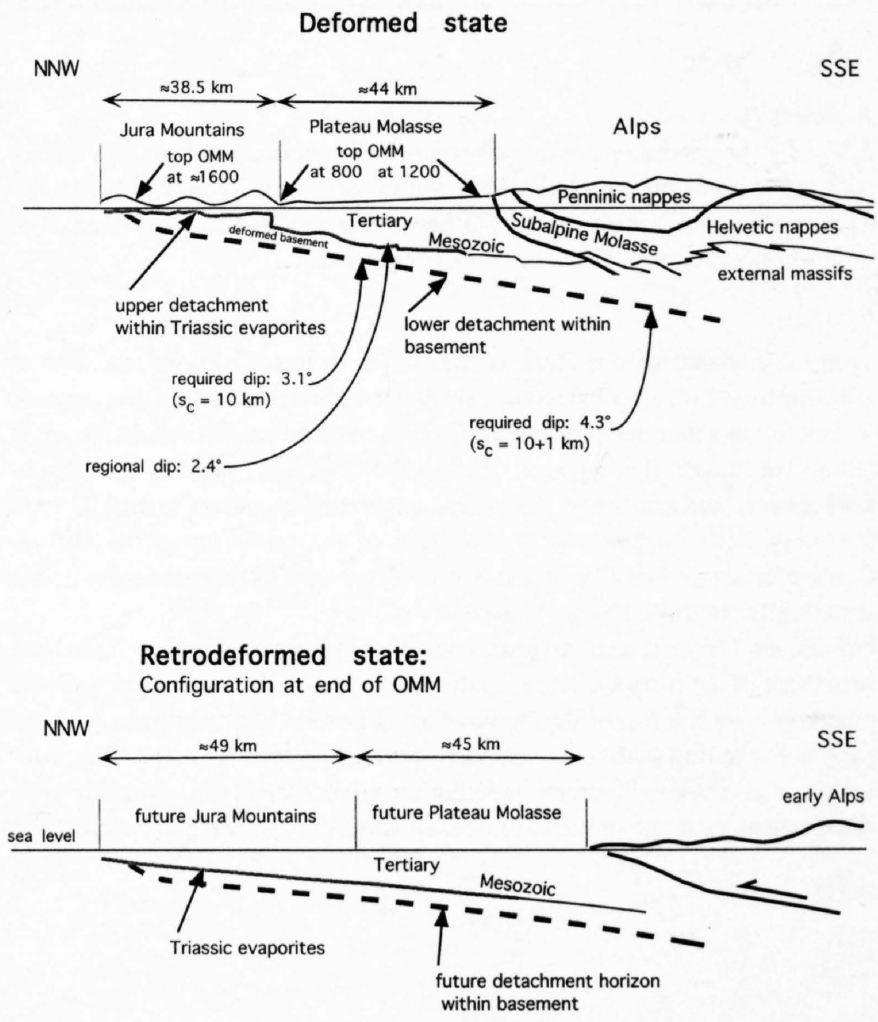

Figure 8-15
Retrodeformed and deformed state of western Swiss Molasse Basin and Jura Mountains. The Triassic evaporites give way to carbonates in the southern part of the Plateau Molasse. The detachment horizon within basement is taken to be subparallel to the overlying Mesozoic strata.

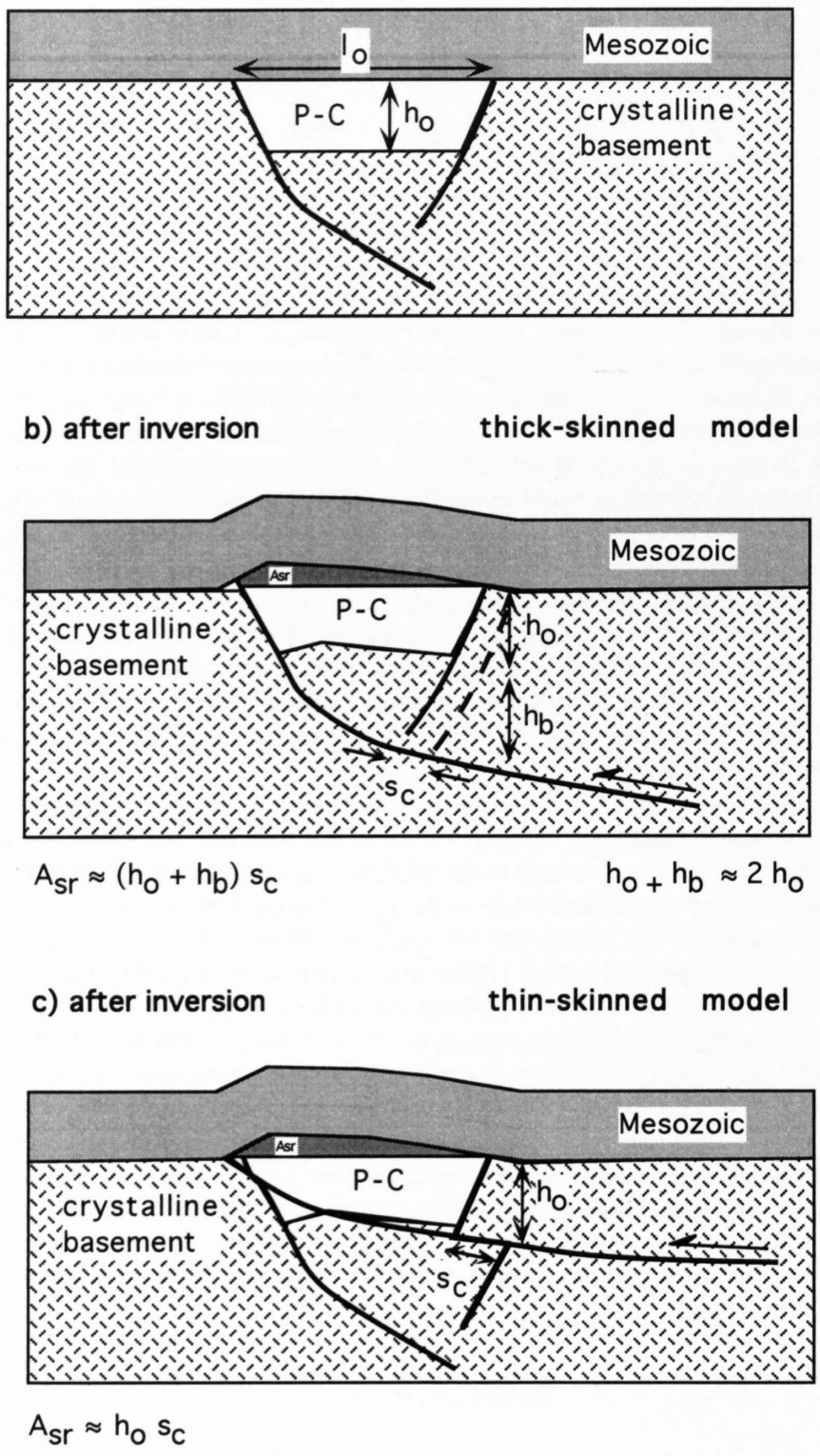

Figure 8-16
Effects of the partial inversion of Permo-Carboniferous grabens. The Mesozoic strata form an anticline above the squeezed-out graben fill. The two graben shoulders approach each other as the graben is compressed. A_{sr}: area of structural relief, s_c: curvimetric shortening.

author speculated on a shallow (evaporite) detachment. The excess area of 100 km^2 used here is considered reasonable and relatively well constrained. It thus follows that the detachment horizon must be sought within the crystalline basement, dipping at 3–3.5° to the SSE and, separating authochthonous foreland crust from a detached uppermost basement of around 1 km thickness. This thickness is of the order of the thickness of the Permo-Carboniferous graben fills and it is speculated that the basement-faults are structurally controlled by these graben structures.
Indications for reactivation (inversion) of these grabens are the anticlinal structures in the Molasse Basin as discussed above. An inversion of such a graben raising the top of the Permo-Carboniferous to an antiform necessitates a shortening across the graben, approaching the two shoulders consisting of crystalline basement (see Figure 8-16). One is thus forced to conclude that at least one of the basement shoulders is displaced horizontally to some extend. Such a displacement can be thought of as taking place in a thin-skinned manner on a subhorizontal fault at the level of the deeper part of the graben infill (Figure 8-16). Another possibility would be a listric shaped fault cutting deeper into basement (thick-skinned model in Figure 8-16). Deeper reaching faults would require a ductile deformation of the crystalline basement, which is unlikely under the low temperatures expected. The area of structural relief defined by the emergent anticline of the Mesozoic strata (dark shading in Figure 8-16) is directly related to the displacement (curvimentric shortening) and the depth of detachment of the moving basement block. If movement of a rigid crystalline basement block is assumed as sketched in Figure 8-16, a structure such as the Hermrigen anticline suggests a horizontal displacement of 3–5 km of the southern graben shoulder. This significant displacement points to basement imbrications on a possibly shallow detachment horizon. Imbrications involving crystalline basement have actually been reported from the well Entlebuch 1 located at the transition from Plateau to Subalpine Molasse in central Switzerland (Vollmayr & Wendt 1987). Other examples are known to exist in the Alps: the Penninic crystalline basement nappes all functioned on shallow detachments (the ductile deformation style as seen today is largely due to post-nappe deformation, as discussed by Schmid et al. in chapters14 and 22). A spectacular example of complete inversion of such a graben is represented by the Glarus nappe of the Helvetic zone, where the graben fill (Verrucano) has been shoved out of the graben and thrust over a distance of at least 30 km (see e. g. Pfiffner 1993). It is clear that in the Jura Mountains the Triassic evaporites acted as (secondary) detachment horizon, permitting the observed tight folding which requires an important flow of mechanically weak material e. g. in anticlinal cores.
Burkhard (1990) analyzed the shortening of the Molasse Basin and the Jura Mountains and estimated a bulk shortening of 25 – 30 km between the NW Jura front and of the crest of the Aar massif. He speculated that the eastward decrease of Jura shortening (non-existent in the eastern transect discussed here) could be compensated by an increase in shortening in the Subalpine Molasse. Shortening in the Subalpine Molasse based on the cross sections in Figures 8-8 and 8-14 can be estimated to be 11.5 km in the western, and 32 km in the eastern transect. Adding the shortening of the Jura Mountains (15 km) and the Plateau Molasse (1 km) along the western transect gives a total of 27.5 km for the latter. Given the uncertainties inherent in these crude estimates (≥ 20% error) the shortening of 27.5 km and 32 km obtained in the two transects are rather similar. It has to be remembered though, that the detachment horizon of the Jura Mountains is at a lower level as compared to the one in the Subalpine Molasse. The en échelon arrangement of Jura Mountains and Molasse Basin already advocated by Burkhard (1991) is thus to be viewed as a 3D feature. Considering the uplift history of the external massifs discussed by Pfiffner et al. in chapter 13 much of the uplift and shortening by folding and thrusting of the Aar massif is related to shortening within the Subalpine Molasse. The westward propagation of basement uplift in Miocene time could reflect a westward propagation of thrusting in the Subalpine Molasse. The Miocene-Pliocene uplift cannot be explained in a straight-forward manner. The young Apatite ages at the western end of the Aar massif and the NE end of the Aiguilles Rouges massif (see Figure 13-23) could be explained by uplift related to Jura shortening on a deep detachment level (involving a soft crystalline basement and being rooted beneath the Aar massif). The (single) data point at the eastern end of the Aar massif tends to suggest a different model, however, with an early uplift through the depth of 4 km recorded by the Apatite fission tracks in the central part of the massifs, which then propagated towards the eastern and western end. In any case the possibly younger lower detachment related to Jura shortening and rooted beneath the Aar massif resulted in a component of vertical uplift (? and rotation) of the structures observed at the northern flank of the Aar massif, which are related to shortening within the Subalpine Molasse and discussed in more detail in chapter 13.

Acknowledgments

The paper benefitted from critical comments by P. Lehner, R. Schoop, G.H. Bachmann & M. Müller, Th. Vollmayr and P.A. Ziegler.

Plates 8-1 to 8-5

SWISS NATIONAL SCIENCE FOUNDATION

E4

FINAL STACK

1: 50'000

RECORDING PARAMETERS

SPREAD LAYOUT	x-412.5-3525 m
CHANNELS	48
SOURCE INTERVAL	75 m
SOURCE TYPE	Vibroseis
SOURCE LAYOUT	3 Vibrators spaced 30 m
SWEEP FREQUENCY	10-35 Hz
SWEEP LENGTH	14 s
SWEEPS/VP	16
GROUP INTERVAL	75 m
GEOPHONE LAYOUT	24 geophones / 100 m
INSTRUMENTATION	DFS-V
FIELD FILTERS	HC 31 Hz
COVERAGE	24 (nominal)
RECORDING MODE	uncorrelated and vert.stacked
SAMPLING RATE	4 ms
RECORDING LENGTH	18 s
RECORDED BY	PRAKLA SEISMOS AG
DATE RECORDED	1975

PROCESSING PARAMETERS

1. Demultiplex with gain recovery
2. Vibroseis correlation
3. CMP-Sort
4. Resample to 8 ms
5. Predictive deconvolution
6. Time variant bandpass filter
7. Elevation statics
8. Time variant trace equalisation
9. Mute application
10. NMO-Correction
11. Surface consistent residual statics
12. CDP-Stack
13. Coherency filter
14. Predictive deconvolution
15. Bandpass filter 7/11 - 34/38 Hz

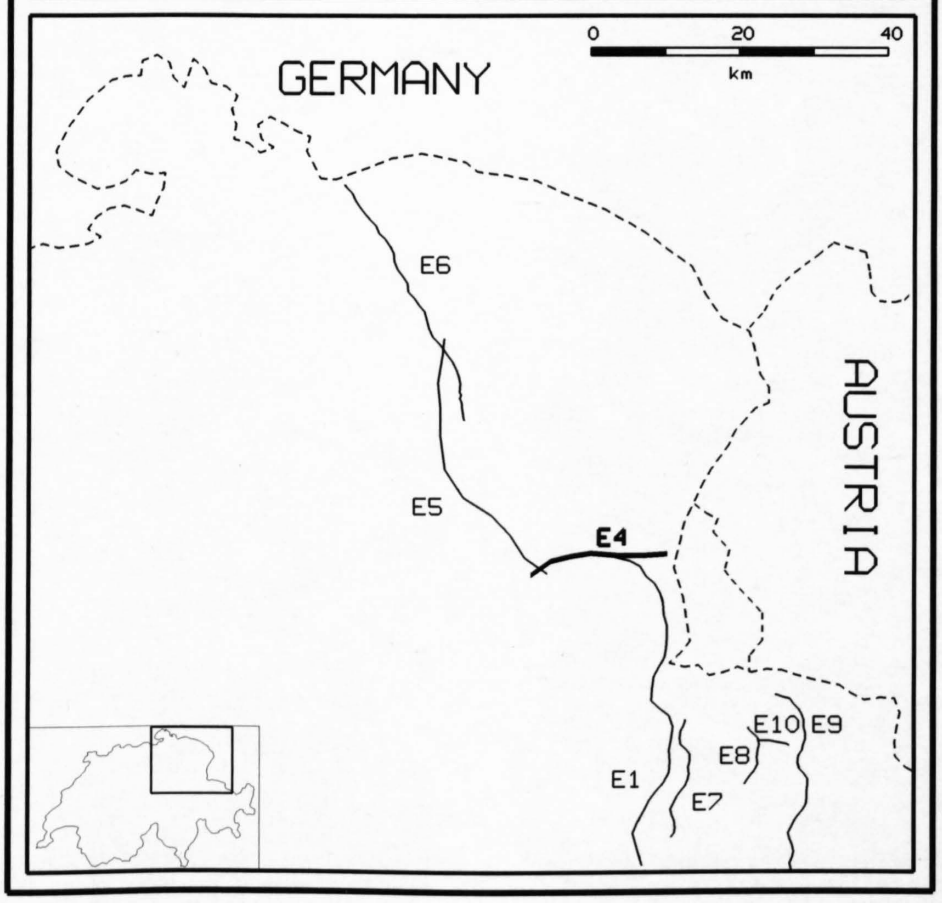

Plate 8-1

E4 (SE9)

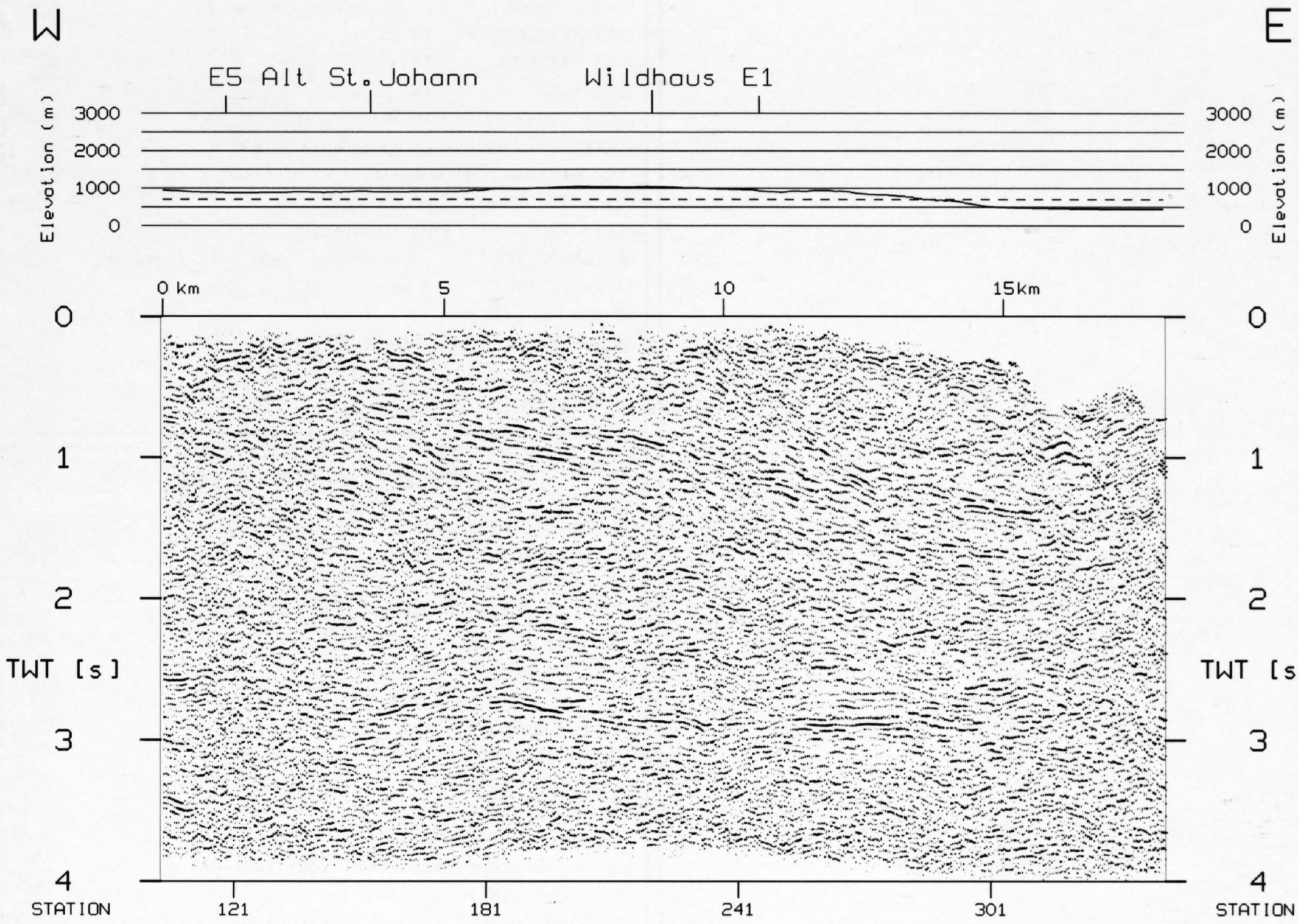
W
E
E5 Alt St. Johann
Wildhaus E1
Elevation (m)
3000
2000
1000
0
0 km
5
10
15km
TWT [s]
STATION
121
181
241
301

SWISS NATIONAL SCIENCE FOUNDATION

E5

FINAL STACK

1: 50'000

RECORDING PARAMETERS

SPREAD LAYOUT	x-412.5-3525 m
CHANNELS	48
SOURCE INTERVAL	75 m
SOURCE TYPE	Vibroseis
SOURCE LAYOUT	3 Vibrators spaced 30 m
SWEEP FREQUENCY	10-35 Hz
SWEEP LENGTH	14 s
SWEEPS/VP	16
GROUP INTERVAL	75 m
GEOPHONE LAYOUT	24 geophones / 100 m
INSTRUMENTATION	DFS-V
FIELD FILTERS	HC 31 Hz
COVERAGE	24 (nominal)
RECORDING MODE	uncorrelated and vert.stacked
SAMPLING RATE	4 ms
RECORDING LENGTH	18 s
RECORDED BY	PRAKLA SEISMOS AG
DATE RECORDED	1975

PROCESSING PARAMETERS

1. Demultiplex with gain recovery
2. Vibroseis correlation
3. CMP-Sort
4. Minimum phase conversion
5. Spiking deconvolution
6. Time variant bandpass filter
7. Notch filter 16.66 Hz
8. Elevation statics
9. Surface consistent residual statics
10. Random scaling
11. NMO-Correction
12. Mute application
13. Surface consistent residual statics
14. CDP-Stack
15. Time variant trace equalisation

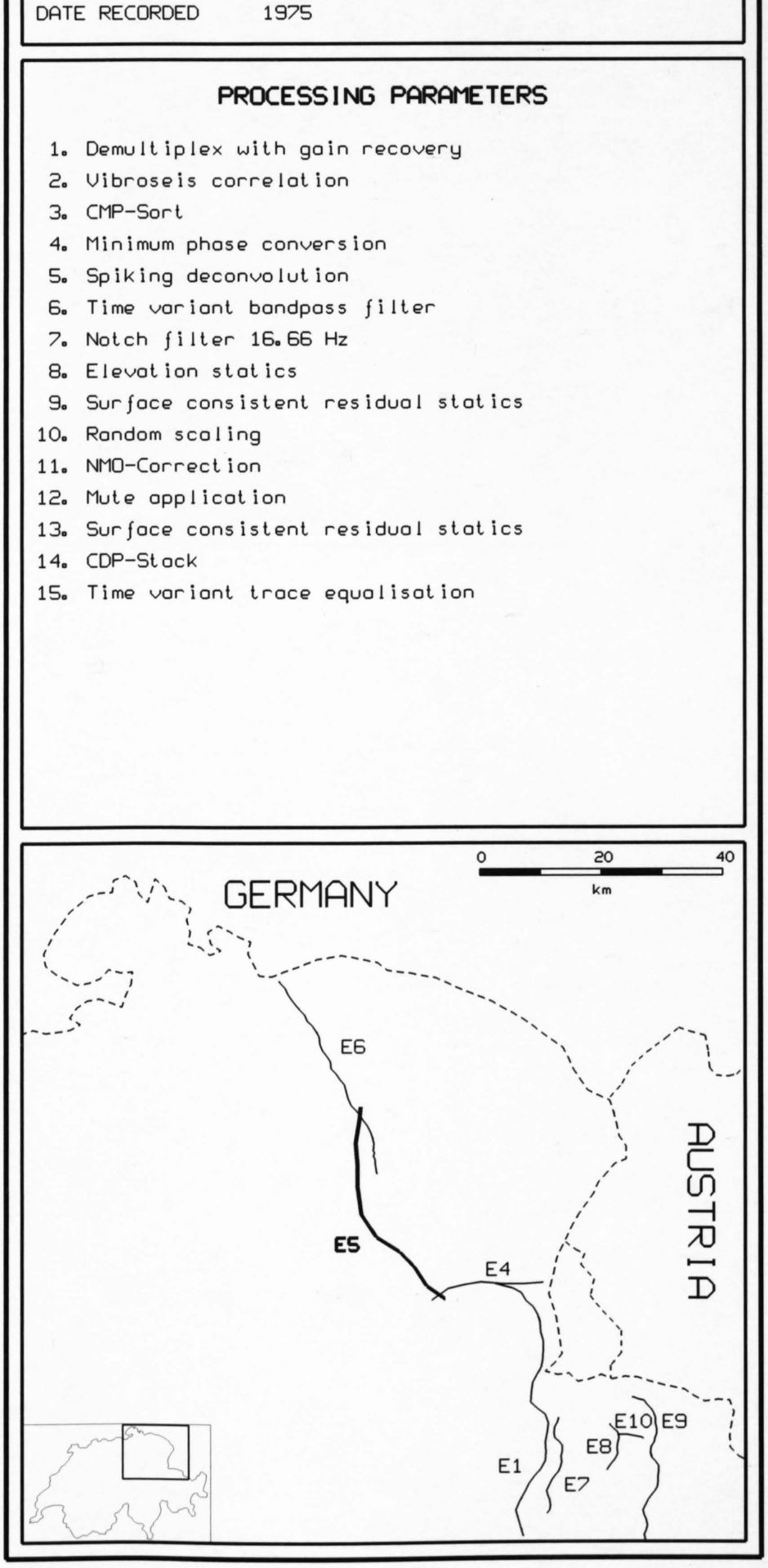

E5 (SE4)

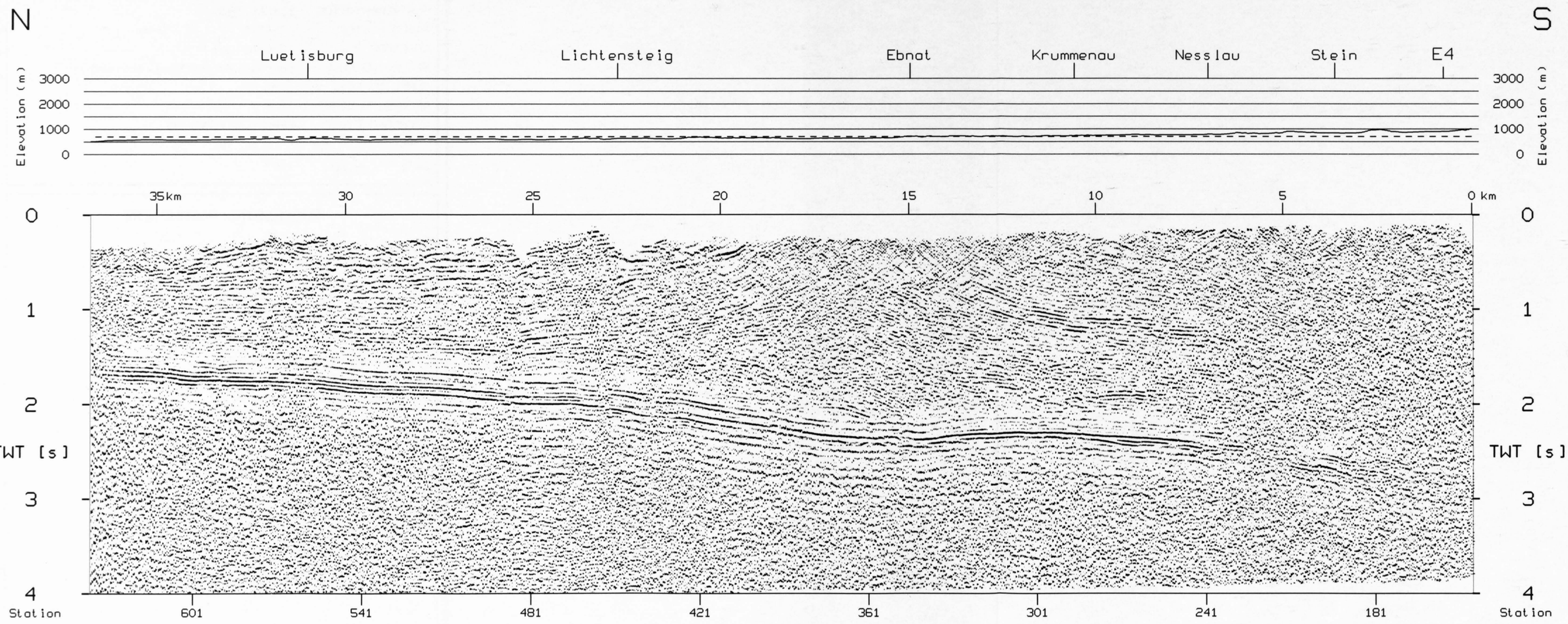
N
S
Luetisburg
Lichtensteig
Ebnat
Krummenau
Nesslau
Stein
E4
Elevation (m)
3000
2000
1000
0
35km
30
25
20
15
10
5
0 km
TWT [s]
0
1
2
3
4
Station
601
541
481
421
361
301
241
181

SWISS NATIONAL SCIENCE FOUNDATION

E6

FINAL STACK

1: 100'000

RECORDING PARAMETERS

SPREAD LAYOUT	1475-87.5-x-87.5-1475 m
CHANNELS	120
SOURCE INTERVAL	25 m
SOURCE TYPE	Vibroseis
SOURCE LAYOUT	3 Vibrators spaced 10 m
SWEEP FREQUENCY	18-90 Hz
SWEEP LENGTH	7 s
SWEEPS/VP	7
GROUP INTERVAL	25 m
GEOPHONE LAYOUT	12 geophones / 25 m
INSTRUMENTATION	SERCEL 348
FIELD FILTERS	LC 12.5 Hz / HC 72 Hz
COVERAGE	60 (nominal)
RECORDING MODE	correlated and vert.stacked
SAMPLING RATE	2 ms
RECORDING LENGTH	11 s
RECORDED BY	PRAKLA SEISMOS AG
DATE RECORDED	1983

PROCESSING PARAMETERS

1. Demultiplex with gain recovery
2. Bandpass filter 12/19 - 95/110 Hz
3. Minimum phase conversion
4. Scaling
5. Trace editing
6. CDP-Sort
7. Spiking deconvolution
8. Time variant bandpass filter
9. Elevation statics
10. Random scaling
11. Mute application
12. NMO-Correction
13. Surface consistent residual statics
14. CDP-Stack
15. Time variant trace equalisation
16. Trace mix (2-fold horizontal sum)

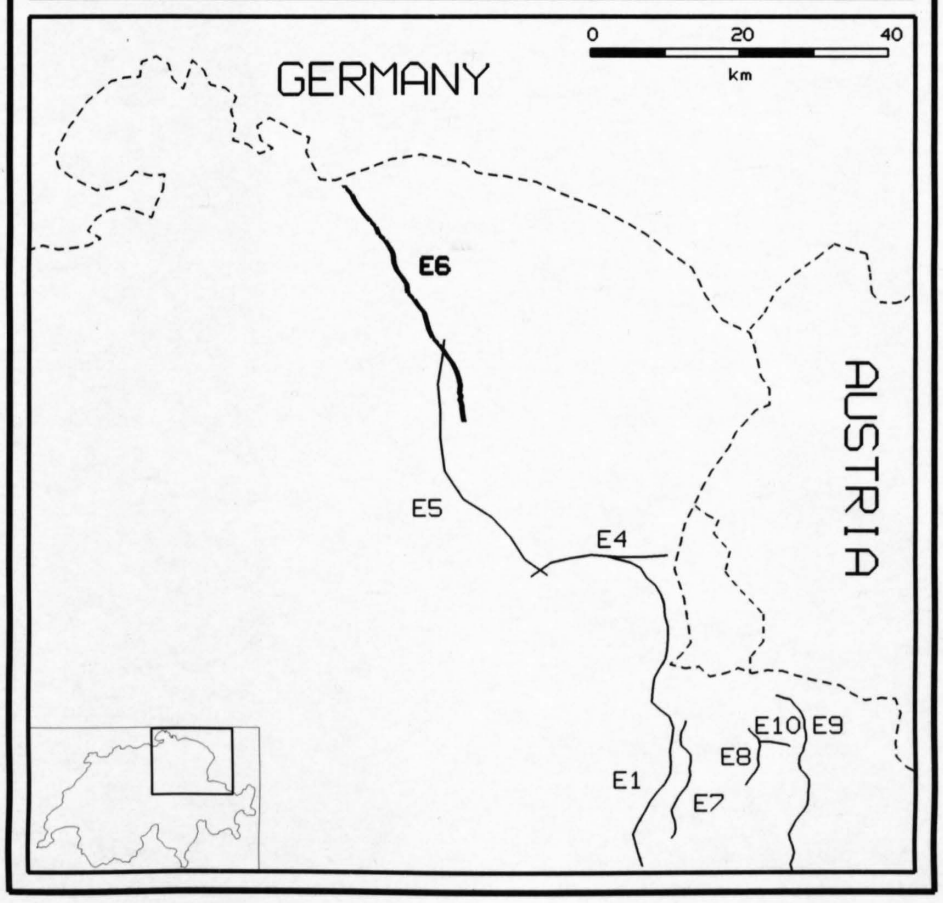

E6 (SE83)

N

E5

S

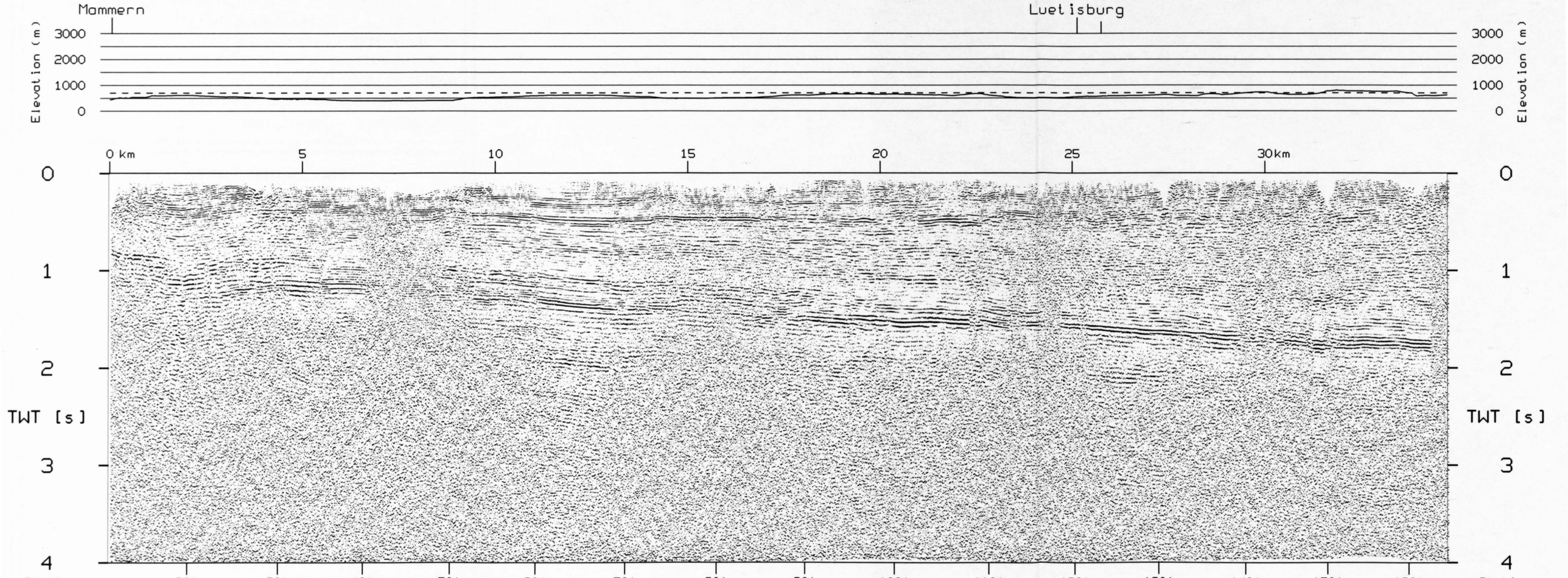

Station	201	301	401	501	601	701	801	901	1001	1101	1201	1301	1401	1501	1601	Station

SWISS NATIONAL SCIENCE FOUNDATION

W7 (BSE1)

FINAL STACK

1: 50'000

RECORDING PARAMETERS

SPREAD LAYOUT	1890-510-x-510-1890 m
CHANNELS	48
SOURCE INTERVAL	60 m
SOURCE TYPE	Vibroseis
SOURCE LAYOUT	3 Vibrators
SWEEP FREQUENCY	16-65 Hz
SWEEP LENGTH	12 s
SWEEPS/VP	16
GROUP INTERVAL	60 m
GEOPHONE TYPE	10 Hz
GEOPHONE LAYOUT	36 geophones / 105 m
INSTRUMENTATION	CFS I
FIELD FILTERS	LC 8 Hz/HC 90 Hz/NT 16.7 Hz 50 H
COVERAGE	24 (nominal)
RECORDING MODE	Correlated
SAMPLING RATE	4 ms
RECORDING LENGTH	16 s
RECORDED BY	PRAKLA SEISMOS AG
DATE RECORDED	Sept. 1981

PROCESSING PARAMETERS

1. Reformatting and gain recovery
2. Crooked line geometry
3. Time variant zero-phase deconvolution
4. Mute application
5. Elevation static corrections
6. NMO-Correction
7. Surface consistent residual statics
8. CDP-Stack

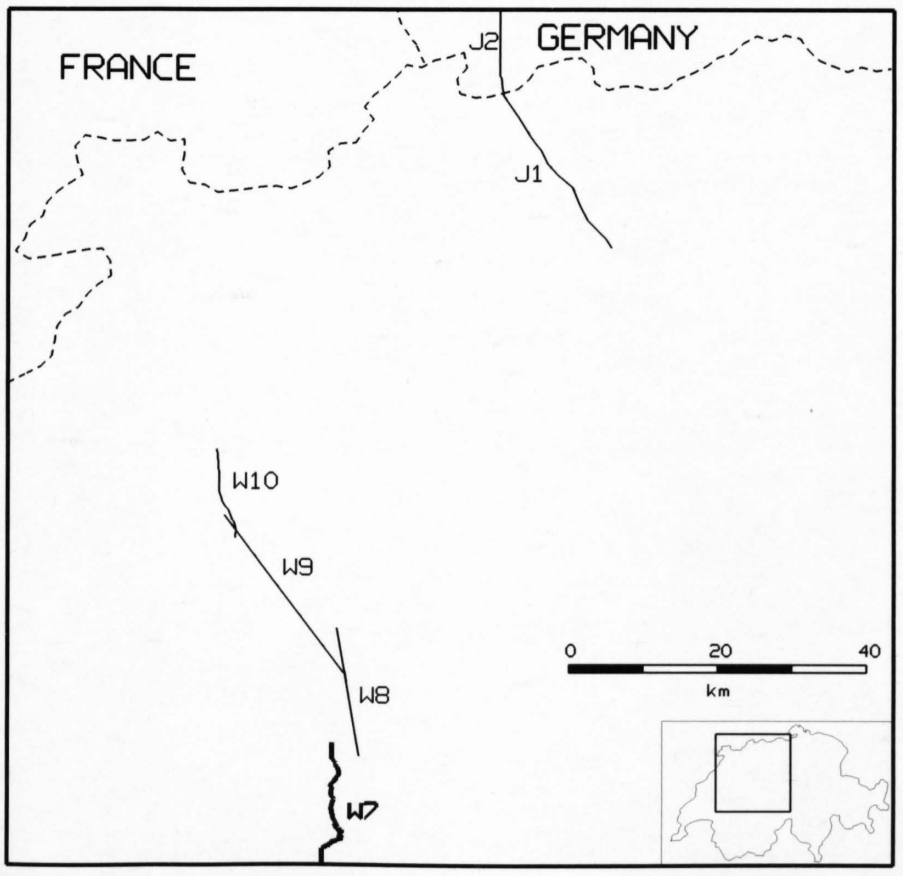

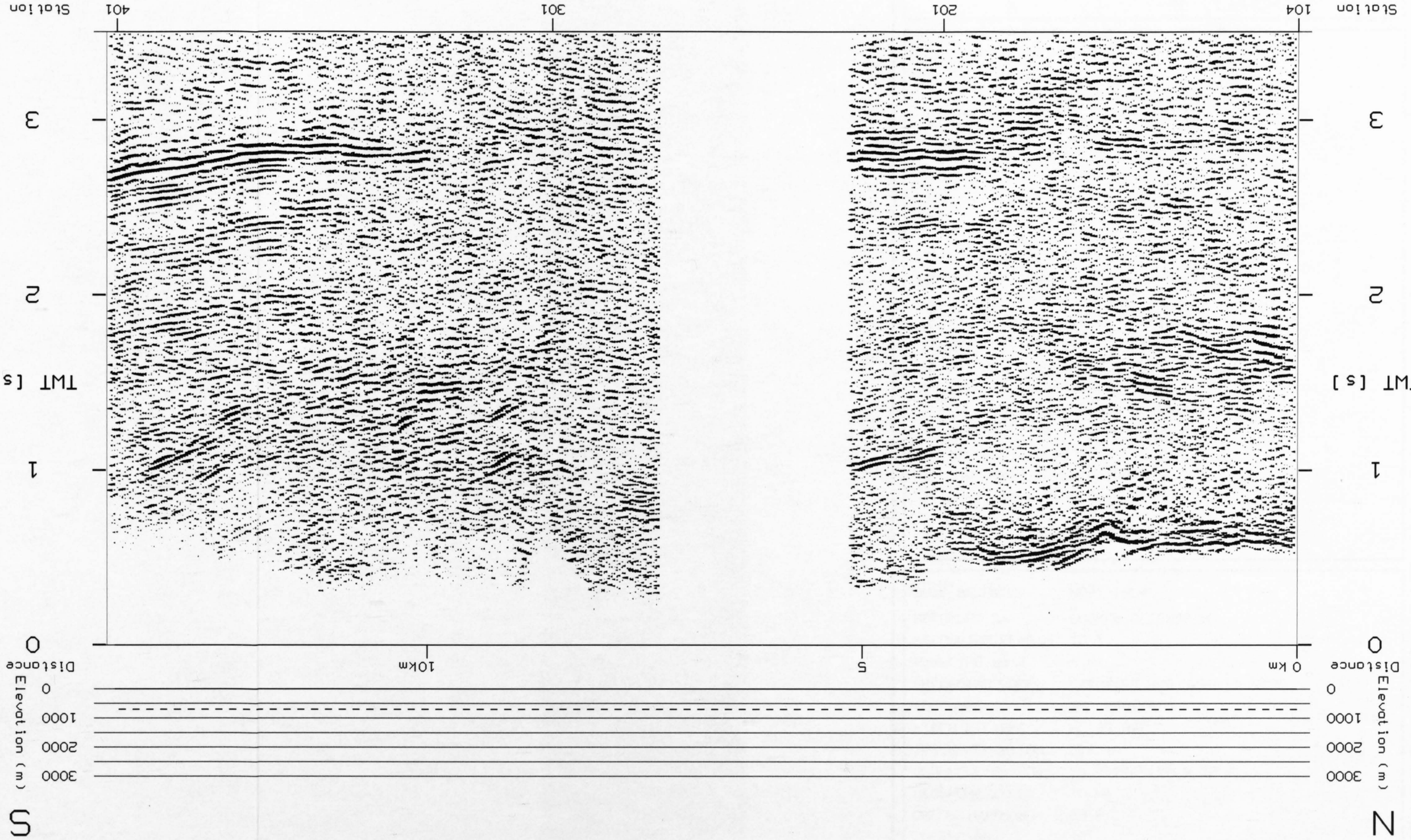
Station
401
301
201
104
Station
Distance
0
10km
5
0 km
TWT [s]
1
2
3
Elevation (m)
0
1000
2000
3000
S
N

M7

SWISS NATIONAL SCIENCE FOUNDATION

W10 (BN7)

FINAL STACK

1: 50'000

RECORDING PARAMETERS

SPREAD LAYOUT	1380-210-x-210-1380 m
CHANNELS	48
SOURCE INTERVAL	60 m
SOURCE TYPE	Vibroseis
SOURCE LAYOUT	3 Vibrators
SWEEP FREQUENCY	15-50 Hz
SWEEP LENGTH	7 s
SWEEPS/VP	15
GROUP INTERVAL	60 m
GEOPHONE TYPE	10 Hz
GEOPHONE LAYOUT	24 geophones / 75 m
INSTRUMENTATION	DFS IV
FIELD FILTERS	HC 52 Hz
COVERAGE	24 (nominal)
RECORDING MODE	unsummed and uncorrelated
SAMPLING RATE	4 ms
RECORDING LENGTH	10 s
RECORDED BY	PRAKLA SEISMOS AG
DATE RECORDED	Aug. 1974

PROCESSING PARAMETERS

1. Demultiplex and gain recovery
2. Vibroseis correlation
3. Vertical stack
4. Crooked line geometry
5. Spherical divergence compensation
6. Zero-phase deconvolution
7. Notch Filter 16.67 Hz
8. Mute application
9. Elevation static corrections
10. NMO-Correction
11. Surface consistent residual statics
12. CDP-Stack

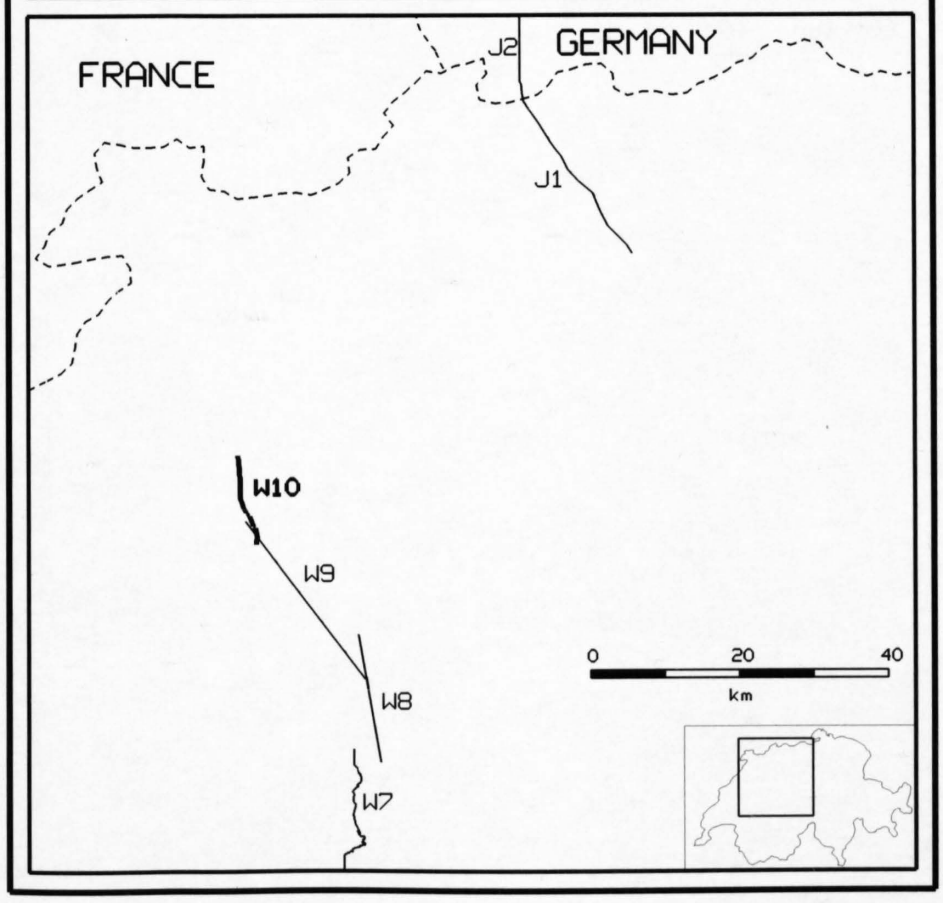

W10 (BN7)

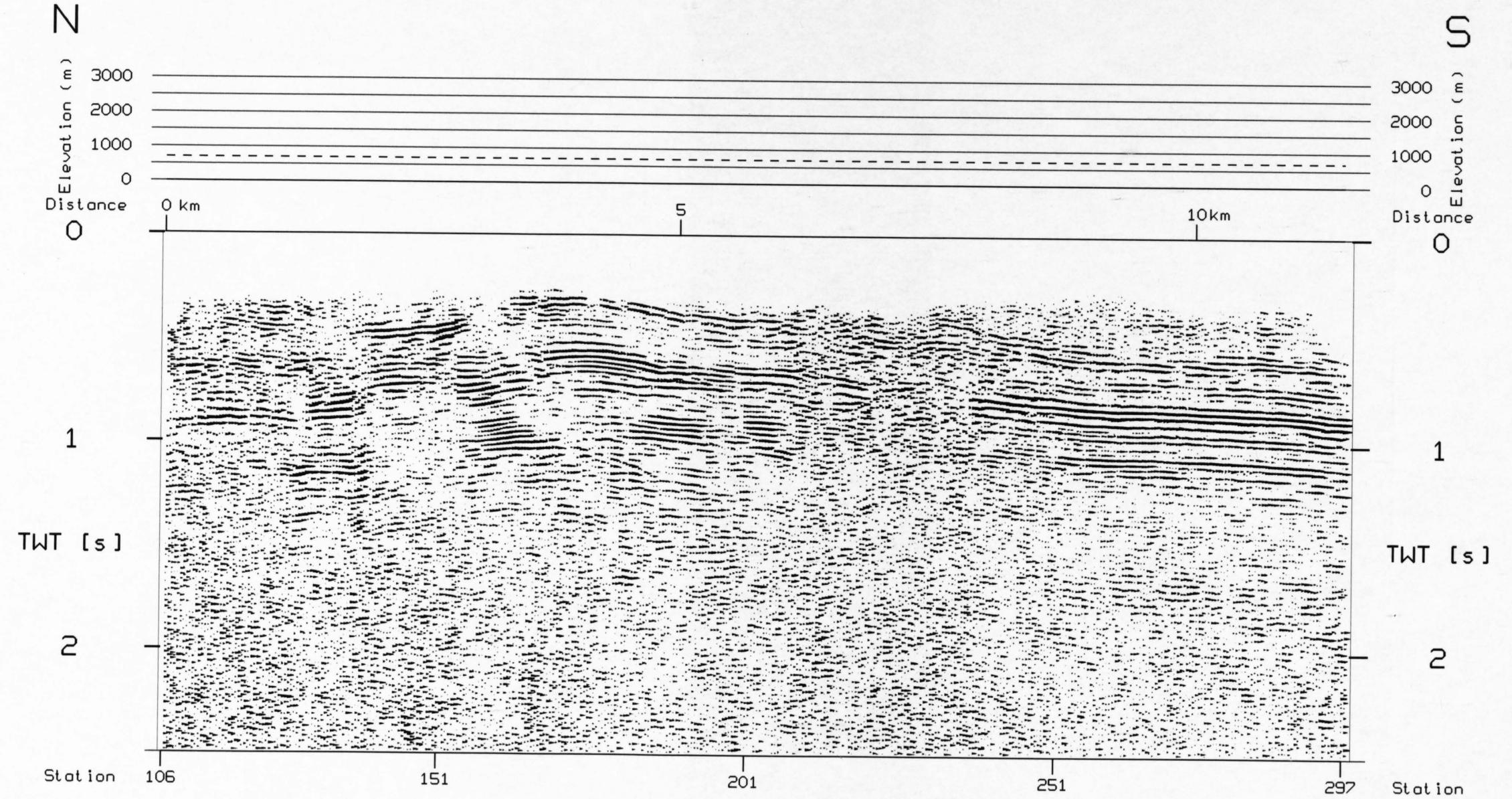
N
S
Elevation (m)
3000
2000
1000
0
Distance
0 km
5
10km
0
1
2
TWT [s]
Station
106
151
201
251
297